HELSINKI UNIVERSITY OF TECHNOLOGY
Department of Electrical and Communications Engineering
Laboratory of Electronics Production Technology
Espoo, Finland

Reliability Assessment of Telecommunications Equipment

Olli Salmela*

Dissertation for the degree of Doctor of Science in Technology to be presented with due permission of the Department of Electrical and Communications Engineering, Helsinki University of Technology for public examination and debate in Auditorium S4 at Helsinki University of Technology (Espoo, Finland) on the 11th of March, 2005, at 12 noon.

*Present address:
Nokia Networks
P.O. Box 301, 00045 Nokia Group, Finland
Tel. +358 (0)7 180 36211
Mobile +358 (0)40 513 2714
Fax +358 (0)7 180 30041
Email: olli.salmela@nokia.com

Electronics Production Technology Publication Series HUT-EPT-12

ISBN 951-22-7476-0 (printed)
ISBN 951-22-7477-9 (PDF)
ISSN 1457-0440

Espoo 2005
Otamedia Oy

Abstract

This thesis studies the reliability of telecommunications equipment, its components, and the systems made using those components. Special attention is paid to creating stronger links between the reliability analyses performed at different hierarchy levels.

The thesis starts with a temperature derating study. It is found out that the generic handbook based procedures may not always be very attractive, as they do not take satisfactorily into account the actual lifetime requirements. An alternative approach is proposed as a remedy to the current situation.

Thermal cycling requirement handbooks are surveyed, and based on the findings some enhancements are proposed. Next, a component and product specific approach to create thermal cycling requirements is suggested. When applying the new approach several factors can be taken into account: the product's lifetime requirement, the field environment, the reliability test result, and the statistical distribution of the component population. A new method of how to predict the reliability of a component population that is addressed to several, different field environments is presented.

Ceramic, leadless components are studied by testing and by utilizing Engelmaier's analytical solder fatigue model and Finite Element (FE) simulations. A new approach to interpret the solder joint height in conjunction with solder castellations is introduced. Based on this, a very good correlation between the test results and the predictions based on Engelmaier's model can be obtained. The parameter sensitivity of both the Engelmaier's model and the FE analysis are studied and compared. Error margins based on the parameter sensitivity studies are given.

Time-averaged hazard rate functions are studied in order to be able to use component level test data in simplistic parts-count method type reliability predictions. Finally, the availability of a full 3rd generation telecommunications network is studied.

Keywords: reliability, availability, MTTF, MTBF, hazard rate, derating, solder joint, fatigue, 3rd generation telecommunications network.

Preface

The work for this thesis has been carried out during my time in Nokia Corporation that started in 1995. The opportunity to prepare the thesis was given to me by Nokia Networks who has been my employer since 1st of April 2001. The initiative to write this thesis came from Dr. Esa Kemppinen. I am very grateful for this chance to finalize my doctoral thesis.

I would like to thank Professor Jorma Kivilahti for his guidance, support, and time. His helpful remarks and support were key to successfully completing my thesis.

I would like to thank my project team for a great working atmosphere and endless support. Especially, I would like to thank Klas Andersson, Jussi Särkkä, Dr. Markku Tammenmaa, Virpi Pennanen, and Yujie Dong for their personal assistance. Without this project team it would not have been possible to finalize this thesis.

I would like to thank all my colleagues for an inspiring working environment. I would particularly like to thank Vesa Vuorio for his healthy criticism against sometimes stiff reliability engineering conventions.

I would also like to acknowledge Helena Salo for her efforts in finding me relevant information and references. The friendly attitude and the swift service helped me a lot when writing my thesis.

I wish to express my appreciation to Dr. Finn Jensen and Prof. Abhijit Dasgupta for their thoroughness in going over my thesis and the constructive comments, which were a great help in bringing the thesis to its present form.

©Hergé/Moulinsart is acknowledged for giving permission to reproduce an excerpt from the Adventures of Tintin, ‘The Shooting Star’. These excellent visuals, in addition to being funny, describe the passionate attitude towards the research work that many scientists share. They also give a hint that predicting things that will happen in the future, be it the end of the world or the end of a component’s lifetime, is not always very easy.

I would also like to express my sincere thanks to my parents, Aarre and Salme Salmela, for supporting me during my university studies

Finally, I would like to thank my wife, Kirsi, for her love.

Espoo, November 2004

Olli Salmela

Contents

List of Symbols

a	crack length in solder material
A	availability
A_{avg}	average availability
$A_{2/3}$	2/3 of the solder-wetted pad area
$A.F.$	acceleration factor
$A.F.(N)$	acceleration factor (in cycles)
$A.F.(t)$	acceleration factor (in time)
c	fatigue ductility exponent
$C.F.$	Conversion Factor
CL	Confidence Level
$C.R.$	Comparison Ratio
$DR_{^oC}$	‘derating factor’, Celsius degrees used
DR_K	$=T_2/T_1$, ‘derating factor’, T_1, T_2 in Kelvin degrees
E	mean lifetime
E_a	activation energy
$E[\cdot]$	expected value for a random variable
F	empirical non-ideality factor
$f(t)$	probability density function
$F(t)$	cumulative density function
f_c	cyclic frequency
$h(t)$	hazard rate
$h_{s.j.}$	height of the solder joint
k	Boltzmann’s constant
K_D	diagonal flexural stiffness of the lead
K_3, K_4	constants in crack growth model

L_D	half of the maximum distance between two solder joints of a component under study
n	number of parameters in a lifetime prediction model
N	number of cycles
n_t	number of tested items
$N_{1st\ failure}$	the first failure found in the test
N_{1/n_t}	the anticipated first failure in the test based on the Weibull distribution
p	number of failed items
p_i	share of component population
R	reliability
$ROCOF$	Rate of Occurrence of Failures
t	time, lifetime
t_{acc}	accumulated number of device hours
t_o	constant
t_1	lifetime without derating
t_2	lifetime after derating
$t_2^{'}$	lifetime after derating taking into account parameter uncertainty
t_D	half of the dwell time during one temperature cycle
T	temperature in Kelvin degrees
T_j	junction temperature
T_1, T_2	temperatures in Kelvin degrees, non-derated and derated, respectively
$T_2^{'}$	derated temperature taking into account parameter uncertainty
$T_i(^oC)$	temperature in Celsius degrees
T_{sj}	average temperature of the solder
U	uncertainty
$U_{\max}$	maximum uncertainty
UCL	Upper Confidence Limit

Var	variance
w_i	weight function
X_i	interarrival time
β	Weibull shape parameter
χ^2	chi-squared distribution
ΔD	cyclic hysteresis energy
ΔT	$= T_1 - T_2$, the difference between the initial and the derated temperature
ΔT_e	equivalent cycling temperature swing
ΔW_{ave}	average viscoplastic strain energy density per cycle
$\Delta\alpha$	difference between the coefficient of thermal expansion values of the component and the substrate (absolute value)
ϕ	diameter
γ	parameter in 3-parameter Weibull distribution, failure-free time
$\Gamma(x)$	Euler gamma function
$\Gamma(a,x)$	incomplete gamma function with parameter a
η	Weibull characteristic lifetime
λ	parameter in exponential distribution, failure rate
θ	mean time to failure
ρ	correlation factor
υ	degrees of freedom
$2\varepsilon_f^{'}$	fatigue ductility coefficient

Abbreviations

AN	Access Network
BGA	Ball Grid Array
BSC	Base Station Controller
BTS	base station
CALCE	Computer Aided Life Cycle Engineering
CBGA	Ceramic Ball Grid Array
CLLCC	Ceramic Leadless Chip Carrier
CN	Core Network
CNET	Centre National D’Etudes des Telecommunications
CS	Circuit Switched
CSP	Chip Scale Package
CTE	Coefficient of Thermal Expansion
DIL	Dual In Line
DNP	Distance to Neutral Point
EDGE	Enhanced Data rated for GSM Evolution
F/C	flip chip
FCBGA	Flip Chip Ball Grid Array
FE	Finite Element
FEA	Finite Element Analysis
FEM	Finite Element Method
GERAN	GSM/EDGE Radio Access Network
GGSN	Gateway GPRS Support Node
GSM	Global System for Mobile Communications
HLR	Home Location Register
HPP	Homogeneous Poisson Process
HTCC	High Temperature Cofired Ceramics
IC	Integrated Circuit
IF	Intermediate Frequency

IID	Independent and Identically Distributed
IIED	Independent and Identically Exponentially Distributed
IP	Intellectual Property
IPC	Institute for Interconnecting and Packaging Electronic Circuits
kB	kilobyte
LEO	Low Earth Orbit
LTCC	Low Temperature Cofired Ceramics
MC	Monte Carlo
MCM	Multi-Chip Module
MDT	Mean Down Time
MSC	Mobile Switching Centre
MTBF	Mean Time Between Failures
MTTF	Mean Time To Failure
MTTR	Mean Time To Recovery
NE	Network Element
NHPP	Non-Homogeneous Poisson Process
Node B	base station in WCDMA system
NTT	Nippon Telegraph and Telephone
OSP	Organic Surface Protectant
PAE	Power Added Efficiency
PS	Packet Switched
PWB	Printed Wiring Board
RAC	Reliability Analysis Center
RAM	Random Access Memory
RAN	Radio Access Network
RBD	Reliability Block Diagram
RNC	Radio Network Controller
RP	Renewal Process
SAW	Surface Acoustic Wave (filter)
SGSN	Serving GPRS Support Node
SMA	Surface Mount Assembly

SMT	Surface Mount Technology
SRP	Superimposed Renewal Process
SSC	Site Support Cabinet
TBF	Time Between Failures
TBGA	Tape Ball Grid Array
TDMA	Time Division Multiple Access
UMTS	Universal Mobile Telephony System
UTRAN	UMTS Terrestrial Radio Access Network
WCDMA	Wideband Code Division Access
µBGA	micro Ball Grid Array
3G	3rd Generation (telecommunications network system)
3GPP	3rd Generation Partnership Project

1 Introduction

Reliability engineering is becoming a multidisciplinary science. In earlier days, reliability engineering was considered as equal to applied probability theory and statistics. Nowadays, the reliability research area has been clearly sub-divided into smaller entities. The research topics may be divided by the methodology it applies; mathematics based approaches have a long history, especially in reliability analysis of large systems, while physics based approaches are being introduced, especially in component level studies. New concepts in mathematics are swiftly being introduced to reliability engineering. These include, for example, fuzzy logic [1] and Petri Nets [2]. Physical reliability science has benefited from the increasing computing power that has enabled accurate modeling of complex structures [3], [4], [5].

The specialization trend has many desired implications: The accuracy of reliability predictions is getting better [6], and therefore the required safety margins have become smaller. Research in specialized areas also has a tendency to create better results than those achieved when working on a wide research area. One might even state that through specialization, reliability is becoming a science instead of being more or less a philosophy.

However, specialization has also some negative impacts. The most obvious one is that as reliability specialists are nowadays focusing on their area of interest only, the interaction between different research topics is getting weaker. In a worst-case scenario, reliability experts cannot understand anymore the neighboring research area problems. Now, it is already evident that component level reliability analysis cannot be fully applied at higher system hierarchy level reliability considerations. On the other hand, the component level reliability requirement should originate from system level requirements.

In this thesis, one of the main objectives is to provide some useful tools to link component and system level reliability considerations. The ultimate goal would be to create a *holistic approach*, in which reliability data could be fully applied and not depend on which hierarchy level it originated. Interaction between different reliability experts can create useful ideas that would never occur if the experts would only focus on their specific area.

Instead of optimizing the reliability performance of some specific area, much more could be gained if all reliability information can be fully utilized. This gives freedom to make clever choices related to component selection, printed wiring board partitioning, and product and system architecture.

Although a wide area, from physical component level to system level reliability studies, is covered in this thesis, in-depth analysis on each of the sub-sections is performed. This is necessary in order to create new results that are scientifically valuable. Nonetheless, the focus is always to obtain useful results on specific areas that help in creating stronger links between different research areas.

In the following chapters, mostly ceramic components will be analyzed from the reliability point of view. New methods to guarantee the reliability requirements to be fulfilled will be presented. The analysis is based on the application of physical models and statistical methods. The analysis starts with Chapter 3, where the effect of constant temperature on active devices is studied and a new temperature derating method is proposed.

The effect of temperature cycling is studied in the two following chapters. First, the general methodology, of how thermal cycling tests are usually interpreted and of how the requirements are set, is studied by analyzing the IPC (the Institute for Interconnecting and Packaging Electronic Circuits) guidelines. In this part, the general methodology to create generic requirements is critically reviewed. Then, certain ceramic components with a second level interconnection reliability risk are tested and the results are analyzed by utilizing the developed component specific reliability requirement methodology. Test methods, statistical analysis, and physical modeling are described in this section. Computer simulation results and results obtained by utilizing analytical solutions are also compared. This part includes a comparison of test results and forecasted results, the field performance prediction benchmark, and the applicability study of the computer simulations and analytical methods.

A link between component level reliability estimates and the analysis of a printed wiring board (PWB) and higher-level entities is established in Chapter 7. The inconsistency between component level test results with increasing hazard rate and the higher-level

reliability analysis with constant failure rate assumption is discussed. Methods to estimate the time-dependent hazard rate function are compared and the best solutions are proposed. Following that, component level test result information is ready to be applied in simplistic parts-count type reliability estimations.

Finally, the effect of introducing high-risk components at system level is studied. As an example, 3rd generation telecommunications network performance is evaluated. Useful simplifications when modeling the availability of the network are presented. It is shown, that the different viewpoints (component vs. system level) may result in an opposite conclusion on the applicability of the component.

2 Component Level Reliability Analysis

2.1 The Definition of Reliability

Reliability may be defined in several ways. The definition to be used in this thesis is the commonly used definition adapted from [70]:

“Reliability is the probability that an item operating under stated conditions will survive for a stated period of time.”

The above definition has its roots in military handbook MIL-STD-721C [7]. The above definition is valid for non-repairable hardware items. The “item“ may be a component, a sub-system or a system. If the item is software instead of hardware, the definition will be somewhat different [8].

2.2 Empirical Models

Component level reliability analysis conventions have their background in the military and space industries. As the components used in these applications were clearly safety critical, it was necessary to create qualification criteria and reliability prediction methods [9]. These reliability prediction models were typically based on large field failure databases. The empirical models give a generic estimate for a certain component or technology. Although, also being based on empirical data, the effect of field environment was taken into account by ‘factors‘ responsible for the degradation effects related to temperature, voltage, or some other stress factor. The temperature dependence was taken into account by the so-called Arrhenius equation [10] that was originally developed when modeling the rate of chemical reactions.

However, although since the early 1970s the failure rates for micro-electronic devices have fallen ca. 50% every 3 years [11] and the handbook models were updated on the average every 6 years, the models became overly pessimistic. Finally, in 1994, the U.S. Military Specifications and Standards Reform initiative led to the cancellation of many military specifications and standards [12]. This, coupled with the fact that the Air Force had re-

directed the mission of the Air Force Research Laboratory (the preparing activity for MIL-HDBK-217) away from reliability, resulted in MIL-HDBK-217 becoming obsolete, with no government plans to update it.

The cancellation of MIL-HDBK-217 was by no means the end of empirical models. Several similar kind of handbooks still exist, such as Bellcore Reliability Prediction Procedure [13], Nippon Telegraph and Telephone (NTT) procedure [14], British Telecom Handbook [15], CNET procedure [16], and Siemens procedure [17]. The predicted failure rates originating from different standards may, however, deviate from each other [18].

Empirical models can, in principle, also take into account early failures and random failures, which is not usually the case when considering physical models. Empirical models are also easy to use.

2.3 Physical Models

Each physical model [19], [20] is created to explain a specific failure mechanism. First, the testing is performed, the failed samples are analyzed, and the root cause for the failures is discovered [21]. Then, a suitable theory that would explain the specific failure mechanism is selected and used in order to calculate the acceleration factor and the predicted mean-time-to-failure (MTTF) value. This means, that the acceleration factor relevant to the failure mechanism is not usually known prior to the testing and analysis of the root cause. Physical modeling may be based on either an analytical model or on Finite Element Analysis (FEA) simulations. Physical models are most widely applied in solder joint fatigue modeling. Some other phenomena that have been studied by physical models are electromigration [22], and other thermally induced failure mechanisms [23].

When applying physical models it is possible to study the effects of material properties, dimensions, and field environment. The problem lies in the large parameter sensitivity of these models. Many models are applying exponential or power equations. The generic solutions to second-order differential equations, usually solved by running FEA simulations, are of exponential type. Therefore, even slightly inaccurate parameter values may result in tremendous errors. Despite this fact, proper error estimates are given far too

seldom, although some examples of this do exist [24], [25]. Another aspect that may possibly degrade the level of confidence towards predictions based on physical models is the fact that the models are developed in a well-controlled laboratory environment and there is little reliability data originated in a real field environment [6].

Presently, there are still situations in which no model that would explain the failure mechanism encountered can be found. In those cases, no prediction based on physical models can be given. Physical models usually address to wear-out phenomena and therefore, are of little value if early failures or random failures are in question. The exception to this is overstress events that can be analyzed by stress-strength analysis. Also, methods to assess early failures of defective sub-populations are being developed [26].

2.4 Development in Component Reliability

Despite the fact that there has been evident progress in component quality and reliability [11], there are some signs of degradation of component reliability. One reason for this is the abandoning of the military handbooks that provided clear guidelines. Therefore, common requirements on acceptable reliability levels do not exist. Today's market is driven by consumer electronics instead of electronics that require long-lasting, high-reliability performance. This has sometimes resulted in a lack of components conforming to high-reliability requirements. This lack has caused some problems, especially in the application areas where long lifetime and high reliability are required, such as military [27] and telecommunications infrastructure products [28].

New surface mount component types without interconnection leads cannot always be adapted due to their limited reliability in demanding applications [29]. Several new component types have been introduced to the market, but the second level interconnection reliability of all these components is not at a sufficient level. In Figure 1, some thermal cycling test results are depicted [30]. It can be easily seen, that most of the components do not conform to the no-failures-in-1000-cycles criterion.

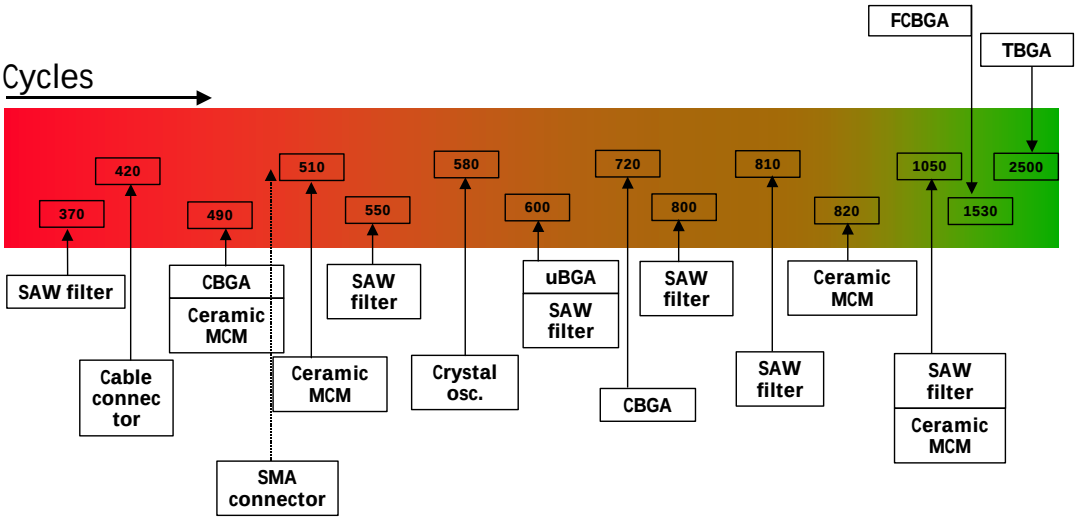

Figure 1. Thermal cycling (-40…+125°C, 1-hour cycle) test results of some leadless components. Characteristic lifetimes in cycles are depicted [30].

The complexity of the products is increasing. This may also create further demands on component reliability. Outsourcing of the design and the manufacturing of IP blocks do not eliminate the responsibility of the end-product manufacturer. Outsourcing may even be seen as threat to reliability and quality, unless the end-product manufacturer carefully communicates the reliability targets, and controls the fulfillment of the reliability requirements.

2.5 Reliability Information

As discussed earlier in this chapter, there are different ways to estimate the reliability of electronic components. In order to be able to evaluate the usefulness of such estimates, there should be some key criteria selected for this. One key issue is *how much we can rely on the reliability data.* Reliability prediction with no correlation to the actual field performance is of little value. It is also vital that the *data is available at times* when it is useful. After its service life, it is possible, at least in theory, to know exactly the reliability performance of a certain component population. However, this information may not be very useful, as the components have already failed and there is no means anymore to affect

the retrofit costs. Therefore, timely information that is based on the best knowledge available would be most desirable for the majority of engineering purposes.

In Figure 2, some reliability information sources are judged based on the two aforementioned criteria: the level of confidence on the reliability information and the time span when the information is available. The graph may be somewhat subjective, but should still be quite illustrative. The ranking of the methods based on the level of confidence may be open for discussion. The term ‘level of confidence’ is used here loosely to describe how accurate or trustworthy the information is. Level of confidence should not be confused with the confidence limits or confidence intervals that have exact definitions in statistics.

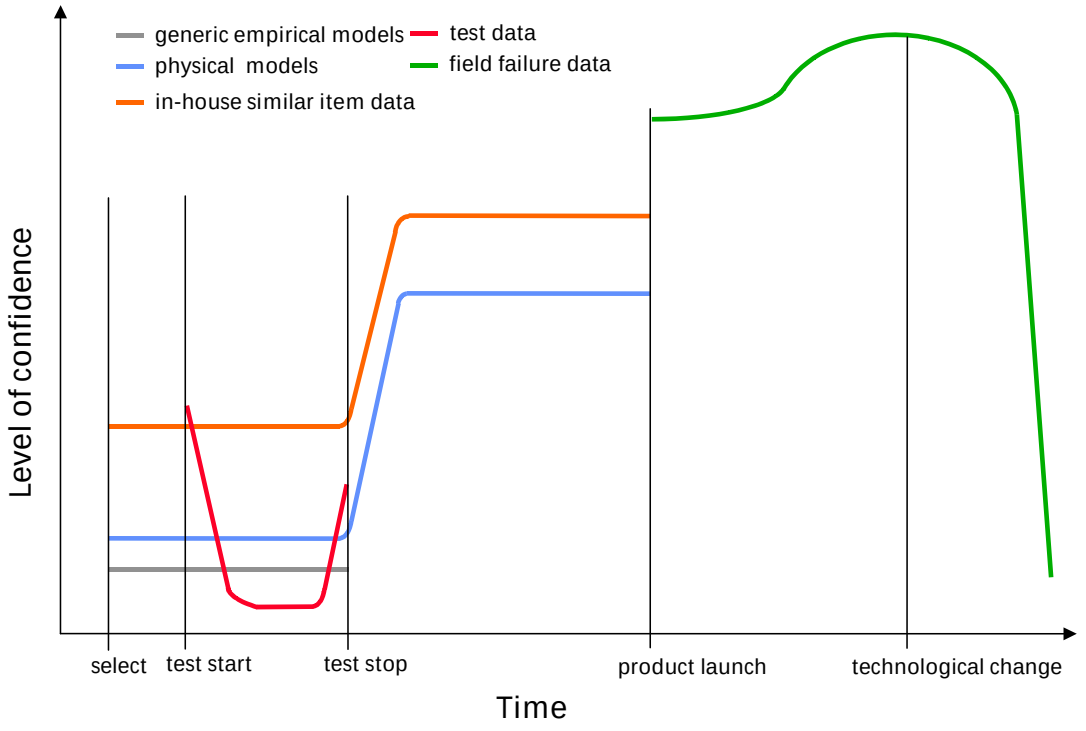

Figure 2. Reliability information sources; the level of confidence of the information and the time when the information is available.

When a component is selected for use in a design, the first indication of its reliability can be based on similar item data. If a similar component has already been used for several years, it is probable that in-house field failure databases can estimate the forthcoming reliability of the introduced component. If the component has not been utilized in a similar product, it is still possible to obtain some generic estimate of its reliability based on the handbooks discussed in Section 2.1. However, it should be noted that such data might be based on out-of-date data.

If there is no field data available, physical modeling may also give an initial estimate. Physical modeling is comprised of the utilization of a suitable analytical model and/or a computer simulation analysis. As physical modeling without calibration information may not be very accurate, it is expected that in-house field data in the initial phase would be superior to physical predictions in terms of level of confidence. However, if the generic handbook values are based on old data, the physical models may give a more accurate lifetime prediction.

Only after the reliability testing has been performed it is possible to improve the quality of reliability predictions. The physical models can utilize the test results as an input (calibration data). After this, a more accurate lifetime prediction for the component can be obtained. Moreover, after the test has been concluded, it is possible to compare the test results of the component to similar items that have been tested in the same way and whose field failure data is available. This enables the reliability prediction to be based on concrete data; if the component has performed in the same way as the reference item, it is also probable that the component studied will have approximately similar field reliability behavior. If the component has performed worse than the item on which field data exists, it is expected that the field reliability performance will be somewhat worse than the reference, and vice versa.

The test itself also gives valuable information. If some early failures occur in a test it is a clear signal that there will most likely be early failures in the field as well. This is very important information, which may be very difficult to obtain unless one actually tests the component. Physical models usually predict the wear-out of the components only, and

therefore may be of little value when it comes to predicting early failures. The exception to this is overstress events that can be analyzed by stress-strength analysis. Empirical models may be better at taking early failures into account. However, currently, they are not updated very often, and therefore may be either pessimistic or they may not contain information on the new component type at all.

The shape of the test data curve resembles the bathtub curve used commonly within the reliability community. The early failure, random failure and wear-out regions are easily recognizable. However, as the level of confidence – instead of hazard rate – is the parameter monitored, it is expected that the shape of the curve deviates somewhat from the conventional bathtub curve. The occurrence of early failures in a test environment is a relatively reliable indicator that real concerns in the field environment are likely to take place. As the test continues, and failures occur, it may be more difficult to predict if these failures are going to be induced also by the real environment during the life span of the component. The random-failure region obtains a relatively small level of confidence value as it is expected that only a minor share of component population is going to fail during this period of time. After wear-out phenomena start to occur, the confidence level is expected to rise again. This time, the level of confidence is, however, less than in case of early failures, as more time has elapsed since the test started. Therefore, it is more difficult to estimate if failures due to wear-out are going to be recorded during the lifespan of the component.

Despite the lack of information on early failures, many times they are responsible for the majority of field failures. This is especially true when it comes to consumer products, whose expected lifetime is limited and therefore wearing out of electronic components is not very probable. Early failures are due to design bugs, manufacturing faults, and quality problems. They should also be considered in conjunction with professional telecommunications equipment. As telecommunications equipment usually have a long life expectancy, both early failures and wear-out have to be taken care of.

After the early failures period in testing, there is usually a period of time, during which not many failures occur. This is often called the ‘random failure’ section of the bathtub curve.

As only a minor share of the equipment fail during this period, the level of confidence is usually low due to limited number of failure observations. In order to gain an acceptable level of confidence, thousands of items should be tested [39]. This is, however, in conflict with the number of test items usually available and the limited test resources.

As discussed earlier, the information on the wear-out period during the test can be used as input data for other prediction methods.

After the product has been launched in the field, field failure data starts to accumulate. Ideally, field data would be the most accurate source of reliability information. Unfortunately, the field data may not always be very useful for reliability engineers. There are several reasons for this. The failure analysis is not always thoroughly performed. This is due to the fact that the primary interest of the repair personnel is to repair the product, not to analyze the cause of failure. The field data also contains some failures that are not actually due to the inherent reliability level of the components. These failures include, for example, misuse of the product. Of course even this kind of information may be valuable, if it is considered that improving the durability of the product is needed. Also, the load history of the failed component is usually lacking, which makes it difficult to understand how the failure was actually initiated. Despite these words of caution, much can be gained if field failure data is utilized effectively. If constantly monitored, the field failure data can provide useful information on subjects of improvement. Improvements based on field data can usually be implemented during the lifetime of the product.

However, field data is valid only for a limited time. Technological advances are mostly responsible for this. It may be that the reliability performance of the component improves very much when the technology gets more mature. This has occurred in conjunction with integrated circuit technology, where constant improvements take place. According to MIL-HDBK-217 version A, a 64 kB RAM would fail in 13 seconds [31]. This very pessimistic prediction is a most unfavorable example of empirical models. Nowadays, the RAM capacity is several thousand times larger than in the example given, and still RAMs are not considered as reliability concerns. Another cause for field failure data becoming obsolete is the fact that components and component technologies have a natural life span. Due to

technology-obsolescence cycle, technologies will be replaced by some other technologies and therefore reliability estimates using the old technologies are of no interest.

2.6 Component Level Reliability Analysis in This Thesis

In this thesis, the reliability analysis at component level focuses on two aspects: the effect of constant temperature on (semiconductor) devices (Chapter 3) and the effect of cyclic thermal loads on solder joints (Chapters 4-6). The selection is motivated by the practical needs in those areas.

Derating affects heavily the component selection and the thermal design of products. Therefore, it would be expected that this procedure is well motivated and that the derated temperature is selected so that the component after derating meets the reliability requirements, but on the other hand, the derating should not add too large safety margins. Too large safety margins may easily result in unnecessary and expensive cooling arrangements. Also, the utilization of certain components may be limited in vain due to unrealistic derating procedures.

The reconsideration of derating practices has become more important as telecommunications is adapting WCDMA technology, where heat dissipation may become an issue both in case of terminals and infrastructure equipment. This is due to the high linearity requirement for the RF components, which in turn has inevitably resulted in relatively small PAE (Power Added Efficiency) figures. Small PAE value indicates that a large share of electrical energy is converted into heat.

Semiconductor manufacturing processes have developed greatly during the last decades. This has resulted in higher yields, smaller number of defects and better quality of the manufactured devices. Therefore, derating practices that were developed earlier on, may add unnecessarily large safety margins.

As discussed earlier in this chapter, the failure rates of micro-electronic devices have fallen radically since the early 1970s, thus, the microelectronic devices themselves are not currently presenting as large risk as they did in the past. On the other hand, consumer

electronics has taken the leading role in the industry. This has resulted in the pronounced requirements for small size and weight and low cost. This, in turn, has resulted in the wide utilization of leadless component attachments. When component leads are not used, the assembly becomes more rigid and the external loads – that were earlier taken partly by the leads – are now almost fully addressed to solder material. The increased loading of the solder material presents a risk that must be assessed, especially if products with long lifetime expectancy are in question. An additional risk lies in the adaptation of new lead-free solder materials [84] that are going to replace old SnPb material system. Lead-free solder materials are not discussed in this thesis; the future research will concentrate on this aspect. However, most of the findings of this thesis can be applied also in conjunction with lead-free solder materials.

3 The Effect of Constant Temperature

3.1 Introduction

Temperature derating is the practice of using an electronic device in a narrower operational environment than its manufacturer designated limits. The purpose of this is to lower the stress level on the device and thus to extend the device's lifetime. The derating guidelines provided limit the environmental stresses by using linear relationships. Usually, the junction temperature of an active device, Tj, is limited to a certain percentage of the maximum rated temperature given by the device manufacturer. However, the reliability of electronic devices typically has non-linear, often exponential, temperature dependence. Therefore, the conventional derating procedures may result in not optimal lifetime extensions.

In this chapter, the effect of using linear derating guidelines on lifetime is studied. After that, an alternative derating approach, that takes better into account the temperature dependency of the lifetime, is introduced.

3.2 Background

Derating has its roots in military industry practices that were developed in order to increase the lifetime of the devices used in high-reliability products. Military standards [32], [33] were created to give generic guidelines on how to perform derating. Besides the military industry, the electronics industry also, in general, adopted this approach, and currently, most companies have their own derating guidelines. Some military standards have been abolished by now, but there is still a need for generic derating guidelines. Reliability Analysis Center (RAC) has recently published a new version of their electronic derating guideline [34] that serves this purpose.

Derating has raised a heavy debate. It has been questioned whether derating has any merits in terms of reliability or if it is just causing extra costs to those who are applying it, without any significant reliability performance increment [35]. It is also claimed that the reliability of active devices does not only depend on the constant maximum temperature,

but also on the temperature excursions and temperature gradients. In many cases, those may have a more serious effect on reliability than the constant temperature has. Furthermore, in some rare cases, relatively high temperature may be advantageous, for example, in the case of hot electrons. Another example on this is the increment of fracture toughness of some electronic packaging materials at high temperatures. Nevertheless, temperature has a significant effect on reliability. The actual form of temperature dependency depends on the specific failure mechanism. Sometimes even uprating has been proposed [36] in order to be able to utilize more cost-efficient technologies/components to replace expensive ones. However, this approach has not, at least yet, reached common acceptance [37].

In this chapter, the effect of derating on the lifetime of electronic devices is studied. The lifetime of the devices studied is assumed to follow a simple Arrhenius-type relationship. As the temperature dependence of Arrhenius lifetime model is exponential, it is expected that the lifetime of the derated device be increased more than linearly, when applying linear derating on temperature.

The effect of parameter uncertainties on lifetime prediction is studied, as well. Finally, a new derating procedure that utilizes a physical lifetime model and compensates for the parameter uncertainty is proposed.

3.3 The Effect of Derating on Lifetime

In the following, the Arrhenius lifetime model is utilized. The reasons for selecting this model are twofold: it is very simple, and it has a very strong temperature dependency, typical to many lifetime prediction models. Moreover, according to a recent survey all companies studied continue to rely on the Arrhenius methodology in lifetime prediction [38]. However, although Arrhenius lifetime model is utilized, it is expected that similar, large parameter sensitivity would have been noted if some other physical lifetime model were chosen, instead. This is due to the fact almost all physical lifetime models have either exponential or power-law type temperature dependency [23].

The Arrhenius model suggests that the lifetime t of a component, having a temperature-activated failure mechanism, has the following form [39]:

$$t = t_o e^{\frac{E_a}{kT}}, \tag{1}$$

where t_o is constant, E_a is activation energy, k is Boltzmann's constant, and T is temperature in Kelvin degrees. Let's assume that the reliability of an identical device is monitored at two temperatures T_1 (initial) and T_2 (derated). The ratio of the lifetimes at these temperatures can be written

$$\frac{t_2}{t_1} = \frac{e^{\frac{Ea}{kT_2}}}{e^{\frac{Ea}{kT_1}}} = e^{\frac{E_a}{k}\cdot\frac{\Delta T}{T_1 T_2}} = \left[e^{\frac{E_a}{kT_1}} \right]^{\left(\frac{1}{DR_K}-1\right)}, \tag{2}$$

where $\Delta T = T_1 - T_2$ and $DR_K = T_2 / T_1$. Looking at the above equation, it is noted that the lifetime depends on the activation energy, the initial temperature T_1, and the 'derating factor' DR_K. Activation energy E_a obtains different values depending on the semiconductor technology and failure mechanism. Typical values range from 0.3 to 2.6 eV [40].

Although activation energy is a useful concept, some words of caution are in place. Activation energy may be temperature dependent, i.e., the values given are typical values for a certain temperature range. The temperature dependency is due to non-linear material behavior. Despite this, the temperature range, where the activation energy value actually was obtained, is not always mentioned. If activation energy is heavily temperature dependent, it may be impossible to utilize Arrhenius' law. Furthermore, a certain failure mechanism may have a relatively wide range of possible activation energy values. Therefore, there is a possibility of selecting a wrong activation energy value although the failure mechanism would have been correctly identified. Measuring the lifetime at multiple temperatures and obtaining the activation energy based on the temperature dependency of

the lifetime enables to obtain accurate, manufacturing process specific activation energy value.

As temperature derating is typically performed utilizing Celsius degrees, it is useful to be able to present DR_K factor in terms of Celsius degrees $DR_{\circ C}$, as well:

$$DR_K = \frac{DR_{\circ C} T_1(^oC) + 273}{T_1(^oC) + 273}, \tag{3}$$

where $T_1(^oC)$ is the initial temperature. $DR_{\circ C} = T_2(0C)/T_1(0C)$ is the 'derating factor' that is often used to derate the maximum rated temperature. It should be noted that the above equation results in an undefined value when $T_1(^0C) = 0$ ºC. This is due to division by zero in $D_{\circ C}$ term. In practice, this is not an issue, as usually $T_1(^0C) >> 0$ ºC. The derated temperature $T_2(°C)$ is obtained by multiplying the maximum rated temperature by $DR_{\circ C}$. The actual derating procedure may be more complicated than presented above, but all such procedures are based on linear transformation of the maximum rated temperature.

Equation (2) may also be presented in terms of lifetimes as:

$$t_2 = \left(\frac{t_1}{t_o}\right)^{\left(\frac{1}{DR_K}-1\right)} \cdot t_1 = t_1^{\frac{1}{DR_K}} \cdot t_o^{(1-\frac{1}{DR_K})}. \tag{4}$$

This is a simple form and easy to utilize.

3.4 Parametric Study

Typical derating procedure is simply using linear transformation of maximum rated temperature (in Celsius degrees). This seems not to be very sensible as lifetime depends exponentially on temperature (in Kelvin degrees). Acceptable reliability of the component during operational use is the ultimate goal of derating, therefore it would be expected that derating procedure would operate using lifetime, not temperature. Actually, it does not

matter which value the (derated) temperature obtains as long as the lifetime requirement is met.

The purpose of this section is to demonstrate that derating based solely on $DR_{^\circ C}$ may result in a variety of lifetimes and therefore cannot be considered as a viable way to extend lifetime. It will be shown that similar derating procedure when utilized on different devices may result in either an acceptable lifetime, or alternatively, it is also possible that derating lowers the maximum acceptable temperature too much.

Let's select the following values for the parametric study: E_a =0.4 eV, $T_1(^oC)$ =150 °C (initial temperature), and $T_2(^oC)$ =125 °C (derated temperature). The derating from 150 °C to 125 °C corresponds to a 'derating factor' of $DR_{^\circ C}$ =0.83.

In Figure 3, the effect of derating on lifetime is depicted. It is noted that when derating by a factor of 0.83, a double lifetime is gained compared to the initial situation. The large effect of temperature on lifetime can be clearly seen. Therefore, even minor changes in the temperature may have a profound effect. The effect of derating on lifetime is far from being linear. Careful control on the operational temperature is therefore of utmost importance. It can be clearly seen that there is a significant potential for lifetime extension, if it is possible to lower the temperature further.

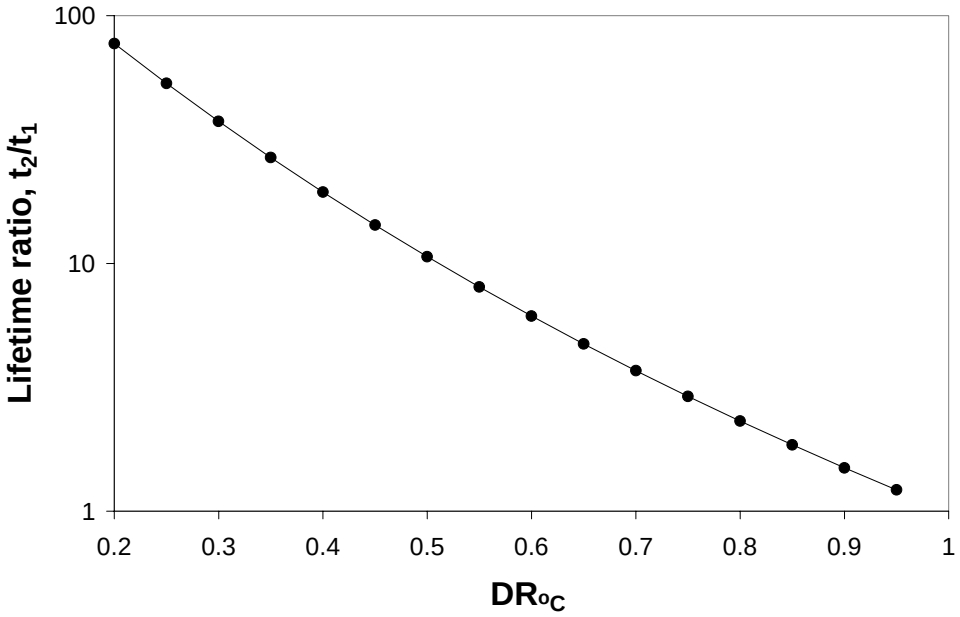

Figure 3. The effect of the 'derating factor' $DR_{\circ C}$ on the lifetime of an electronic component.

If the derating factor would have remained the same, but the initial (not derated) temperature would have been higher, the related relative lifetime extension could have been even larger, as can be seen in Figure 4.

As discussed earlier, activation energy E_a gains values over a wide range, typically 0.3…2.6 eV, depending on the failure mechanism. As Arrhenius relation has an exponential dependency on this parameter value, the expected lifetime of the component depends heavily on the activation energy (Figure 5). Therefore, derating procedures that do not take into account the differing failure mechanisms and the related different activation energy values seem to be quite rough. The same derating procedure may result in completely different lifetime extension. The effect of activation energy may be up to two decades.

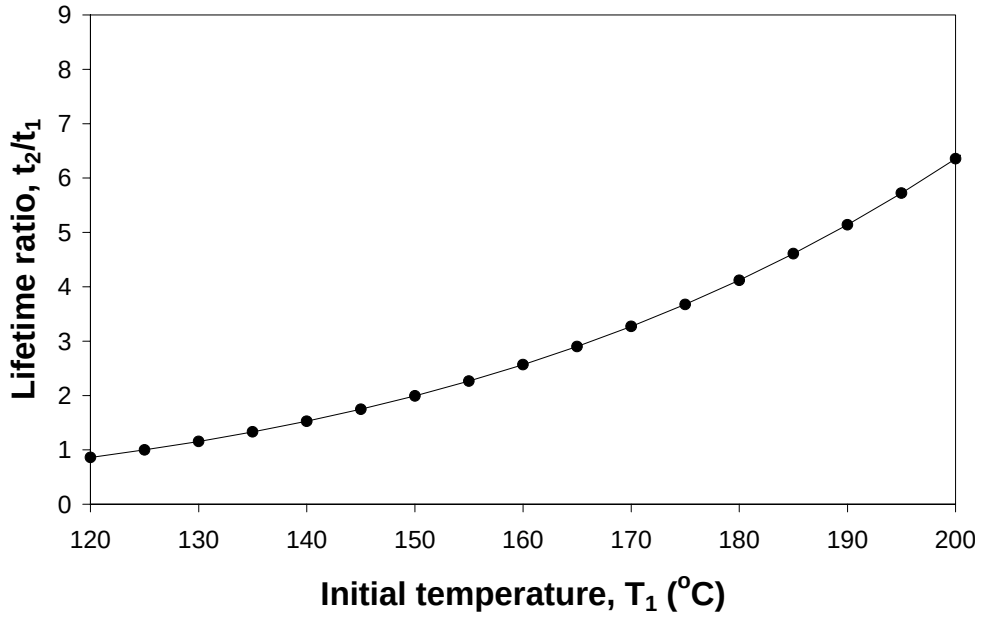

Figure 4. The effect of initial temperature T_1 on the lifetime of an electronic component.

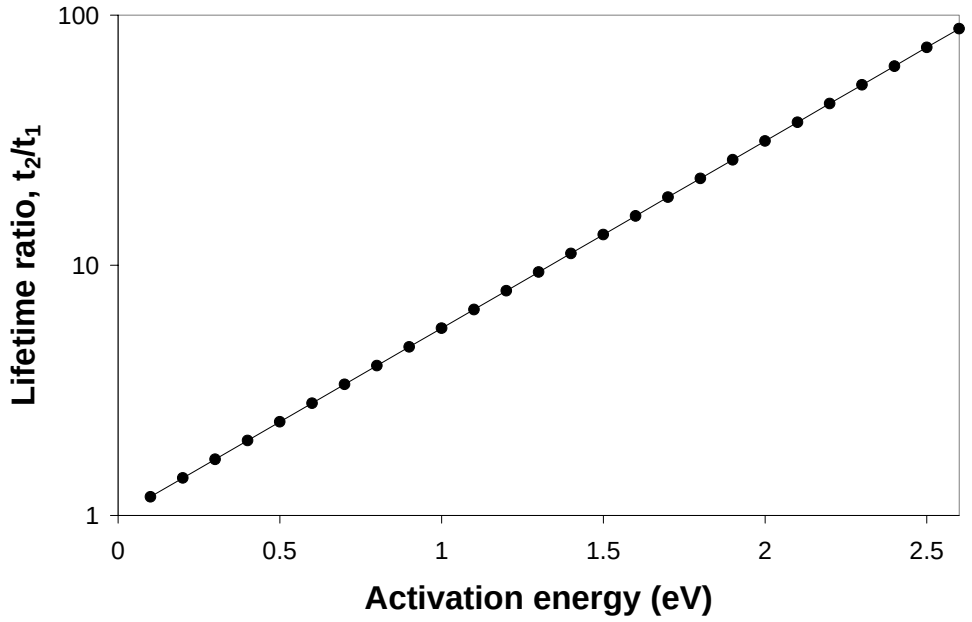

Figure 5. The effect of activation energy on the lifetime of an electronic component.

This short demonstration should already make it clear that conventional derating procedure is quite rough and that the hoped-for life elongation may obtain almost any value. Therefore, a more refined derating procedure, that takes into account the temperature dependency of the lifetime, is needed.

3.5 The Need for a New Derating Procedure

In Section 3.4 it became apparent that as the lifetime is quite heavily dependent on temperature, derating has its motivation. By derating one can gain lifetime extension by lowering the temperature below the maximum rated temperature. Although the failure mechanism would not directly depend on *constant* temperature, lowering of the maximum temperature can still have a positive effect. This may occur, for example, in case of failures due to temperature cycling. Limiting the temperature range of the temperature cycling by its high-temperature end can increase the lifetime of the components.

The lifetime expectations of the product and the reliability requirements should specify if derating is required or not. Whilst components used in consumer products with a short lifetime expectation may not need to be derated, the products that have long lifetime expectations usually require derating to fulfill the reliability expectations. Derating may also be needed, in case a component with a low initial reliability level is about to be utilized in an application that requires a long lifetime [41].

On the other hand, the criticism against derating seems to be felicitous when it comes to the way it is applied in many cases. Far too often this methodology is applied ‘blindly’; not considering what can actually be gained in terms of lifetime increment if this procedure is applied. This was demonstrated in the previous section. It is clear that different components, component technologies, manufacturing processes, failure mechanisms, and the related lifetime prediction models should be studied carefully in order to be able to effectively utilize this procedure. It is vital to utilize correct parameter values. The parameter sensitivity related to Arrhenius is a characteristic that is also common to other physical reliability models [23]. Many of these models are assuming that lifetime has an exponential or a power dependency on temperature.

Another aspect worth noting is that derating is performed utilizing Celsius degrees, although the lifetime prediction models are typically presented in terms of Kelvin degrees. Therefore, the true effect of derating on lifetime may be even more difficult to realize, unless careful lifetime analysis is performed.

Utilizing *linear* derating procedures does not seem to be very reasonable as the temperature dependency of the electronic devices is not linear. It would also be expected that the derating procedure would somehow take into account the true temperature dependency of the component. Therefore, it is proposed that physical lifetime models should be used as a basis for creating the derating procedures. This can be done, for example, by setting a goal for lifetime in the field environment and then finding out the required temperature reduction that the physical reliability model proposes. This approach is demonstrated in the following Section 3.6.

The careful analysis of the failure mechanism, its temperature dependency, and the related lifetime is a very tedious task. However, the end result may be cost savings resulting either from the reduced warranty costs or the ability to utilize inexpensive components in relatively demanding applications. As the reliability models are very parameter sensitive, care must be taken so that accurate parameter values are utilized; generic values originating from handbooks may not be accurate enough. Quite often semiconductor manufacturers have readily the data that is needed to estimate the safe operational temperature. This data is recommended to be utilized.

3.6 The New Derating Procedure

3.6.1 General

In the following section, Arrhenius lifetime model is used as a basis for derating. First, the lifetime requirement is set. Then, the temperature corresponding to this lifetime requirement is derived. After that, the parameter sensitivity is taken into account by further lowering the temperature so that the lifetime requirement t_2 can guarantee fulfillment, even in a scenario where all the parameter uncertainties add up.

Taking into account uncertainty is a standard procedure in circuit simulations when it comes to electrical performance. Uncertainty of electrical parameters is usually accounted for by running Monte-Carlo simulations [42]. Certain failure mechanisms occurring at IC level have been studied by circuit simulation [43], [44]. Failure mechanisms studied include electromigration [45] and the degradation due to hot electrons [46]. However, derating procedures, as such, have been based on the assumption of nominal lifetime performance of certain component technologies [34] - without any specific consideration of uncertainty.

Finally, a step-by-step example on this methodology is given. One should, however, note that this methodology is not to be limited to Arrhenius type lifetime models, but can be applied in conjunction with any physical lifetime model.

3.6.2 Setting the reliability target

First, the reliability target for the component in field environment is set. The target can be stated, e.g., as $F(10\,years) = 1\%$. This means, that at the end of component's lifetime (10 years) 1% of the whole component population is allowed to have failed. Some alternative lifetime lengths and failure percentages may be considered, as well. The requirement setting depends heavily on the application, the complexity of the product and the reliability target for the whole product. All this should reflect the target setting. Therefore, product specific reliability targets should be preferred over fixed reliability requirements.

3.6.3 Obtaining the temperature to fulfill the requirement

After that, the reliability requirement is translated into a temperature value. After studying the temperature dependency of the lifetime of the component, this can be done. Let's say that the lifetime requirement is fulfilled if temperature is equal to T_2. If all components would be identical, keeping the temperature below this value would guarantee the fulfillment of the lifetime requirement. However, statistical lifetime behavior of the component population is expected. This must be taken into account by further lowering the

obtained temperature in order to make sure that the fulfillment of the reliability requirement is guaranteed at all times.

3.6.4 Obtaining uncertainty values and taking into account their effect

As derating should guarantee an acceptable operation even if the component studied performs worse than the component of average quality, it is necessary to add some safety margin to the derated temperature. One way to do this is to estimate the effect of uncertainties on the lifetime of the component - and after that - to compensate for those by lowering the temperature to a value $T_2^{'}$ that satisfies the fulfillment of the reliability requirement at all times.

Next, the needed equations are derived, after which, uncertainty and its effect on lifetime is estimated, and finally, a step-by-step example on the whole derating procedure is given.

One can solve Equation (2) for lifetime t_2

$$t_2 = t_1 e^{\frac{E_a}{kT_1}(\frac{1}{DR_K}-1)}. \tag{5}$$

To estimate the maximum uncertainty $U_{\max}$ related to t_2, based on the individual uncertainties related to parameters X_i used, it can be stated that [11]

$$U_{\max} = \sum_{i=1}^{n} \left| \frac{\partial t_2}{\partial X_i} \right| U_{\bar{X}_{i,\max}}, \tag{6}$$

where $U_{\bar{X}_{i,\max}}$ is the maximum uncertainty related to parameter X_i and n is the number of parameters used. Utilizing Eqs. (5) and (6), it can be written that

$$U_{\max} = \left| \frac{\partial t_2}{\partial t_1} \right| U_{\bar{t}_{1,\max}} + \left| \frac{\partial t_2}{\partial E_a} \right| U_{\bar{E}_{a,\max}} + \left| \frac{\partial t_2}{\partial T_1} \right| U_{\bar{T}_{1,\max}}. \tag{7}$$

In the above, it has been assumed that all three parameters are independent of each other. The partial derivatives can be easily derived. The uncertainties are due to measurement uncertainties and statistical variation in and between manufacturing processes and manufacturing lots.

When the maximum uncertainty $U_{\max}$ of lifetime t_2 is known, how much extra derating is needed can be calculated so that even in the worst-case scenario (all uncertainty terms add up), the lifetime requirement is still fulfilled. The derated temperature $T_2^{'}$, taking into account parameter uncertainties, can be calculated by writing the lifetime requirement in this case as $t_2^{'} = t_2 + U_{\max}$. After inserting these values into Eq. (5) and solving for $T_2^{'}$, it can be written that

$$T_2^{'} = \frac{T_1}{\frac{kT_1}{E_a}\ln\left(\frac{t_2 + U_{\max}}{t_1}\right)+1} \; . \tag{8}$$

Each uncertainty component should preferably be estimated based on actual test data. As actual lifetime vs. temperature data on a specific component and failure mechanism represents the most accurate data available, it is believed that using this data results in the most realistic uncertainty estimate. Furthermore, this approach results in a derated temperature value that guarantees an optimal acceptable operation during the whole lifetime, but on the other hand, does not add unnecessarily large safety margins.

The uncertainty related to the last term of Eq. (7) is expected to originate from temperature measurement uncertainty. The measurement of ambient temperature is a quite straightforward task, and therefore, it is expected that the uncertainty originating from this is relatively small, let's say ± 1 °C. However, if junction or channel temperature of an active device is considered, the accurate measurement is quite much more demanding due to small dimensions of the semiconductor device and the limited resolution of the infrared cameras. Therefore, if the device is powered, the uncertainty related to temperature measurement is expected to obtain a much larger value, in the range of ± 2 °C.

The lifetime t_1 measured at an elevated temperature T_1 is expected to obtain fluctuations due to statistical behavior of the component population. A common practice is to assume that the components tested possess a constant hazard rate and that the probability density function is an exponential [70]. If making this assumption, it is possible to account for statistical fluctuation by utilizing confidence limit values related to exponential distribution. This means that the measured hazard rate value λ_{meas} is replaced by a larger value related to a selected confidence level (CL) value. An usual choice used in the semiconductor industry is CL=60%. The upper confidence limit (UCL) for the hazard rate can be written as [70]

$$\lambda_{UCL} = \frac{\chi^2_{CL,\upsilon}}{2t_{acc}}, \tag{9}$$

where $\chi^2_{CL,\upsilon}$ is the chi-squared distribution value with υ degrees of freedom and t_{acc} is the accumulated number of device hours. Based on the above, the uncertainty related to the lifetime t_1 can be described by

$$U_{t_{1,\max}} = \frac{1}{\lambda_{meas}} - \frac{1}{\lambda_{UCL}}. \tag{10}$$

This approach to estimate the uncertainty is very simple and easy to apply. The drawback of the above is that it is based on an assumption that the lifetimes of the component population would follow an exponential distribution. This is not necessarily realistic in all cases. The utilization of some other lifetime distribution and the related confidence limits is possible, as well. The selection of using exponential distribution is motivated by the fact that it is the standard choice used by most semiconductor device manufacturers.

The uncertainty related to activation energy may be estimated graphically from the lifetime-temperature curve, as shown in Figure 6. The uncertainty of the activation energy usually lies in the range of ± 0.05 eV [47].

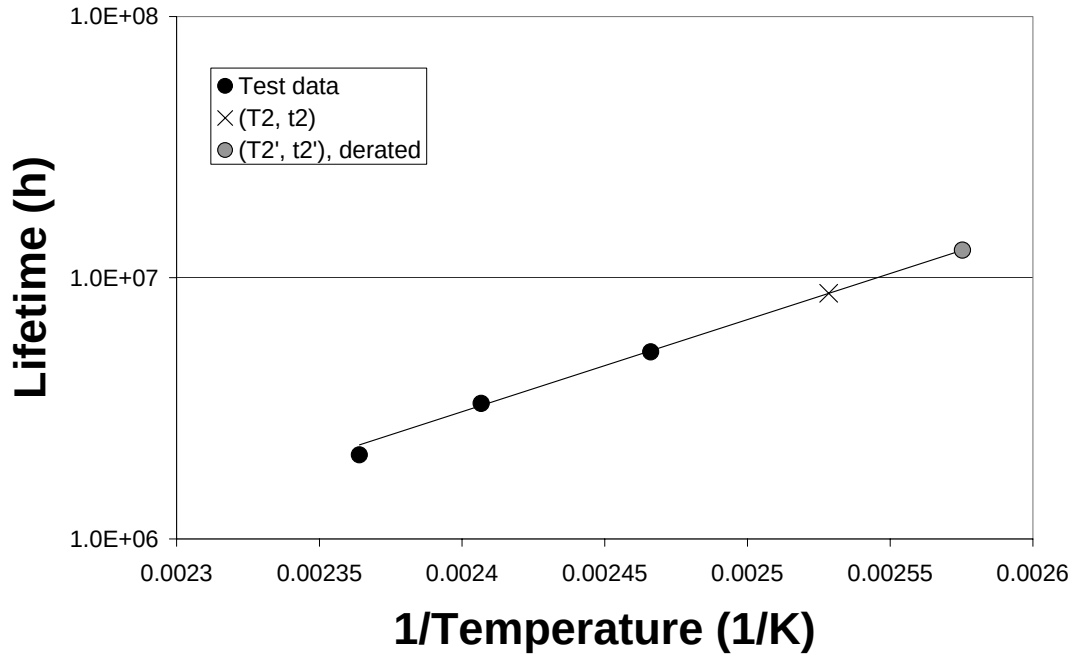

Figure 6. Lifetime data obtained from the accelerated life test and the derated temperatures.

An example:

The new derating method is demonstrated here by a step-by-step example. Let's assume that the reliability requirement for the component is that 1% of the population is allowed to have failed after 10 years of operation. Reliability tests at elevated temperature have been run and Figure 6 presents the results. The activation energy obtains a value of 0.7 eV and t_o =0.01047 h. The absolute maximum temperature the manufacturer suggests is $T_1(^oC)$ =150 °C.

$F(10\,years) = 1$ % translates to a hazard rate value of 115 FITs (or mean lifetime of $8.7 \cdot 10^6$ h) assuming that lifetime is exponentially distributed. This requirement can be met if temperature is kept below $T_2(^oC)$ =122.5 °C (Figure 6).

Nominal values and uncertainties related to parameters are listed in Table 1. The uncertainty related to term T_1 originates from uncertainties in temperature measurement, as discussed earlier in this section. The uncertainty related to activation energy is obtained by studying Figure 6. As can be seen, all data points do not follow exactly the fit line. Therefore, the slope (=activation energy) may obtain an alternative value. The uncertainty is estimated by obtaining the maximum deviation of the data points from the fit line.

The uncertainty related to the lifetime result at 150 °C is estimated by utilizing the upper confidence limit. The test run consisted of 4580 vehicles out of which 2 failed during the 1000-hour test period. Therefore, the measured failure rate was $\lambda_{meas} = 437\ FITs$. As the test was time-truncated, the degrees of freedom obtains the value of $\upsilon = 2 \cdot r + 2$, where r is the number of failed items. In this case, $\upsilon = 2 \cdot 2 + 2 = 6$. When selecting the confidence level CL=60%, the chi-squared distribution obtains a value of $\chi^2_{60\%,6} = 6.2$. Therefore the upper confidence limit obtains the value of $\lambda_{UCL} = 677\ FITs$ and using Eq. (10) the uncertainty related to lifetime at temperature $T_1(^0C)$=150 °C is estimated to be $0.8 \cdot 10^6$ hours.

As now all the uncertainty components are known, the maximum uncertainty can be calculated by using Eq. (7). The results are listed in Table 2. It is noted that due to the large parameter sensitivity, the maximum uncertainty $U_{\max}$ is ca. 46 % of the lifetime value t_2. The most significant uncertainty factor originates from the measured lifetime in the accelerated life test. The second most important factor is the uncertainty related to the activation energy value. In order to obtain smaller uncertainty values, larger sample sizes should be tested for longer times. This is not always easy due to limited test resources.

Already keeping the operational temperature below $T_2(^0C)$=122.5 °C could guarantee the fulfillment of the reliability requirement in a nominal situation. After utilizing Eq. (8), the new, derated temperature of $T_2^{'}(^oC) = 115.4$ °C is obtained. This value is higher than the value suggested by the new RAC derating manual [34] for silicon devices (95 °C) in severe environment. The higher allowable temperature enables to reduce the cooling

arrangements and thus can result in lower costs. Using the new derating procedure makes it possible to use the component studied in applications where components with better thermal and/or electrical performance are traditionally employed.

Table 1. The parameter values used in uncertainty analysis.

Parameter	*Nominal value*	*Uncertainty*	*Unit*
t_1	$2.3 \cdot 10^6$	$\pm 0.8 \cdot 10^6$	h
E_a	0.7	± 0.05	eV
T_1	423	± 2	K

The new derated temperature $T_2^{'}$ adds some extra conservatism to the design compared to the case when utilizing T_2, but it is necessary to somehow take into account the huge effects related to possible wrongly chosen parameter values. It is possible to utilize some other estimate for the uncertainty instead of the maximum error. One choice could be the uncertainty U given by [48]

$$U = \sqrt{\sum_{i=1}^{n} \left(\frac{\partial t_2}{\partial X_i} U_{\bar{X}_i} \right)^2} \ . \tag{11}$$

The maximum uncertainty in Eq. (6) is based on the assumption that all the uncertainty terms would add up. In case there are many parameters, this is highly improbable. When maximum uncertainties are utilized, the uncertainty estimate value is increased. Eq. (6) presents the ultimately unfortunate case. Eq. (11) is probably more 'realistic' estimate on uncertainty, as nominal uncertainty terms are utilized and the errors not necessarily add up. The choice which uncertainty estimate to use is somewhat speculative, but if one wants to guarantee that derating can guarantee acceptable performance of the component even in the most unfortunate circumstances, the maximum uncertainty of Eq. (6) is preferred.

When utilizing U, a more moderate derating would be sufficient. In this case, the derated temperature would have been $T_2^{'}(^0C)$=116.6 °C, assuming that the uncertainty terms $U_{\bar{X}_i}$

were equal to uncertainty terms $U_{\bar{X}_{i,\max}}$ of the maximum uncertainty. The difference between this estimate and the temperature obtained by utilizing the maximum uncertainty is therefore not very large.

In an ideal situation, the exact statistical distributions of each parameter value would be known and this knowledge could be used to solve the lifetime distribution of the components in the field environment. In case the lifetime prediction model has many parameters, Monte-Carlo simulation would be needed in order to be able to estimate the lifetime distribution. However, in practice, this complete information is rarely available. Therefore, the method introduced in this section is considered to be a more feasible choice.

Table 2. Uncertainty terms gained utilizing Eq. (7).

Uncertainty term	$\left\lvert\frac{\partial t_2}{\partial t_1}\right\rvert U_{\bar{t}_{1,\max}}$	$\left\lvert\frac{\partial t_2}{\partial E_a}\right\rvert U_{\bar{E}_{a,\max}}$	$\left\lvert\frac{\partial t_2}{\partial T_1}\right\rvert U_{\bar{T}_{1,\max}}$	$U_{\max}$
Value/ h	$3.1 \cdot 10^6$	$8.3 \cdot 10^5$	$5.5 \cdot 10^4$	$4.0 \cdot 10^6$

3.7 Conclusions

In this chapter, the effect of temperature derating on lifetime has been analyzed. The conventional, linear derating approach to temperature does not seem to be sensible for electronic devices. Understanding on the temperature dependency of the lifetime of electronic components should be employed, instead. This is demonstrated here by introducing a new derating method that utilizes a physical lifetime model.

The introduced derating procedure is based on the actual lifetime requirement of the component and the sole purpose of the derating procedure is to fulfill this requirement under all circumstances. When test information from semiconductor manufacturer is available, it is possible to base the derating on specific component type and failure mechanism. This data is used as an input when estimating the required temperature that fulfills the lifetime requirement. However, physical lifetime models have very large

parameter sensitivity. To avoid premature failures, it is therefore necessary to take into account the effect of uncertainties in the derating process. This is accomplished by lowering the temperature in order to guarantee the safe operation of the component population, even if the parameters deviate heavily from their nominal values.

Utilizing the new derating method, optimal operational temperature is obtained. Furthermore, cost savings due to reduction of unnecessary cooling arrangements can be gained, as operation at higher temperatures may be allowed.

4 Commentary on the IPC Surface Mount Attachment Reliability Guidelines

4.1 Introduction

The rest of this thesis concentrates on studying the effect of thermal excursions on solder joint reliability. This is started with a survey on a surface mount attachment reliability guidelines by IPC.

The Institute for Interconnecting and Packaging Electronic Circuits (IPC) has published guidelines and standards related to surface mount solder attachments. The latest standard IPC-9701 was published in 2002. In this chapter, the general methodology for creating the aforementioned documents and the related qualification requirements are reviewed and discussed. Corrections to the standards and guidelines are also proposed. The corrections are related both to the use of formulas and to inaccuracies in the units used.

4.2 Background

The Institute for Interconnecting and Packaging Electronic Circuits (IPC) has published guidelines and standards related to surface mount solder attachments based on Werner Engelmaier's work on solder joint interconnection reliability. During the early 1980s, a semi-empirical solder joint fatigue model that is the basis for both IPC-SM-785 [49] and IPC-9701 [50] documents, was created. The model is based on general fatigue life models for metals developed by Morrow [51] and Manson [52]. These models have parameters whose values may be difficult to obtain, as they are somewhat abstract in nature.

After extensive testing and curve-fitting procedures, Engelmaier could transform these representations into a model that has parameters that are easy to understand and measure, such as physical dimensions, material parameters and thermal cycling characteristics. Besides having easily applicable parameters, Engelmaier's model is relatively accurate due to the semi-empirical nature of the model. The model includes a 2-parameter Weibull

lifetime distribution. It gives a reliability prediction both for leaded and leadless solder attachments.

The model has some limitations. It should not be applied to leaded components that have very stiff or very compliant leads. It does not take into account all structural details. For example, it makes no difference whether the component lead configuration is of peripheral or area array type. Therefore, by using Engelmaier's model accurately describing the actual physical situation may not always be possible.

This chapter first describes Engelmaier's model. Then, the general methodology used in creating the IPC guidelines is described and discussed. After that, the failure-free criterion and the applicability of the guidelines are covered. Finally, some corrections related to formulas used in IPC-SM-785 are proposed [53].

4.3 Engelmaier's Model

Engelmaier's model is a semi-empirical physical model that was developed by extensive testing to modify the Coffin-Manson type solder fatigue model and give it a more easily applicable form. The Engelmaier model mostly has easily measurable parameters, such as physical dimensions and material parameters. However, not all structural details (for example, the shape of the solder ball/column) can be taken into account when using this model.

Engelmaier proposes not to use this model below 0 °C, as the failure mechanism changes from creep fatigue into elastic/plastic fatigue when cooling the solder material under 0 °C. Therefore, the use of this model in conjunction with -40…+125 °C temperature cycling or a similar test profile may not be recommended.

Engelmaier's model gives an estimate of the solder joint reliability both for leaded and leadless component packages.

The acceleration factor $A.F.(t)$ according to Engelmaier's model can be written in the form

$$A.F.(t) \cong \frac{\left(\Delta D(use)\right)^{\frac{1}{c(use)}} f_c(test)}{\left(\Delta D(test)\right)^{\frac{1}{c(test)}} f_c(use)}\ , \tag{12}$$

where *use* denotes the operational environment and *test* the accelerated (test) environment. ΔD is the cyclic hysteresis energy at complete stress relaxation, $f_c(test)$ is the temperature cycling frequency in the accelerated environment, $f_c(use)$ is the temperature cycling frequency in the operational environment and c is the fatigue ductility exponent defined by

$$c = -0.442 - 6 \cdot 10^{-4} T_{sj} + 1.74 \cdot 10^{-2} \ln\left(1 + \frac{360}{t_D}\right), \tag{13}$$

where T_{sj} is the average temperature of the solder (in Celsius degrees) and t_D (in minutes) is the half-cycle dwell (= time of the half cycle – time used in temperature transitions). Cyclic hysteresis energy ΔD receives different values depending on whether the component is leaded or without leads. In the case of a leaded component, we get

$$\Delta D = \frac{F K_D \left(L_D \Delta\alpha \Delta T_e\right)^2}{(0.917 MPa) A_{2/3} h_{s.j.}} \tag{14}$$

where F is an empirical non-ideality factor, which obtains values between 0.7..1.5, K_D is the diagonal flexural stiffness of the lead, L_D is half of the maximum distance between two solder joints, $\Delta\alpha$ is the difference of the coefficient of thermal expansion values of the component and the substrate (absolute value), ΔT_e is the equivalent cycling temperature swing, $A_{2/3}$ is 2/3 of the solder-wetted pad area, and $h_{s.j.}$ is the height of the solder joint.

In case of a component without leads, the cyclic average shear strain is

$$\Delta D = \frac{FL_D \Delta\alpha \Delta T_e}{h_{s.j.}}. \quad (15)$$

When the values for ΔD into Eq. (12) are introduced, the acceleration factor value for a component with leads is gotten

$$A.F.(t) \cong \left(\frac{FK_D}{(0{,}917MPa)A_{2/3}h_{s.j.}} \right)^{\frac{1}{c(use)}-\frac{1}{c(test)}} (L_D\Delta\alpha)^{\frac{2}{c(use)}-\frac{2}{c(test)}} \frac{(\Delta T_e(use))^{\frac{2}{c(use)}}}{(\Delta T_e(test))^{\frac{2}{c(test)}}} \frac{f_c(test)}{f_c(use)}, \quad (16)$$

and for the component without leads

$$A.F.(t) \cong \left(\frac{FL_D\Delta\alpha}{h_{s.j.}} \right)^{\frac{1}{c(use)}-\frac{1}{c(test)}} \frac{(\Delta T_e(use))^{\frac{1}{c(use)}}}{(\Delta T_e(test))^{\frac{1}{c(test)}}} \frac{f_c(test)}{f_c(use)}. \quad (17)$$

The approximate nature of Eqs. (16) and (17) should be noted. This will be discussed further in Appendix A.

4.4 The Methodology for Creating Reliability Requirements

It is a demanding task to create a general reliability requirement for components. This requirement should depend, for example, on the lifetime specification, the complexity of the product and the acceptable field return level. However, this kind of information varies depending on the application, the product, and the specification. Therefore, some kind of compromise is needed if general requirements are to be given. IPC documents have been successful in giving this kind of general level advice on the acceptance criteria of certain components in certain specific applications.

In IPC-SM-785, Table 2, both typical use conditions and suggested accelerated test profiles, and the related required thermal cycle numbers for certain specific service lives are given. Furthermore, the requirements are sub-divided based on the application area. These include consumer electronics, computers, telecommunications, commercial aircraft, automotive, space, and military avionics. For each category an acceptable risk level is

given. This is presented in terms of an acceptable percentage of failed items at the end of the lifetime of the product.

In the following sections, the above-described method to create reliability requirements is discussed.

4.4.1 Use environment

Use environments are very difficult to specify. There are several reasons for this. One major reason is that there is not much actual measured data on the use environment. Even if it exists, the question remains, which kind of data to apply. Meteorological data that is available for different regions of the globe might be used. Of course, there is a large scatter of temperature values depending on the geographical location and time of year and, usually, there is a large daily variation.

If it is considered that the temperature variation is not due to the 'outside world' but to the product's internal heat generation/cooling, then of course this kind of data should be used instead.

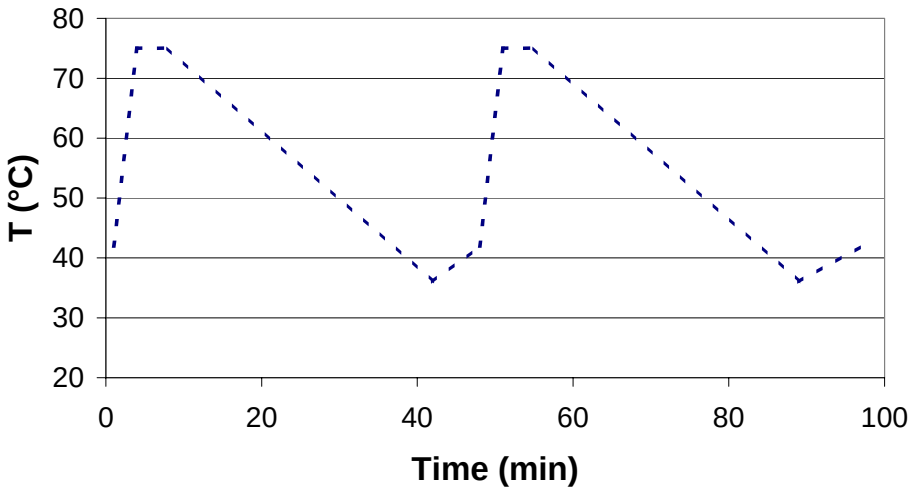

Figure 7. Average thermal profile based on measurements inside telecommunications equipment.

Also, in this case the question remains, which temperature should be measured? It is evident that there are large temperature gradients in the electronic apparatus, as certain power devices and processors are almost solely responsible for the heat generation. Therefore, it should be studied where exactly the temperature was measured and whether this data can also be considered representative in general.

Due to temperature fluctuations it is evident that some kind of approximation is needed in order to be able to reduce the complex temperature behavior into a simple thermal cycle profile. This is necessary as the temperature profile is based either on meteorological data or on in-situ electronic apparatus measurements.

The above argumentation should show that it is a complex task to select a generic thermal cycling profile representative of a whole product segment, such as telecommunications equipment. In IPC-SM-785, the typical telecommunications use condition is selected to be one daily cycle from +10 °C to +45 °C. It seems that this profile has been selected based on meteorological data. This, however, seems to be in conflict with data that has been recorded in actual telecommunications equipment. The data recorded by us shows that there are several thermal cycles per day, which are due to cooling (Figure 7). The data has been collected from a Site Support Cabinet (SSC) located in an outdoor environment in Cyberjaya in Malaysia. Therefore, it seems that the assumption for the use environment used in IPC-SM-785 is not always directly applicable.

Criticism on the selection of field environment can also be found in the literature. In [54] the field environment proposed by IPC-SM-785 for computer applications was considered to be acceptable in general level, although it was noted that the obtained temperature depended very much on the computer platform. The maximum temperature rise on PWB level varied in the range +4…+32 °C. IPC-SM-785 suggests a generic value of $\Delta T_e = 20$ °C for computers.

4.4.2 Test environment

IPC-SM-785 proposes not to use the lifetime prediction model below 0 °C, as the failure mechanism changes from creep fatigue to elastic/plastic fatigue when cooling the solder

material under 0 °C. Therefore, the IPC-SM-785 and IPC-9701 documents, both recommend to use a 0…+100 °C thermal cycling test profile. The use of a -40…+125 °C temperature cycling test profile or similar is not recommended. However, IPC-9701 also provides the acceleration factors for the three non-conforming thermal cycling profiles, such as the -40…. +125 °C profile mentioned above.

In IPC-SM-785, the required number of thermal cycles is tabulated for each application category. For example, for telecommunications equipment with a 20-year lifetime expectancy, 14,600 cycles are required if the component is leadless. Beyond 14,600 cycles, a maximum of half of the test population is allowed to fail. In IPC-9701, application-specific requirements are no longer given. However, the acceptance criterion for the preferred thermal cycling profile, 0…+100 °C is 6,000 failure-free cycles.

One obvious observation is that if one follows the requirements in the IPC documents, very long test times can be expected. 14,600 1-hour thermal cycles, as proposed by IPC-SM-785, require over 600 days to complete. Even the 6,000 failure-free cycles proposed by IPC-9701 takes 250 days, in other words, more than 8 months. Test times this long are not ideal for practical testing purposes.

The argument used in the IPC documents to limit the thermal cycling temperature excursion only to positive Celsius degrees was that the failure mode changes below 0 °C as solder material properties change. However, there is evidence that similar kinds of failure modes are obtained despite the fact that certain thermal cycling profiles may include negative Celsius degrees [54], [55].

Also, in our tests, it has been noted that when two different temperature profiles are used and one of them violates the IPC-SM-785 guideline, similar kinds of solder fatigue phenomena are noted. The temperature profiles of the tests are depicted in Figure 8. Our test vehicles consisted of 5 different solder-castellated ceramic components assembled on an FR-4 printed wiring board. The failure mode was inspected by cross-sectioning the test items, and it was identified as solder fatigue. Furthermore, the fact that the shape factor β value was not affected by the thermal cycling profile also supports the conclusion that the

failure mode was the same in both tests. Usually, if the failure mode changes, so does the shape factor value. If the failure mode remains the same, the β value remains the same as well. Only one component (B) indicates any change of the β value. In this case, a significantly smaller β value in Test 2 compared to Test 1 was obtained. This can, however, be explained by the fact that only a few components (4 out of 15) actually failed during Test 2, and therefore there were only a few data points available. This fact adds uncertainty to the Weibull parameters obtained after the curve fitting, and therefore the β value obtained may not be a very representative one.

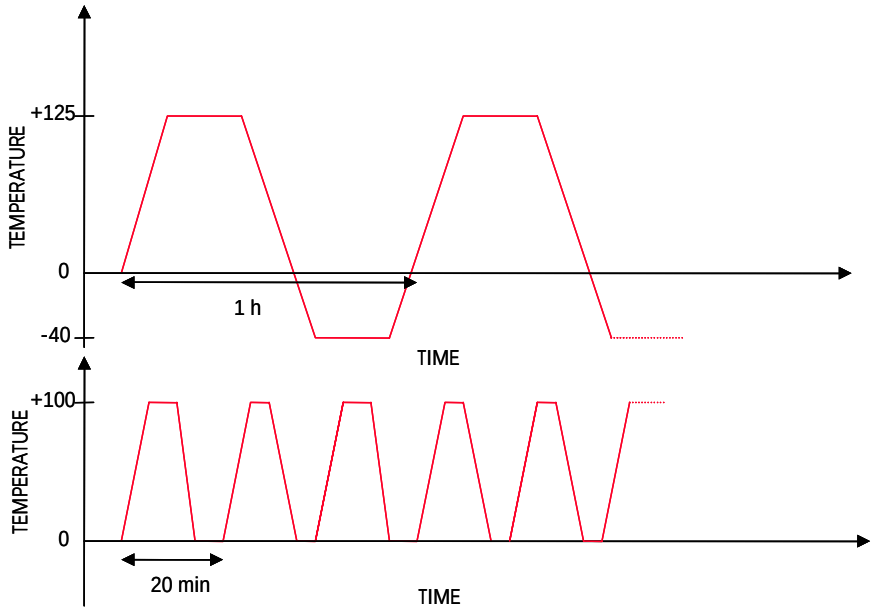

Figure 8. Two thermal cycling profiles used in the reliability tests.

Moreover, it was noted that there was a clear correlation between the mean number of cycles in the two tests (Table 3). This fact can be easily seen when looking at the ratio η_2 / η_1, where η_2, η_1 are the characteristic lifetimes for the test profiles 2 and 1, respectively. The ratio obtained values from ca. 3.3…3.9. This indicates that even highly accelerated tests may be correlated easily.

Table 3. Test results of the reliability tests using two temperature profiles.

Component	*Test 1, -40…+125 °C, 1-hour cycle*	*Test 2, 0…+100 °C, 20-minutes cycle*	η_2 / η_1
A	η_1=609, β_1=7.8	η_2=1988, β_2=8.3	3.27
B	η_1=1072, β_1=8.9	η_2 =4210, β_2=3.5	3.93
C	η_1=612, β_1=9.1	η_2 =1919, β_2=6.9	3.13
D	η_1=663, β_1=5.4	η_2=2228, β_2=5.9	3.38
E	η_1=365, β_1=10.1	η_2 =1277, β_2=11.1	3.50

4.4.3 Assumptions within the requirements

The IPC-SM-785 and IPC-9701 documents both give solid guidelines on the minimum number of cycles until a certain share of the test items is allowed to fail. In Table 2 in IPC-SM-785 these numbers are clearly stated. One may, however, wonder how these numbers have been obtained, as this is not explicitly explained in the documents. It is not a very difficult task to discover the procedure after some consideration. In this section, the procedure is described: The test requirement is based on the field reliability requirement. This is presented as an acceptable share of failed items at the end of the lifetime of the component. Both the acceptable share of failed items and the lifetime of the component are dependent on the use category. For example, in the telecommunications use category it is assumed that the lifetime is either 7 or 20 years, and that an acceptable share of failed items at the end of the lifetime is 0.01%.

Table 4. Acceleration factor values used when creating IPC-SM-785 thermal cycle requirements.

Use category	*Acceleration factor, lifetime assumption 1*	*Acceleration factor, lifetime assumption 2*	*Attachment type, leadless (ll), leaded (ld)*
Consumer	3.3	3.0	ll
	9.5	8.7	ld
Computer	15.9	15.0	ll
	340.1	320.2	ld
Telecomm	5.0	4.6	ll
	51.9	47.1	ld
Aircraft	21.2	16.0	ll
	800.8	600.6	ld
Automotive	2.3	1.9	ll
	7.3	6.0	ld
Military ground & ship	0.7	0.6	ll
	2.3	2.0	ld
Space, leo	120.5*)	12.2	ll
	149.8	150.4	ld
Space, geo	4.2	3.5	ll
	39.4	33.1	ld
Military avionics, a	3.8	6.9	ll
	104.8	108.5	ld
Automotive, under hood	1.5	1.4	ll
	1.0	0.9	ld

*) The correct value should be 12.1. 120.5 is a value that is gained from the reliability requirement given by the IPC-SM-785, Table 2.

This may be a reasonable assumption, but it can be argued that some other values might have been chosen as well. This is especially true when it comes to the share of failed items, as 0.01% seems to be quite a tough requirement. Usually a 1-3% limit is used.

After the field requirement is selected, this requirement is converted into a test requirement. There are two things that must be considered: first, the test requirement is for 50% of failed items instead of, for example, the 0.01% requirement for the field environment. Secondly, the acceleration effect of the test environment compared to the actual field environment must be taken into account.

To take into account the translation along the Weibull distribution from x% to 50%, the number of cycles in the field requirement must be multiplied by the factor:

$$\left(\frac{\ln 0.5}{\ln(1-0.01x)}\right)^{\frac{1}{\beta}}. \tag{18}$$

This factor gives the value of 9.12, assuming that x =0.01 and β=4 (This is the assumption for leadless components in IPC-SM-785. For leaded components β=2).

The acceleration factor used to convert the field requirement into a test requirement is not stated in the documentation, but it can be easily deduced when looking at the requirements. The number of cycles in the field environment must be divided by the acceleration factor used in order to obtain the number of cycles in the test environment.

When using both of the above transformations, the acceleration factor is obtained for the 20-year lifetime telecommunications application having a test requirement of 14,600 cycles as follows: $A.F.(N)=((365\cdot 20)\cdot 9.12)/14{,}600=4.56$. This acceleration factor value is quite reasonable, but it should, however, be remembered that there is no generic acceleration factor value. It always depends on the specific component used, the attachment type and even on the printed wiring board and its characteristics. Moreover, the shape factor β values that IPC-SM-785 proposes are somewhat smaller compared to the values often recorded both in the literature [56] and our tests (cf. Table 1). As values given

by Eq. (18) are very dependent on the shape factor value, the use of arbitrary values has a big effect on the requirement to be created. For example, if the true shape parameter value is β=10, then the factor defined in Eq. (18) would be 2.42. This results in an almost 4 times larger thermal cycle test requirement than the one given in IPC-SM-785. Therefore, it is evident that the IPC-SM-785 requirements in Table 2 should not be taken as such, but that the true statistical behavior of the component population should be investigated and only after that is it possible to use an Eq. (18) type of translation along the Weibull distribution.

For the sake of thoroughness, the acceleration factors that were used in the creation of the IPC-SM-785 document, Table 2, are deduced and tabulated in Table 2. In most cases, the acceleration factor is for the test environment 0…+100 °C, 1-hour cycle. It is noted that there is a wide variety of acceleration factor values. In general, they seem to be acceptable – keeping in mind, once again, that in principle no generic acceleration factor values exist. The reader familiar with a specific use category should now be able to judge if the acceleration factor values are relevant or if other values might be more representative. There is one misspelling in the space low earth orbit (leo) category requirement for a 5-year lifetime in the original document. This results in an acceleration factor value of 120.5 instead of 12.1. To correct this, the 5,900-cycle requirement in IPC-SM-785 should be changed to 59,000 cycles.

4.4.4 The Failure-Free Cycles Criterion

The required number of test cycles given in the IPC documents is very large in many use categories. This is mostly due to the relatively mild test environment (0…+100 °C, 1-hour cycle). The other explanation for the long test times is that it is required that the test should be continued until 50% of the items have failed. Long test times are not very practical, especially when considering the time pressure in the qualification of new components and products.

In order to shorten test times, Equation (17) in the IPC-SM-785 document gives a way to turn the 50% requirement into a failure-free requirement. This requirement $N(test,0\%)$ will result in shorter test times compared to $N(test,50\%)$. The Eq. (17) is

discussed in more detail in Appendix A. The use of the failure-free criterion may lead to pitfalls related to statistical considerations. For example, it may be that a poor quality component happens to be selected for the test population. Then the whole population will be judged (rejected) based on one single component that, in actual fact, is not representative of the full component population. If the test was continued after the first failure, then there would be a possibility to look at the full component population and no false judgment, based on one single weak component, would be made. On the other hand, as many times there is no possibility to test statistically, meaningful sample sizes, there is a risk that components of exceptionally high quality only are selected for the test population. In this case, the first failure indication would be recorded too late and the test result would be a non-justified ‘pass’.

4.5 The Applicability of the Guidelines

Reliability considerations are performed at three levels at least: at component level, at PWB level and at product/system level. The IPC guidelines are solely related to component level considerations. However, it would be very useful if component level reliability data could also somehow be utilized in higher hierarchy level reliability evaluations.

Currently, the component level reliability requirement given by the IPC documents is not affected by the complexity or the architecture of the product. This means that any possible redundancy is not taken into account. It is just assumed that an acceptable share of failed items at the end of the product’s lifetime is a well-enough defined link to the higher-level reliability considerations. However, as discussed earlier, the acceptable share of failed items in the IPC documents is not necessarily representative in all cases.

An alternative approach would be to turn the test results into figures that can also be easily applied to the PWB and product level reliability considerations. This can be done, for example, by applying the reliability block diagram (RBD) technique [57], where the interconnection reliability of the component would be one additional block in the total reliability calculations. RBD is a well-known technique, and the solution to the diagrams

can be found either in closed-form, if the product is not very complex, or by simulation if the closed-form solution is not easy to obtain.

A clear advantage of using RBD is that the whole product can be analyzed simultaneously against the *product* reliability target, not only against a fixed component level requirement. It is also possible to take into account the fact that one single component or multiple similar components are used. Furthermore, the redundant elements may be considered. One additional benefit is that availability and maintenance can be evaluated as well. This is not possible if a fixed criterion, such as those given by the IPC guidelines, is applied.

One approach to analyze PWB level reliability is to utilize calcePWA software developed by Maryland University [58]. This software enables to study several possible failure mechanisms that may occur, depending on the load conditions the PWB assembly experiences. The software includes product modeling, stress assessment, and failure modeling capabilities. The user is supported with material, environmental profile, and failure models. It is also possible to update these databases.

The main purpose of this software is to highlight design flaws in an early development phase. The software serves this purpose well. However, as physical lifetime models are sensitive to parameter values, good care must taken if accurate lifetime predictions are expected. The generic values, such as material properties, given by the software may not always be accurate. The user should confirm that the values selected present the actual situation before running the simulation tool. Another word of caution is related to the models utilized. For example, in case of interconnection failure assessment first order models are employed. More refined tools, such as finite element simulators, are not utilized. This fact results in limited capabilities to take into account structural details, and in some cases, limited prediction accuracy. However, as this software tool is primarily meant to be applied in an early product development phase, it is expected that it serves this purpose well enough.

4.6 Discussion

In this chapter, the IPC guidelines for solder attachment are reviewed and discussed. In particular, the thermal cycling test requirements are discussed. The assumptions used in creating the requirements are revealed. They include assumptions on the use environment, the acceptable share of failed items at the end of the product's lifetime, and the shape parameter value of the Weibull distribution. In general, the values used seem to be in the range typically recorded. However, in some cases it may be argued that not all selections are valid. For example, the use environment and the resulting acceleration factor for telecommunications equipment might have been chosen differently. Moreover, the pre-selected Weibull shape parameter values seem to be too small in the light of our experience. Shape factor values that are too small give rise to a too stringent reliability requirement.

At a more philosophical level, it might be argued as to whether generic reliability requirements with a fixed thermal cycle count should be given at all. This is because there are several parameters that have a very large impact on the requirements. Therefore, even a small deviation in the assumed parameter values may result in a much altered requirement level. However, generally accepted guidelines are useful as they provide common rules. Having common rules makes communication between component suppliers and customers easier, as there is a mutual understanding on the reliability requirement on which the components should conform.

In order to obtain the best accuracy level, the acceptance of a component should be considered case-by-case, and not based on generic guidelines. By doing so, accurate parameter values can be utilized. They include the acceleration factor value for a specific component and a specific use environment. The acceleration factor value may be obtained, for example, with analytical models, such as Engelmaier's model, or with thermo-mechanical simulations. Also, if the Weibull shape parameter value used is from the tests actually run on the component, the true quality distribution of the component is utilized in the creation of the requirement.

Creating component-specific reliability requirements is a very demanding task. Only trained persons are able to perform the testing, the statistical analysis of the results and the lifetime prediction. Therefore, creating component-specific requirements is both time-consuming and labor-intensive. For those who do not have the capability or the time needed, the generic requirements given by the IPC guidelines are a good alternative.

The test profile suggested in the IPC documents is relatively mild and results in very long test times. There is an effort to compensate for this by concluding the test after the first failure in the test. This approach raises certain statistics-related concerns. Also, it can be shown that when using a more stringent test profile the failure mechanism may not always change, although the IPC guidelines claim that this is so.

One shortcoming in the requirements given is that they do not depend on the product's complexity, the architecture of the product and the number of components used. In order to obtain a better link to the product level reliability considerations, a reliability block diagram technique in conjunction with the interconnection reliability assessment could be used. The interconnection reliability of a single component would be an additional reliability block.

Finally, some errors found in the IPC documents are rectified in Appendix A.

5 Analysis of Ceramic Leadless Components

5.1 Introduction

In the previous chapter, a handbook-based approach of setting 2nd level interconnection reliability requirements was reviewed. In this chapter, an alternative, component-specific approach is discussed. The approach is demonstrated by actual test data on five leadless ceramic components. These components are tested and the results are interpreted by utilizing a component-specific reliability requirement tool created for this purpose. The analysis starts with thermal cycling tests that are run using two temperature profiles: –40…+125 °C 1-hour cycle and 0…+100 °C 20-minutes cycle. The test results are interpreted with statistical analysis combined with Finite Element Analysis (FEA).

The second part of this chapter consists of the interpretation of the test results utilizing the tool created. By using the tool it is possible to evaluate if the test result is compatible with the component level reliability requirement given.

5.2 Background

Ceramic leadless chip carriers (CLLCC) have several desired properties: they have high thermal conductivity, it is possible to create hermetic cavities inside them, and the size of such components can be small, as both the footprint and the thickness of the packages is small. However, due to coefficient of thermal expansion (CTE) mismatch between the ceramic components and the organic printed wiring boards (PWB), there is a reliability risk related to the second level interconnections. This risk is pronounced in case of CLLCCs as this component type does not have any leads that would add some flexibility to the interconnections.

The reliability issues related to CLLCC type components have already been studied for some time [59]. In the mid-1980s, it was recognized that the solder column size and shape have a profound effect on the reliability [60]. Studies on SnPb solder materials are known from the literature, but lately studies on lead-free solder materials have also been published [61], [62], [63], [64], [65].

In this chapter, five leadless ceramic components are tested and the results are interpreted by utilizing a method created for this purpose. The analysis starts with thermal cycling tests that are run using two temperature profiles: –40…+125 °C 1-hour cycle and 0…+100 °C 20-minutes cycle. After the tests are run, failure analysis is performed. The lifetime data is analyzed by utilizing Weibull distribution. In the Weibull analysis phase, it is also studied if the test data contains some early failures or if the test data seems to consist purely of components in the wear-out region. Then the acceleration factor that relates the test result and the field lifetime is calculated by utilizing Finite Element Analysis (FEA).

The second part of this chapter consists of the interpretation of the test results by utilizing a tool created for this purpose. The tool enables taking into account several aspects of the test results, such as, how many items were tested, what was the share of failed items, what is the lifetime requirement of the component and what was the test profile used.

5.3 Test Setup

Thermal cycling tests were run employing two cycle profiles [66]: the first one was a –40…+125 °C test with 1-hour cycle time and the second one was a 0…+100 °C test with a cycle time of 20 minutes.

In Figure 8, Section 4.4.2, the test profiles are depicted. It is noted that in addition to having a smaller temperature excursion, a thermal cycle in 0…+100 °C test is three times shorter than the one in –40…+125 °C test. The smaller temperature excursion of the 0…+100 °C test is expected to alleviate the test compared to –40…+125 °C, but the higher cyclic frequency will accelerate the fatigue phenomena and therefore may compensate for the smaller temperature swing.

The idea behind using two temperature profiles was to test if the –40…+125 °C test will create failure mechanisms different to the ones observed in the 0…100 °C test. It has sometimes been claimed that this would be the case [49]. However, opposite results have also been recorded in the literature [67].

5.4 Test Vehicles

The test board used was a FR-4 board (CTE=16…21 ppm/°C) with the OSP surface finish. The thickness of the board was 1.6 mm (8 layers).

The test vehicles consisted of five component types. Four of them were IF frequency SAW filters and one was a crystal clock oscillator. Each component had two manufacturers except for one SAW filter, which had three manufacturers. All component packages were manufactured of alumina (CTE=7 ppm/°C) and they were assembled on a PWB by using castellated solder attachments. Due to the interconnection structure the amount of solder material between the component and the PWB was small (typically 50…70 microns). Solder fillets on the side of the components consists of a thicker layer of solder material (200…400 microns).

In Table 5, components, component package types and component manufacturers are listed.

Table 5. Ceramic test vehicles.

Component	*Package*	*Manufacturers*
a, SAW IF filter	QCC12	I, II
b, SAW IF filter	DCC18	I, II, III
c, SAW IF filter	QCC12B	II, III
d, Crystal clock oscillator	2560NK component	IV, V
e, SAW IF filter	QCC10B	II, III

The DCC18 package was of dual-in-line (DIL) type, whereas all others were of quad type, in other words, there were solder joints on all four sides of the component. The crystal oscillator had solder contacts at four corners.

It should be noted that the component package codes are according to the manufacturer datasheets. The detailed geometry measures and the details on the components can be found in the manufacturers' Web pages.

5.5 Test Results

During the tests, the test vehicles were continuously monitored using an event detector apparatus. Failure events could therefore be accurately recorded. The –40…+125 °C test lasted for 1,000 cycles, whereas 0…+100 °C test continued for 3,008 cycles. After completing the tests, a thorough failure analysis, including cross sectioning and X-ray inspection, was performed.

The test results were analyzed by using a 2-parameter Weibull distribution. First, it was attempted to fit components of the same type from different vendors as one population, but it became apparent that there were quite large performance deviations between components from different manufacturers. Therefore, the components from different manufacturers had to be analyzed separately; otherwise the convergence of the fit would have been quite poor. Some apparent early failures were taken out from the test results before the Weibull distribution was fitted to the test results.

5.6 Statistical Analysis of the Results

2-parameter Weibull distribution was used as a default fitting function. This selection was motivated by the good fit of our experimental data. This will be shown in this section. Similar, good fit results have been recorded also in case of lead-free solder materials [63]. Another obvious choice, instead of 2-parameter Weibull distribution, would have been 3-parameter Weibull distribution. This is due to the fact that in case of wear-out, an incubation period without failures is expected [5]. Therefore, 3-parameter Weibull distribution, with the failure-free period of time γ included, would have been an appropriate choice. A more detailed discussion on the selection of the statistical distribution functions can be found in Section 7.7.

In most cases, the selection of 2-parameter Weibull distribution proved to be acceptable. However, in some cases, early failures occurred and their existence did complicate the analysis somewhat. Even small amounts of early failures can deteriorate the convergence of the fitting, especially when small sample sizes are considered. In order to gain a better fit, it was necessary to distinguish early failures from the rest of the population. However, this was not a straightforward task to accomplish. In the literature, some methods on how to analyze results containing data consisting of the 'main' population and the 'freak' population are presented, cf., for example, [68], [69] for suspended data technique and [70] for infant mortality *distribution* parameter estimation methods. Because in this case only *individual* freak data points, and not multiple data points, were recorded, the methods mentioned earlier could not be applied. Instead, some new method was needed in order to distinguish the freak data points from the main population and to gain an acceptable curve fitting result.

In most cases, it was easy to visually recognize the apparent deviations from the main population, but some general, 'neutral' criterion was still needed. For this purpose, a term called Comparison Ratio ($C.R.$) was introduced. This term gives an indication if the data point representing the first failure fits well the main population. The definition of the Comparison Ratio ($C.R.$) is

$$C.R. = \frac{N_{1/n_t}}{N_{1st\ failure}}\ , \tag{19}$$

where N_{1/n_t} is the number of cycles to first failure according to Weibull distribution (or some other distribution) after fitting the whole data to Weibull function, and $N_{1st\ failure}$ is the number of cycles to first failure observed in the test. The rule of thumb selected was that the curve fitting is considered successful, if $C.R.$ lies in the range 0.9…1.1. As an example, the data with one early failure and the Weibull fit, functioning with and without the early failure data point is depicted in Figure 9.

There was one component (component *c*, from manufacturer II) whose test population fitted relatively poorly the 2-parameter Weibull distribution. This is probably due to some

other underlying statistical distribution that the component population might have. In this case, a low value of *C.R.* factor was related to a poorly chosen distribution function, and not due to the inclusion of early failure data. This was verified by utilizing 3-parameter Weibull distribution instead of 2-parameter Weibull distribution (Table 6), after which larger correlation coefficient ρ indicated a better convergence (-40…+125 °C test, ρ: 0.9366->0.9925; 0…+100 °C test, ρ: 0.9502->0.9884).

Table 6. 3-parameter fit results of component *c*, vendor II.

3-parameter Weibull parameters	*-40…+125 °C test*	*0…+100 °C test*
γ	454	1273
β	1.8	1.8
η	143	598

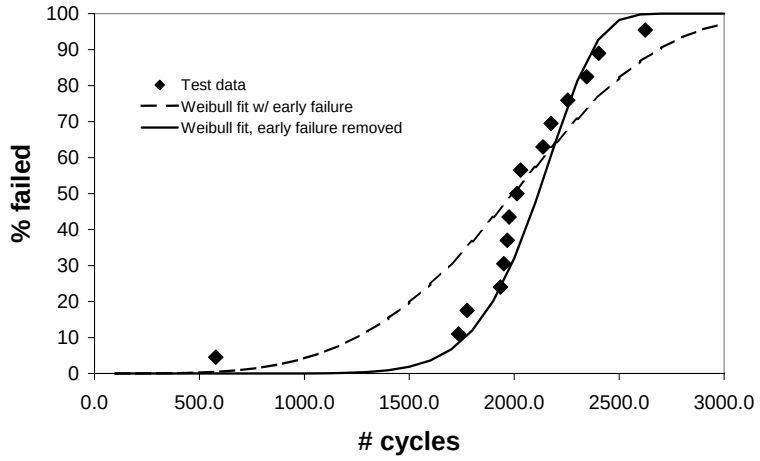

Figure 9. Test data with early failure data point and the effect of that in the fitting of the 2-parameter Weibull distribution.

Sometimes it has been argued, that the use of 2-parameter Weibull distribution is not in line with historical failure data [71]. Also, it has been claimed that the use of this distribution may result in false conclusions related to the reliability of the component, especially when small values of cumulative distribution function are concerned. However, in our case, the 2-parameter Weibull distribution was successful in explaining the underlying component statistical behavior (Table 31, in Appendix B).

Looking at Table 31, one can conclude that the failure mechanism is not changing due to different thermal cycle test profiles. This is due to the fact that the 2-parameter Weibull distribution shape parameter β is not affected by the different test profiles. The failure analysis further confirms this conclusion as the failure mechanism in the case of both test profiles was recognized as solder fatigue.

It looks like that the characteristic lifetimes in terms of number of thermal cycles scale by a factor of ca. 3. This means that it takes approximately 3 times more cycles in 0…+100 °C compared to –40…+125 °C until the same share of components has failed. However, as the cycle time in the case of the 0…+100 °C test was only 20 minutes and one cycle in the –40…+125 °C test lasted for one hour, the two tests induce failures almost simultaneously time-wise.

The performance differences between the vendors proved to be significant. Although virtually identical components from different manufacturers were studied, lifetime differences of up to a factor of 2 could be noticed. The reason for the performance difference probably lies in the different solder column shapes and different amount of solder in the interconnection area. This will be discussed in more detail in Section 6.3.2. In Figure 10, the solder columns of two virtually identical components (*e*) from two vendors are depicted. The difference in the solder width W is clearly visible.

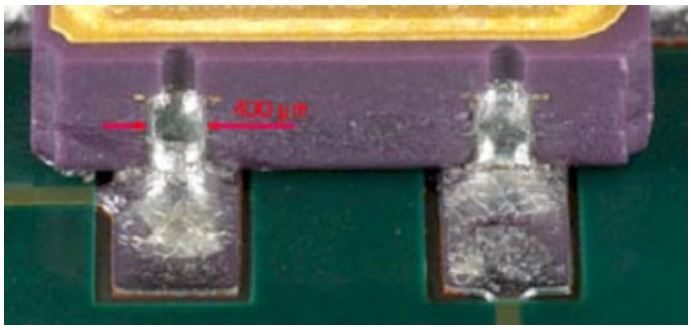

a)

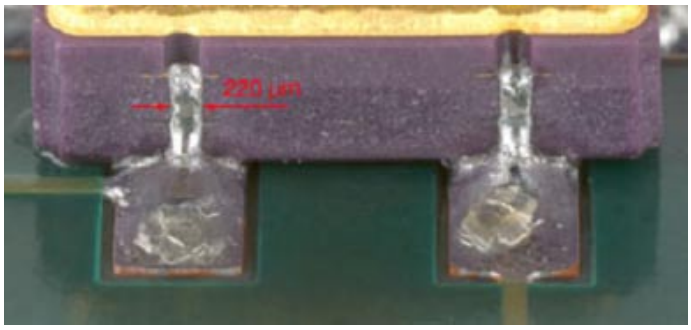

b)

Figure 10. Solder interconnections of two identical components (*e*) from two different vendors. a) Vendor: II. W=400 microns. b) Vendor: III. W=220 microns.

5.7 Finite Element Analysis

Finite Element Analysis was run on each of the test vehicle structures. Test data was used to calibrate the FEA model. Four thermal profiles were selected to be able to study the effect of field environment, which the components are exposed to. Those are listed in Table 7.

Table 7. Test and field environment profiles.

	Cycle profile					
	Test -40…+125 ℃	*Test 0…+100 ℃*	*Fast soft*	*Fast hard*	*Day soft*	*Day hard*
Start temp. [°C]	25	25	27.5	37.5	30	50
Max. temp. [°C]	125	100	37.5	75	40	80
Min. temp. [°C]	-40	0	17.5	40	20	20
Time min->max [min]	15	5	8	5	360	360
Dwell time at max [min]	15	5	43	5	360	360
Time max->min [min]	15	5	10	34	360	360
Dwell time at min [min]	15	5	3	5	360	360

Structural details were carefully modeled. For example, solder pad sizes and solder fillet geometries were input separately for each component. The acceleration factor values obtained are listed in Table 8.

It is noted that there are significant differences in $A.F.(N)$ values depending on the component type and the field environment the components are about to be subjected to.

Table 8. Acceleration factors obtained by FEA modeling [82].

	$A.F.(N)$ $-40\ldots+125\,℃$				$A.F.(N)$ $0\ldots+100\,℃$			
Component	Fast soft	Fast hard	Day soft	Day hard	Fast soft	Fast hard	Day soft	Day hard
a	167.6	44.6	122.4	5.4	66.0	17.6	48.2	2.1
b	84.6	25.1	64.9	7.5	27.6	8.2	21.1	2.5
c	80.8	20.6	55.1	6.1	29.7	7.6	20.3	2.2
d	48.8	13.8	36.5	5.0	21.8	6.1	16.3	2.2
e	175.0	48.8	128.4	7.3	59.0	16.4	43.2	2.5

5.8 Interpretation Tool

In order to validate designs prior to the product launch, the test vehicles are tested. To take into account the acceleration of degradation processes due to test severity, acceleration factor $A.F.(N)$ is used. It converts the test result N_{test} into a number of cycles N_{field} in the field environment

$$A.F.(N) = \frac{N_{field}}{N_{test}}. \tag{20}$$

In order to obtain the acceleration factor value, there are a few options: some analytical models, such as Engelmaier's model [115] and Norris-Landzberg's model [72]. It is also possible to use Finite Element Analysis (FEA) simulations in order to obtain the acceleration factor value, as we did in the previous section.

The acceleration factor values for a leadless assembly are typically in the range of 1…1000, but however, they depend on the actual test vehicle (geometry, physical properties, etc.), the physical properties related to the assembly, the test setup, and the expected field environment. In Figure 11, some typical test and field environments and the

factors relating those to each other are seen. -40…+125 °C temperature cycle is quite often used as a validation test for new technologies [50]. IPC-SM-785 [49] proposes a 0…+100 °C thermal cycle to be used, instead.

The differences in test profiles result in different test results (in other words, Acceleration factor 1 and Acceleration factor 2 obtain unequal values). Therefore, it seems that there is a need for a conversion factor that relates the test results from different test profiles. For practical engineering purposes, introducing a conversion factor is useful. However, care must be taken that the failure mechanism is the same in both tests before utilizing the conversion factor concept.

Let's define the conversion factor ($C.F.(N)$) as

$$C.F.(N) = \frac{\eta_{test2}}{\eta_{test1}} \tag{21}$$

where $\eta_{test2}, \eta_{test1}$ are the characteristic lifetimes (Weibull parameter, which is equivalent to the number of cycles when 63.2% of the samples being tested have failed) obtained in two different tests. In case some other statistical distribution is utilized, the relevant lifetime parameter related to the distribution should be employed, instead.

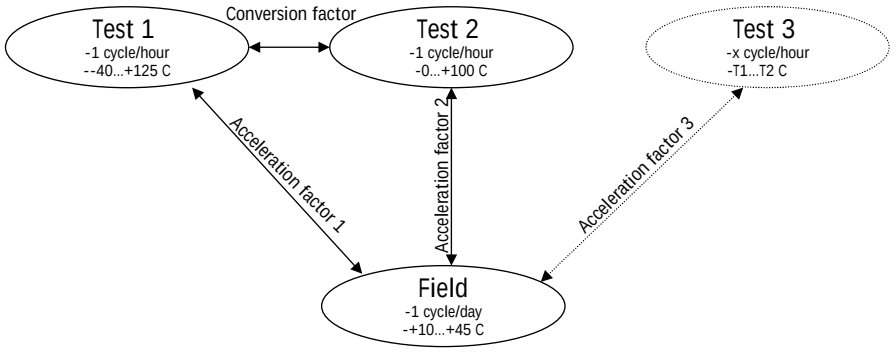

Figure 11. Factors relating the test and the field lifetime performance. Field environment is adapted from the IPC-SM-785 guideline [49].

Tests are typically run until at least half of the test vehicles have failed. In the field environment, the acceptable risk level (in other words, the share of failed components) can vary, depending on how crucial the component is and how stringent the reliability requirement is. Therefore, it is evident that the risk level must be taken into account when comparing test results and field reliability requirements. This can be accomplished by introducing a statistical factor $S.F.$

$$S.F. = \left(\frac{\ln\left(1 - \frac{p+1}{n_t}\right)}{\ln(1-0.01x)} \right)^{\frac{1}{\beta}}, \tag{22}$$

where p is the number of failed devices in the test, n_t is the total number of devices tested, x is the maximum allowable percentage of failed devices in the field environment, and β is the shape parameter of the 2-parameter Weibull distribution.

Based on the above-introduced factors, let's define the minimum number of thermal cycles $N(p/n_t)$ in a test that the field environment reliability goal requires as

$$N(p/n_t) = \frac{N_{field}(x\%) \cdot S.F.}{A.F.(N) \cdot C.F.(N)}, \tag{23}$$

where $N_{field}(x\%)$ is the number of thermal cycles that the devices are addressed in the field environment after which $x\%$ failures is acceptable. $A.F.(N)$, $C.F.(N)$ and $S.F.$ have been defined earlier by Eqs. (20), (21) and (22), respectively.

Now, it is possible to check arbitrary test results against the field environment reliability requirement $N_{field}(x\%)$.

An example: Let's assume that the reliability requirement in the field environment is that a maximum of 1% failed components is allowable after 10 years of operation. If, assuming that there is 1 daily thermal cycle, the total number of thermal cycles the component

experiences in the field environment during 10 years time is $N_{field}(1\%) = 3650$. After performing a –40…+125 °C test, the following results are obtained: η=820 cycles and β=7. Furthermore, we know that the acceleration factor of the 0…+100 °C test is $A.F.(N)$=5 and that the conversion factor between the 0…+100 °C and the -40…+125 °C tests is $C.F.(N)$=3. Then, we obtain $S.F.$=1.94, and from Eq. (23), $N(63.2\%)$=471 cycles. Because $\eta > N(63.2\%)$, the test result can be considered as acceptable.

5.9 Interpretation of the Test Results

In the previous section, we created a method to correlate the thermal cycling test results with the reliability requirement for the field environment. By using this methodology it is possible to judge if components are applicable in certain field environments with certain reliability requirements. Four different field environments were already introduced earlier in Table 7 and the related acceleration factors for each of the components were calculated (Table 8). Furthermore, if we assume that the component should last for 10 years and that at the end of its lifetime $x = 1\%$ failed devices is acceptable, we can create the requirement data $N(63.2\%)$ according to Eq. (23) shown in Table 9. The ratio of the characteristic lifetime value η actually recorded in the test and the required characteristic lifetime $N(63.2\%)$ is presented in parenthesis in Table 9. This gives insight on how the performance recorded in the test compares to the required one. As the acceleration factors for both test profiles were known, the use of a conversion factor in this case was not needed ($C.F.(N)$=1).

It is noted that only if the field environment is of the ‘day soft’ type, test results of the components can be considered acceptable. In many cases there is a considerable deviation from the required performance.

Table 9. Applicability of tested components in different use environments with 10-years lifetime requirement. 1%-failed items at the end of the lifetime is acceptable.

	$N(63.2\%)$ ($\eta / N(63.2\%)$, %), -40…+125 ℃				$N(63.2\%)$ ($\eta / N(63.2\%)$, %), 0…+100 ℃			
Component	Fast soft	Fast hard	Day soft	Day hard	Fast soft	Fast hard	Day soft	Day hard
a	778(19)	3822(4)	47(306)	1074(13)	1867(33)	9150(7)	114(544)	2608(24)
b	1799(17)	7923(4)	104(292)	902(34)	11162(13)	49091(3)	649(219)	5477(26)
c	1467(42)	7521(8)	96(640)	864(71)	5407(53)	27611(10)	352(811)	3244(88)
d	4098(17)	18933(4)	243(291)	1777(40)	9334(35)	43587(7)	555(581)	4111(79)
e	785(44)	3677(9)	48(715)	836(41)	2181(70)	10254(15)	132(1149)	2288(66)

5.10 The Effect of Mixed Field Environments

5.10.1 Background

In the previous section, the applicability of components in one individual field environment was discussed. In the following, a more realistic case, where the component population is addressed to a mixture of field environments, is studied. The ‘mixture of environments’ can be interpreted in such a way that the component population is divided into groups that are placed in different geographical locations for their full lifetime. The underlying principle is to study the environmental effects on reliability in a case, when the field environment is not the same for the whole population.

The environment that an electronic component experiences varies depending on its geographical location, the mechanics of the product, the cooling approach used and the amount of time the component is active/powered. The field environment variation can be taken into account using different approaches. Based on the environmental information available, field environment profiles [73], [74], [75] and the related acceleration factors [6]

have been represented by their typical values. The overly averaged data may, however, result in reliability predictions with poor accuracy. As there is a huge variation within and between different field environments, it would be *natural to consider the field environments as a set of different environments, instead of having one generic environment*. An approach on how to handle this will be introduced in the following Sections, 5.10.3-5.10.4.

5.10.2 Mixture-of-Distributions Concept

Mixture-of-distributions concept is well known in the literature [76]. In their paper, Hansen and Thyregod discuss it as a phenomenon as such and in conjunction with competing-risks concept. Mixture concept is applied in case of early failures, as it is believed that the component population may be *divided* into two; standard components and those with initial defects. With the mixture concept the reliability behavior of the whole population may be handled if the underlying statistical distributions of the two sub-populations are known. All the statistical functions have been derived in the reference.

Wear-out has been studied by utilizing the competing risk concept, instead. According to [76], different wear-out mechanisms are expected to follow different statistical distributions. In case of competing risks, the competing failure mechanisms are operating on *all* the components simultaneously. The mathematical treatment is based on the utilization of competing risk composition. Finally, combination of mixtures and competing risks are established and their use is demonstrated.

In the following, the mixture-of-distributions concept will be applied for the first time in case of multiple field environments. The *failure mechanism* is assumed to be *the same* in the field environments, but the failures are expected to take place at different times. The mixture of distributions is applied in case of wear-out in Section 5.10.3. In Section 5.10.4, random failures in multiple field environments scenario are studied.

5.10.3 Mixed Environment Analysis

In the following section, the methodology to account for the mixed population with 'standard components' and those with initial defects [76] is introduced to a case where components are reliability-wise similar. It is assumed that *only one failure mechanism* exists and that the components are used in *several, different field environments*.

Let's assume that products having the component under consideration are placed in multiple, different field environments. Furthermore, let's mark the share of components placed in each field environment as p_i. Then according to [76] the density distribution function $f(t)$, the cumulative distribution function $F(t)$, and the reliability function $R(t)$ for the whole component population may be described by

$$f(t) = \sum_{i=1}^{n} p_i f_i(t) \tag{24}$$

$$F(t) = \sum_{i=1}^{n} p_i F_i(t) \tag{25}$$

$$R(t) = \sum_{i=1}^{n} p_i R_i(t), \tag{26}$$

where terms with indexes *i* are related to functions of n field environment categories. The probability density function $f_i(t)$ in case of 2-parameter Weibull distribution can be described as

$$f_i = \frac{\beta}{(\eta \cdot A.F._i)^{\beta}} \cdot t^{\beta-1} \cdot e^{-\left(\frac{t}{\eta \cdot A.F._i}\right)^{\beta}}. \tag{27}$$

The reliability function for each environment category can be written as

$$R_i(t) = e^{-\left(\frac{t}{A.F._i \cdot \eta}\right)^{\beta}}, \tag{28}$$

and the cumulative distribution function $F(t)_i$ obtains the value

$$F_i(t) = 1 - R_i(t), \tag{29}$$

where $A.F._i$ is the acceleration factor related to a certain field environment. η and β are obtained after fitting the 2-parameter Weibull distribution to the test data.

The hazard rate $h(t)$ can be presented as

$$h(t) = \sum_{i=1}^{n} w_i h_i(t) \tag{30}$$

with weight functions $w_i(t)$ defined as

$$w_i = \frac{p_i R_i(t)}{R(t)}, \tag{31}$$

where p_i is the fraction on items placed in environment *i*.

An example: Let's study the component *a* from vendor I. The thermal cycling result from –40…+125 °C indicated that the Weibull parameters are η =609 cycles and β =7.8. The related acceleration factors are listed in Table 8. Keeping in mind the different cycle lengths and using Eqs. (26) and (28), the data in Figure 12 is obtained.

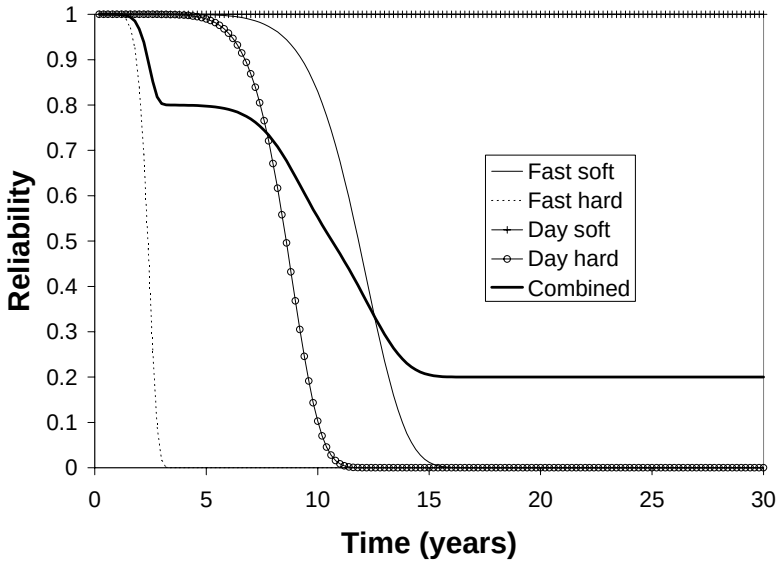

Figure 12. The reliability functions for different field environments and the combined reliability function taking into account the whole population placed in different field environments.

In Figure 12, it was assumed that 40% of devices would be put in a 'Fast soft' field environment, while the remaining 60% of the components would be placed in three other field environments, 20% in each environment. As only a small portion of the components in the 'Day soft' environment failed after 30 years and during the same time almost all components in other field environments failed, the reliability $R(30\,years) \approx 0.2$ in accordance with p_i =20% share of components placed in 'Day soft'. It is noted that the reliability function $R(t)$ is decreasing heavily according to the decrease in each individual reliability function $R_i(t)$, as expected.

In Figure 13, the hazard rate is depicted.

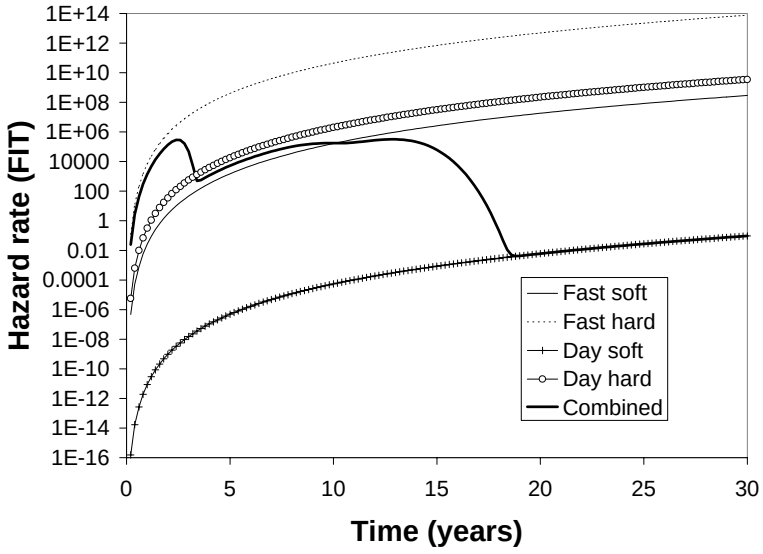

Figure 13. Hazard rate for different field environments and the combined hazard function, taking into account the effect of each population in different field environments.

It can be seen, that the heaviest maintenance load is expected after ca. 2.5 years. It should be noted that in the above figure the repetitive nature of maintenance/repair actions is not taken into account. This means that if the components in a 'Fast hard' field environment are replaced by similar kind of components, it is expected that they will be repaired/replaced again soon.

The above analysis implies that by selecting a set of field environments and balancing the related shares of component populations placed into those, it is possible to predict accurately the expected amount of field returns. In some cases, cost-effective and reliability-wise intermediate components may be feasible, if the main population is placed in a moderate field environment and only a small part of the population is exposed to a harsh environment. Then, the small portion placed in the harsh environment may be taken care of by preventive maintenance. Also, it is possible to consider whether it would be beneficial to use more durable components in the 'Fast hard' environment and use weaker

components in all other field environments if that does not compromise the reliability of the product during its life span. It may also be considered whether it would be beneficial to use more expensive and more durable components - also in mild environments - so that retrofit costs could be avoided and low cost due to the large volume of purchased components could be gained.

5.10.4 The Effect of Mixed Environments in Case of Random Failures

In the following section, the effect of mixed environments, when failures are due to random occurrence of failures, is studied. The characteristic lifetimes at each field environment category is expected to stay the same as in previous section, but the value of the shape parameter β is now set equal to 1. This assumption is in conflict with the test results, which indicated that wear-our takes place and therefore the shape parameter β is larger than 1. However, it is interesting to study what if the failures obtained in the tests were due to random phenomena and how that would affect the reliability behavior of the whole population.

In Figure 14, the reliability functions for different field environments and the combined reliability function are depicted. Compared to Figure 12 the situation is not very much changed. As expected, the changes in reliability are smoother because the shape parameter has a smaller value.

The combined reliability function starts to slope down earlier, but on the other hand, it does not reach the $R(t)=0.2$ value even after the 30-years time period. This indicates that maintenance should be prepared to continuous repair actions. In this case, preventive maintenance is somewhat more demanding to plan, as there is not a very clear instant of time after which the occurrence of failures starts to increase strongly.

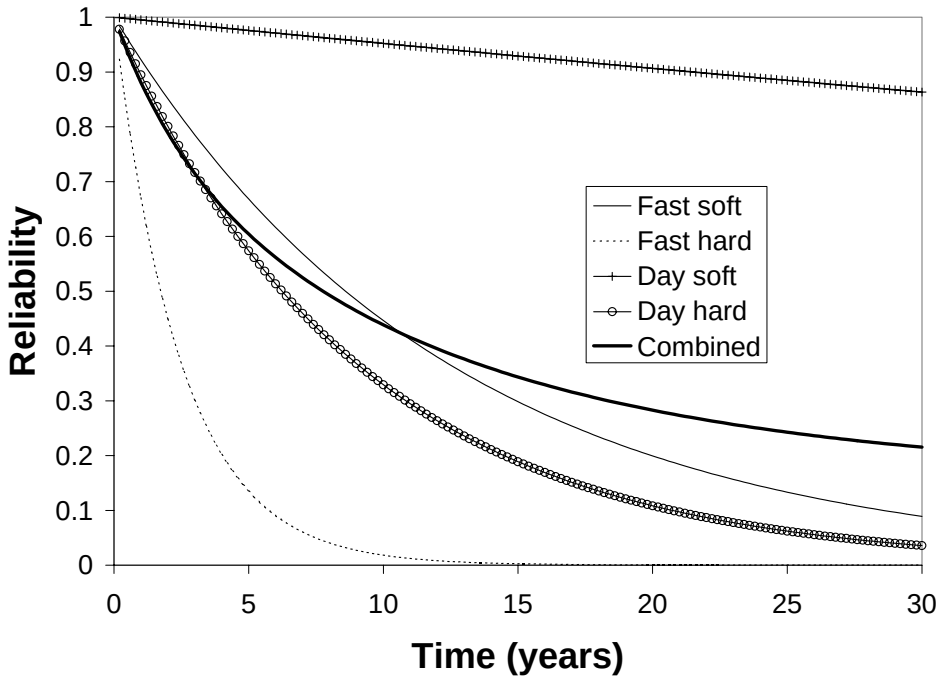

Figure 14. The reliability functions for different field environments and the combined reliability function taking into account the whole population in case β =1.

Looking at Figure 15, this conclusion can be confirmed, as the combined failure rate shows a monotonically decreasing behavior. An interesting finding is that although the hazard rate function in each individual field environment is constant, the combined hazard rate function is not a constant. This apparently controversial behavior can be explained by studying Eqs. (30) and (31). Although the hazard rates $h_i(t)$ are constant, the weight functions w_i are time-dependent.

This can be seen, e.g., by writing the weight function w_1 in terms of its components as

$$w_1 = \frac{p_1 \cdot R_1(t)}{R(t)} = \frac{p_1 \cdot R_1(t)}{\sum_{i=1}^{4} p_i \cdot R_i(t)}, \tag{32}$$

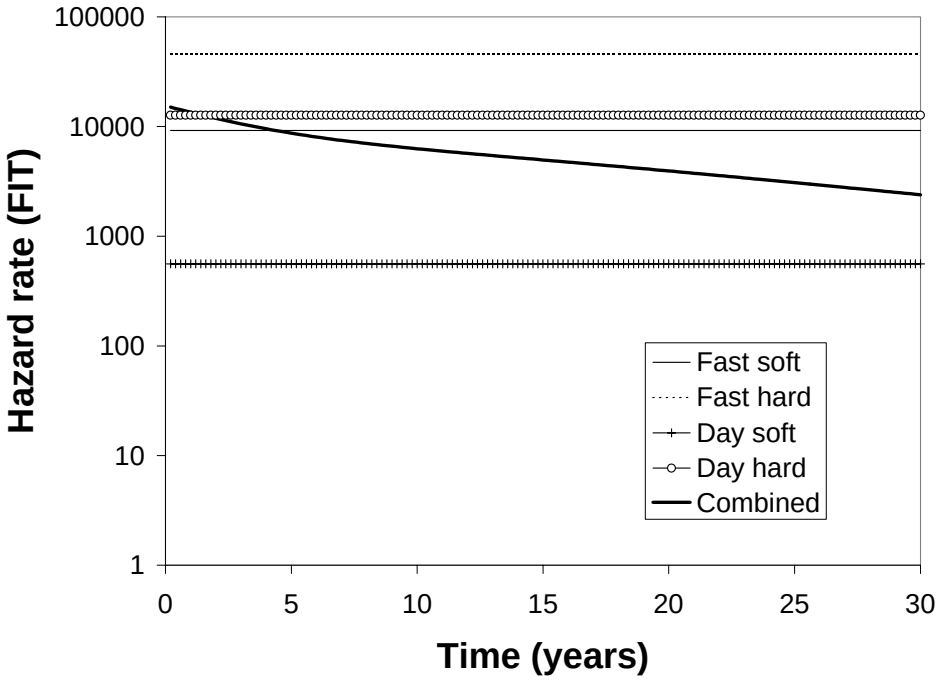

Figure 15. Hazard rate for different field environments and the combined hazard function, β =1.

which can be written as

$$w_1 = \frac{p_1 \cdot e^{-\left(\frac{t}{A.F._1 \cdot \eta}\right)}}{p_1 \cdot e^{-\left(\frac{t}{A.F._1 \cdot \eta}\right)} + p_2 \cdot e^{-\left(\frac{t}{A.F._2 \cdot \eta}\right)} + p_3 \cdot e^{-\left(\frac{t}{A.F._3 \cdot \eta}\right)} + p_4 \cdot e^{-\left(\frac{t}{A.F._4 \cdot \eta}\right)}}. \quad (33)$$

All weight functions are depicted in Figure 16.

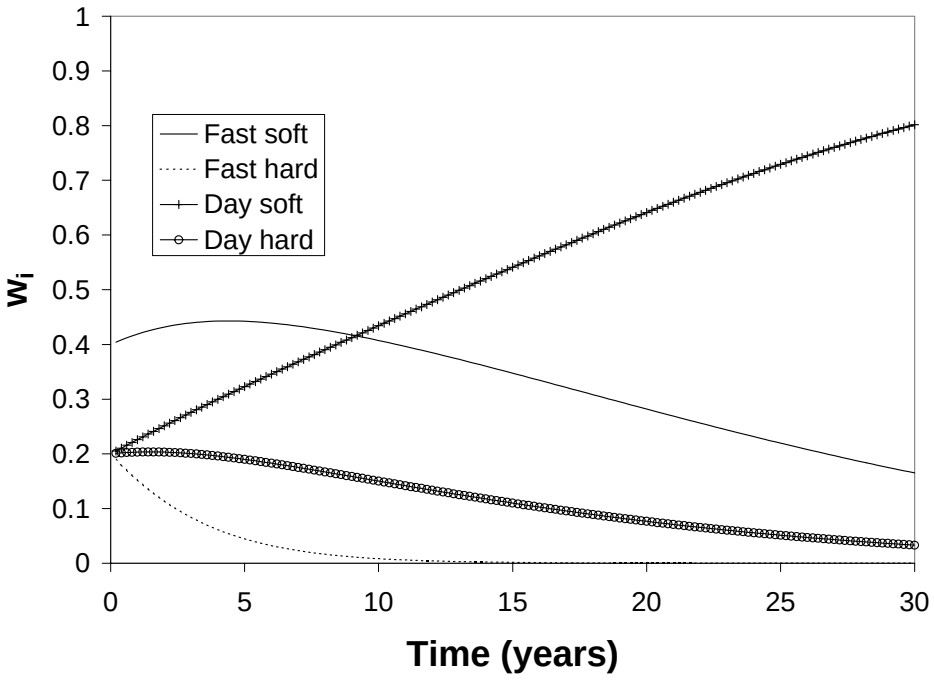

Figure 16. Weight functions in case β =1.

All the weight functions obtain values $w_i = p_i$ at the instant of time $t = 0$. The weight functions in most field environments start to decrease quite soon after the components have been placed in the field, as opposed to the weight function of 'day soft' environment, which increases monotonically during the plotted time period.

As a conclusion, if a component population with random failures is placed in several, different environments, a decreasing total hazard rate is to be expected. This is due to the time-dependency of the weighting factors.

5.11 Conclusions

In this chapter, five leadless ceramic components have been tested by using two thermal cycle profiles. It has been noted, that both test profiles are suitable for inducing solder

fatigue failures. The effectiveness of the tests has been compared and it was discovered that the failures occur time-wise simultaneously although the cycle profiles are not similar.

Significant reliability differences between different component vendors existed. The main reason for this proved to be differences in solder fillet shape.

The developed thermal cycling prediction tool was used to interpret the test results. The tested components proved to be suitable for mild field environments, but they cannot be recommended for use in harsh environments.

Taking an average of several field environments results in over-simplification, that in turn results in poor accuracy of reliability predictions. Instead, the effect of different field environments should be treated as a mixture of different field environments. This approach is demonstrated here for the first time in the literature by utilizing the mixture-of-distributions concept, originally developed to take into account of the initial defects within a component population.

6 Comparison of Analytical and Simulation Based Reliability Prediction Methods

6.1 Introduction

In this chapter, the analytical and simulation based reliability prediction methods are compared. The analytical model used here is Engelmaier's solder fatigue model and the simulation method is based on thermo-mechanical Finite Element Analysis (FEA) using solder material properties defined by Anand [77]. The purpose is to study the reliability predictions, their parameter sensitivity, error margins, and the applicability of the two methods. Finally, some conclusions based on the results are drawn.

Although analytical solder joint models are of power equation type and therefore are very sensitive to parameter fluctuations, the error margins of the reliability predictions are rarely given. Some estimates on error magnitudes do exist [78], [79], but far too often error estimates are completely neglected. In general, the same argument holds for what comes into FEA simulations, although some examples of error estimates do exist [5]. Lately, the response surface technique has given some insight into the parameter sensitivity issue and the related large error margins in FEA modeling [80], [81], [82].

The cases studied here are adapted from the previous chapter.

6.2 Error Sources

As discussed earlier in Chapter 1, reliability predictions are getting more accurate, but they may still have very large error margins. The errors related to the lifetime predictions may originate from several sources: The raw *data on which the models are based* and the way it is analyzed may result in inaccuracies. In Engelmaier's case, the parameters for modified Coffin-Manson-type power law were gained after comprehensive testing. Within standard FEA, 'calibration curves' are utilized in order to correlate the plastic work done to the number-of-cycles-to-failure figures. It is obvious that the calibration curve does not fit the data points perfectly. Therefore, it would be natural that the *confidence bounds* would be

estimated. However, this is rarely accomplished. In Engelmaier's model, a parameter *F*, 'empirical non-ideality constant' takes into account at least part of the non-idealities built in the model. The parameter *F* obtains values in the range 1.0…1.5 for column-like leadless solder attachments and 0.7…1.2 for leadless solder attachments with fillets [49]. Therefore, within the worst-case scenario, the difference between the lifetime predictions due to varying value of parameter *F* may be almost 2 times.

A further source of inaccuracy comes from the fact that the models may be used outside the range (stress/strain/work) they were originally developed for. This happens, for example, when calibration curve within FEA is utilized outside the original calibration data range. Such *extrapolation* may result in a severe lack of accuracy, especially if the *convergence of the original data* was already poor.

Engelmaier's model was developed using ceramic components [116] and Darveaux's model was first demonstrated by using plastic BGA components [83]. Both models have, however, been utilized using several package types and materials assuming that the lifetime prediction models are also valid *outside the original configuration* they are based on. In reality, this may not always be the case. Differences between manufacturing processes may already create large reliability performance deviations.

As both analytical and FEA solutions have a strong parameter dependency, one error source may be the *wrongly chosen parameter values*. The erroneous parameter value selection may be due to *statistical fluctuations*. It is also possible that the parameter value is *not actually measured* but originates from some reference, where typical values are given. For example, the CTE value of organic PWBs may easily vary within a large range, depending on the manufacturer, material, and the amount of copper traces under the component. The effect of parameter sensitivity and the resulting error margins are studied in detail in Section 6.5. The author is not aware of similar studies in the literature in conjunction with solder joint reliability studies, although it is evident that this kind of error estimate should always co-exist with lifetime predictions.

Engelmaier's model is quite simplistic and therefore it *cannot take into account all structural details*. In FEA modeling, all structural details can be taken into account, in

theory. However, typically some structural simplifications are done in order to guarantee affordable solution times for simulations.

Neither Engelmaier's model nor FEA is useful if the failure mechanism is not of thermo-mechanical solder fatigue type. This means that the need for understanding *metallurgy* remains despite the progress in thermo-mechanical modeling. The need for understanding metallurgy is becoming even more important due to the adaptation of lead-free materials [84]. Intermetallics growth in lead-free solder materials [85], [61] has been recognized as a major factor affecting the reliability of solder joints.

Comparisons between the test results and the reliability predictions show some indicative values of the *absolute* accuracy of the models. In [78], it is shown that by utilizing the Solder Reliability Solutions (SRS) methodology it is possible to gain better than ±2.5 times accuracy when compared to the accelerated life test results. According to Darveaux [5], better than ±2.0 times correlation between FEA simulation predictions and lifetime test results can be obtained. However, in the same paper, it is stated, that the predictions obtained by applying different FEA methods diverge at low strain energy values and within the worst-case scenario it is possible that a difference of 7 times can be obtained between different FEA analysis methods.

It is well known that *different analytical and numerical methods* may result in different lifetime predictions. The *relative* accuracy between Anand's [77] and Darveaux's FEA approaches is estimated to be ±25% [5]. In [74], Coffin-Manson, modified Coffin-Manson, Norris-Landzberg, and FEA field performance predictions were compared. The acceleration factor values obtained by applying FEA were smaller than the ones obtained by analytical formulas. The difference in acceleration factor values varied within the range of 3…16 times, depending on the field environment in which the component was about to be exposed. In [6], the acceleration factors for four components were analyzed using Norris-Landzberg, SRS, and FEA. The acceleration factor values were in closer agreement with each other, the deviations being in the range 2…6 times for a component type. Of course, relative accuracy does not actually tell if the prediction is accurate or not, it just indicates the magnitude of differences between different predictions.

6.3 Comparison Between Test Performance Predictions

6.3.1 Introduction

In the next two sections, the absolute accuracy of the Engelmaier's model and FEA are compared. In Section 6.3.2, it is studied as to whether the lifetime performance deviations of the component *e* from two vendors can be explained by using the prediction methods. In the Section 6.3.3, the test performance of all ceramic components *a-e* introduced in Chapter 5 is compared to the ones obtained by utilizing the lifetime prediction methods.

6.3.2 Vendor Related Performance Deviations

In the following, it is investigated, whether differences between the test performance and the predictions based on Engelmaier's model and FEA exist. The component studied here is the component *e* introduced in the previous chapter. Component *e* had two vendors: II and III. Both vendors are studied here, as a large performance deviation existed between them. The performance deviation was due to the different shape of solder fillets. The length of the solder crack path was shorter for the component with the worse performance.

The problem in applying Engelmaier equations in conjunction with CLLCCs lies in the way the 'solder joint height' term is conventionally applied. If the thickness of the solder material between the component and the PWB ($h'_{s.j.}$ in Figure 18) had been considered as this measure – as is usually done – the reliability prediction would have been very pessimistic: It would have been anticipated that the solder joints would only last for 33 cycles in 0…+100 ºC thermal cycling test and for 8 cycles in –40…+125 ºC test. No performance deviations due to different vendors and the varying solder fillet profiles would have been expected either. These anticipated thermal cycle values are, however, grossly in error compared to the actual test results.

Similar problems when applying Engelmaier's model in conjunction with CLLCCs has also been recognized in the literature. In [60], several CLLCC components assembled on ceramic substrates were power-cycled. Different solder fillet shapes were utilized and it was found out that the optimal solder joint profile would be of low standoff (=small solder

joint height), large fillet type. This is in conflict with Engelmaier's model, where increasing the solder joint height should always result in longer lifetime. Therefore, it would have been expected that the optimal solder joint be of tall standoff type. According to Engelmaier's model the fillet shape/the amount of solder material used in the fillet should not have any effect on the lifetime of the CLLCC components. This was, however, proven not to be the case. The lifetime behavior recorded by the reference and us suggests that Engelmaier's model, if applied in a conventional way, cannot explain the thermal cycling test results of the CLLCC components.

However, if the solder joint height is redefined as perpendicular to the crack path ($h_{s.j.}$ in Figure 18) a much better correlation with the test results is obtained. It should be noted, that the normal is placed approximately in the middle of the crack path along its propagation from the solder surface to the edge of the component. This interpretation of the solder joint height is actually analogous to the normal Ball Grid Array (BGA) case,

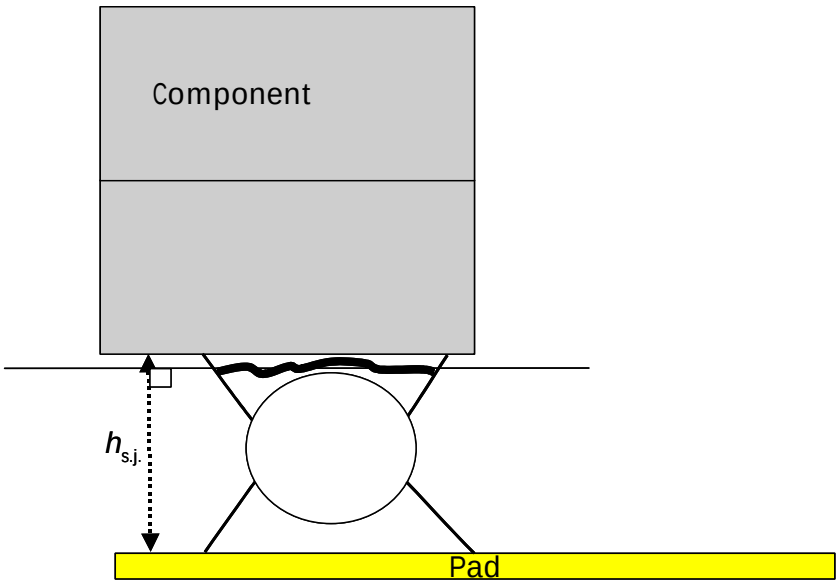

Figure 17. Solder joint height $h_{s.j.}$ measured in case of BGA.

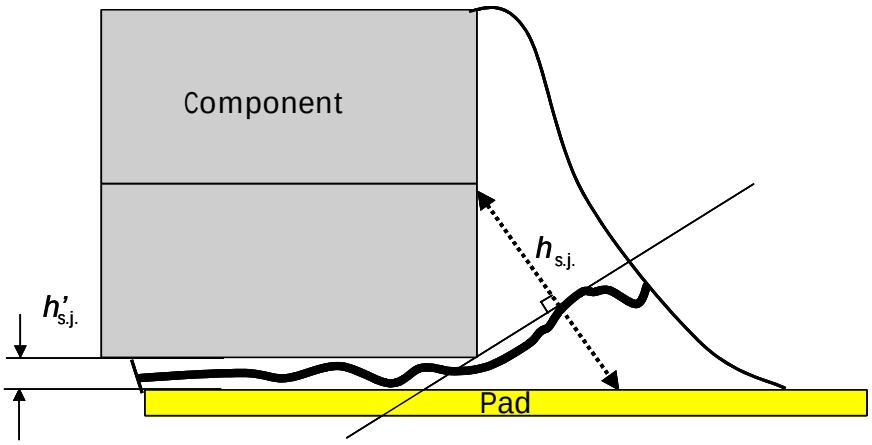

Figure 18. Solder joint height $h_{s.j.}$ as defined here in case of solder castellation.

where the solder joint height is also defined as the distance between the pads measured perpendicular to the crack path (Figure 17). The actual profiles of the solder joints from both vendors are depicted in Figure 19 and Figure 20.

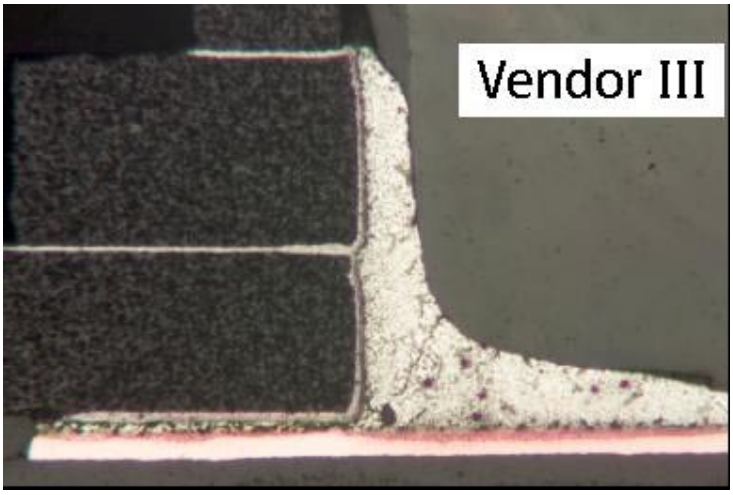

Figure 19. Solder profile of the component *e* in case of vendor III.

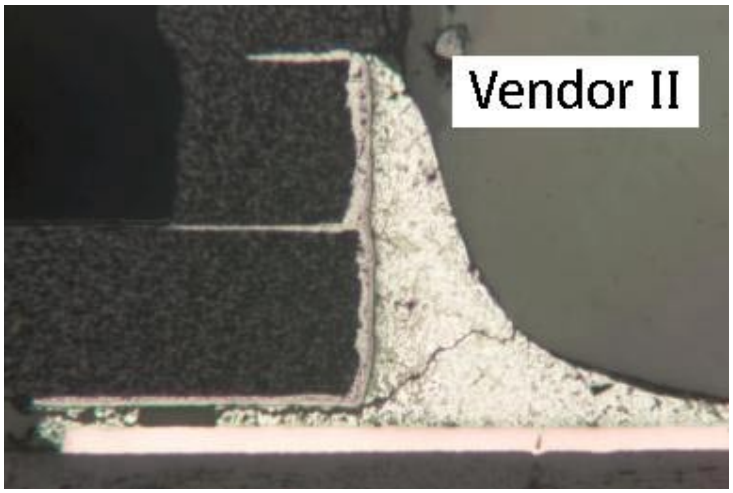

Figure 20. Solder profile of the component *e* in case of vendor II.

The redefined solder joint height obtain values of 200 and 260 microns, for vendors III and II, respectively. When inputting these values together with the other required parameters into Engelmaier's model, the prediction for the test performance shown in Table 10 is obtained.

Table 10. The test performance of the component *e* from two vendors. The predicted characteristic lifetime η values using Engelmaier's model and thermo-mechanical FEM analysis and the actual values recorded in the temperature cycling tests.

Vendor (test env.)	*Engelmaier*	*FEM*	*Actual test result*
III (0…100 ºC)	1064 (-17%)	887 (-31%)	1277
II (0…100 ºC)	2072 (-6%)	1313 (-40%)	2202
III (-40…125 ºC)	243 (-33%)	232 (-36%)	365
II (-40…125 ºC)	464 (-42%)	334 (-58%)	801

The selection of the ‘solder joint height’ term proved to be successful, as the predicted values obtained now by utilizing Engelmaier’s model are relatively close to the values actually recorded in the tests. It looks evident that Engelmaier’s model can explain the large test performance deviation between the two vendors by the different solder joint shapes and the related differences in the ‘solder joint height’ values. The prediction obtained by using Engelmaier’s model proved, in all cases, to be slightly pessimistic, as expected [92]. However, FEA proved to be even more pessimistic.

Although by using Engelmaier’s model it seems that the redefinition of the solder joint height is useful, the question remains, is it permissible to use Engelmaier’s model in the way described above. The original definition of the cyclic hysteresis energy term ΔD was originally defined utilizing *shear strain* $\Delta\gamma$ concept, as can easily be seen

$$\Delta D = F \cdot \frac{L_D \Delta\alpha \Delta T_e}{h_{s.j.}} = F \cdot \Delta\gamma . \tag{34}$$

The only deviation between the classically defined shear strain and the cyclic hysteresis energy is the non-ideality factor F, whose value is usually close to 1. Shear strain is the relative distortion of a solid caused by a force parallel to the planes of the object. It is therefore expected that the crack in the solder due to shear strain propagate parallel to the direction of the force causing shear strain. When looking at Figure 18, this would implicate that the direction of the force should be parallel to the crack path, in other words, pointing slightly upwards from the horizontal plane. This, however, may be in conflict with the assumption used in Engelmaier’s model that the force should act parallel to the PWB. This apparent contradiction can be, at least partly, explained by the fact that the PWB under thermal cycling load bends. This means that, in reality, the force related to the CTE mismatch may point out of the horizontal plane. This has been verified by Engelmaier himself [116], and by some other studies [86], [87], [88], [89] in the case of thermal cycling and power cycling

In the most comprehensive study [86] of those mentioned above, the deformation modes are divided into three categories: in-plane displacement, out-of-plane rotation, and out-of-

plane displacement. The first one represents a typical (horizontal) shear stress situation, whereas the last one is related to (vertical) tension strain. The out-of-plane rotation is the mode that takes into account the PWB bending. In the reference, a thorough analysis is presented where the strains related to all the above-mentioned deformation modes are measured during a temperature cycling of –40…+125 ºC. The maximum bend angle was measured as α=1 mrad at 55 ºC (Figure 21). At higher temperatures the bending decreases due to the stress relaxation related to the solder material plastic deformation.

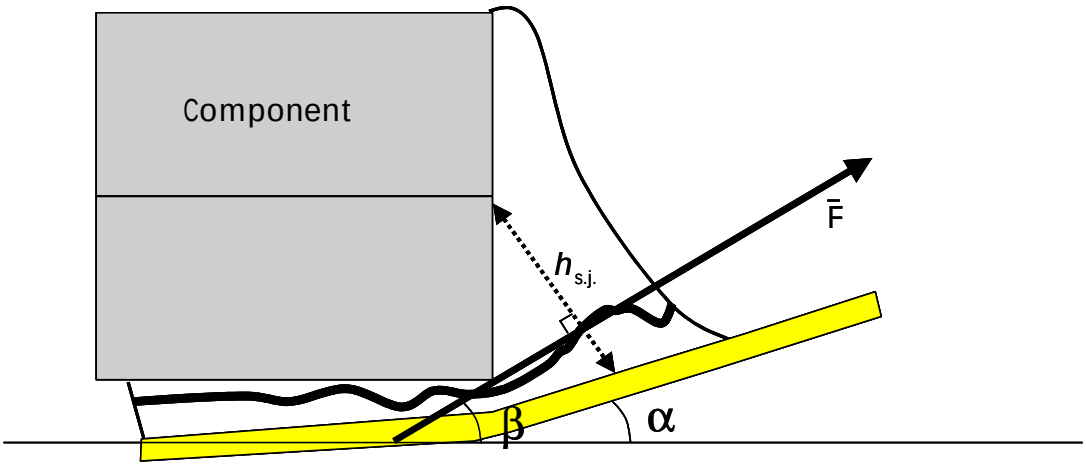

Figure 21. Ceramic component assembled on organic PWB during thermal cycling at elevated temperature. Bending of PWB is clearly visible.

Although the PWB bend angle α recorded was relatively small, it gives a clear indication that the force $\overline{F}$ due to the PWB expansion does not point horizontally. Furthermore, it can be assumed that the angle β between the horizontal plane and the force $\overline{F}$ is larger than the bend angle α. Therefore, one may estimate that force $\overline{F}$ is almost perpendicular to the solder joint height $h_{s.j.}$, as re-defined earlier. Due to this fact, the strain observed can be considered as predominantly of shear type, despite the PWB bending. This, in turn, satisfies the requirement related to the utilization of Engelmaier's model, in other words, that the solder fatigue should occur due to shear strain.

An explanation, why only solder castellation is taken into account when considering fatigue life, needs still to be given. This is due to the fact that according to [90] more than 90% of the fatigue life of CLLCCs is due to solder castellation. In the reference, the crack propagation velocity in different parts of the CLLCC type solder interconnection was studied. This information was used as an input when running FE simulations on this kind of solder geometry. Only a minor share of fatigue life was due to solder material between the component and the PWB. Therefore, the solder joint height may well be re-defined as the normal dimension in the middle of the solder castellation.

6.3.3 Test Performance Predictions of Some Ceramic Components

In this section the lifetime of components *a*-*e* in a test environment is studied. The predicted performance using Engelmaier's analytical model and FEA computer simulation is compared to the actual test performance. The difference between the following analysis and the one presented in the previous chapter lies in the fact that here average performance is considered. This means that the analysis is based on average values and the differences due to various vendors are not considered.

Table 11. The test performance in 0…100 °C thermal cycling test. The deviation from the actual test performance is inside parenthesis.

Component η *(cycles)*	*Average test result*	*Engelmaier*	*FEA*
a	1856	1209 (-35%)	1823 (-1.7%)
b	4209	2774 (-34%)	3567 (-15%)
c	1918	2855 (+49%)	1978 (+3%)
d	2173	3227 (+49%)	2086 (-4%)
e	1739	1517 (-13%)	1116 (-36%)

In Table 11, the actual test performance in 0…+100 °C thermal cycling test and the ones predicted are presented.

It is noted that there are relatively large deviations both in the case of using Engelmaier's model and FEA modeling. One explanation may be that the average performance is studied. This means that the actual test result is the arithmetic mean of the characteristic lifetimes obtained. In some cases, large deviations due to different vendors could be noted. This fact is neglected in the above analysis. Average values for solder joint geometry were used when predicting the lifetime, as well. For example, when using Engelmaier's model the solder joint height, as redefined in Section 6.3.2, was assumed to be 300 microns for components *a* and *b*, and 230 microns for components *c*-*e*.

In Table 12, the actual test performance in -40…125 °C thermal cycling test and the ones predicted are presented.

Table 12. The test performance in -40…125 °C thermal cycling test. The deviation from the prediction of the actual test performance is inside parenthesis.

Component/ η (cycles)	*Average test result*	*Engelmaier*	*FEA*
a	594	275 (-54%)	717 (+21%)
b	981	580 (-41%)	1161 (+18%)
c	562	614 (+9%)	727 (+29%)
d	590	708 (+20%)	930 (+58%)
e	583	343 (-41%)	365 (-37%)

Also in this case, relatively large deviations from the actual test performance can be noted. It seems that FEA usually gives somewhat over-optimistic predictions while Engelmaier's model, in most cases, gives over-pessimistic predictions. Based on the results, it does not

seem that the absolute accuracy of either of the prediction methods is very good. Unless the solder joint height-term in Engelmaier's model was to be redefined as explained in Section 6.3.2, the predictions given by Engelmaier's model would have been grossly over-pessimistic.

It seems, that FEA modeling can predict that component *b* performs the best in both thermal cycling tests. However, using Engelmaier's model, components *c* and *d* outperform component *b*, which is in conflict with reality. The explanation for this may lie in the varying pad size of different components. Component *b* has clearly the largest pads (3.6*1 mm^2) that extend under the component. The pads of the other components are very much smaller and do not extend much under the component. In the above Engelmaier analysis, the distance to neutral point (DNP) was assumed to be equal to the distance between the two corner-most castellations. This is a valid assumption when it comes to all the other components, but in the case of component *b*, the actual center point of the pad lies underneath the component, and therefore the DNP value used is too large resulting in an over-pessimistic lifetime prediction.

By taking into account the true location of the pad center location and using this information in redefining the DNP value, a shift from DNP=5.01 mm to DNP'=4.35 mm is obtained. When using the redefined DNP in Engelmaier's model, the following characteristic lifetimes are obtained for component *b*: in 0…+100 °C test η=3924 cycles and in -40…+125 °C test η=810 cycles. Since the actual test results were 4209 and 981 cycles, it is now noted that there is a relatively good agreement between the predictions and the actual test results.

6.4 Benchmark of Field Reliability Predictions

6.4.1 Introduction

As the actual field failure data on the components did not exist, it was impossible to study the absolute accuracy of the prediction methods when it concerned field lifetime performance. However, it is possible to *compare* the predicted lifetimes obtained by using Engelmaier's model and thermo-mechanical FEA. In this section, the average solder joint

height, as redefined, was assumed to be 300 microns for components *a*-*b* and 230 microns for components *c*-*e*.

6.4.2 Comparison of Field Lifetime Predictions

In Table 13, the characteristic lifetime values obtained by using Engelmaier's model are shown. Also, the difference to the field lifetime values obtained by utilizing FEA is shown. At first glance, it looks like that the magnitudes of predicted lifetimes correlate relatively well. No deviations greater than 2 times exist. This is somewhat surprising, as it is often assumed that FEA modeling is always superior over analytical, sometimes called 1st order models [19]. Therefore, a larger deviation between the predictions would be expected based on Engelmaier's 1st order model and presumably more sophisticated FEA modeling.

Table 13. Field lifetimes obtained by using Engelmaier's model. The difference to the value obtained by applying FEA modeling is inside parenthesis.

	Characteristic lifetime, years			
Component	Fast soft	Fast hard	Day soft	Day hard
a	6.0 (-59.2%)	1.4 (-53.3%)	50.2 (-79.1%)	3.5 (-67.3%)
b	13.0 (+8.3%)	3.1 (+14.8%)	102.7 (-50.3%)	7.0 (-70.8%)
c	13.6 (+88.9%)	3.3 (+135.7%)	106.4 (-3.3%)	7.3 (-39.7%)
d	15.5 (+181.8%)	3.7 (+208.3%)	120.2 (+29.2%)	8.2 (-36.4%)
e	7.5 (-6.3%)	1.8 (+5.9%)	61.5 (-53.4%)	4.3 (-42.7%)

The predicted lifetime of component *d* seems to deviate the most. The optimism of Engelmaier's prediction related to this may originate from the fact that Engelmaier's model does not make any difference based on how many solder joints are used. It just considers the reliability of the corner-most solder joint, as that is usually the most critical one. In FEA modeling it is possible to take into account the whole solder attachment

configuration. This means that the number of solder joints has an effect on the lifetime prediction. The more solder joints, the longer the lifetime. As component *e* has solder joints only in the corners of the component (4 pcs), it is natural that FEA modeling should result in a more pessimistic prediction than Engelmaier's model.

Another finding is that the ranking based on the lifetime length remains the same when using Engelmaier's model in different field environments. The component *e* outperforms the other components in terms of lifetime under all field environment profiles. This is not the case when applying FEA. The best component under a 'day hard' profile is component *b*, while within all other profiles, component *a* seems to have the best performance.

6.4.3 Calibration of FEA

FEA predictions are based on the use of *calibration curves*. Calibration curves are obtained by plotting a set of plastic energy values observed by FEA against the related characteristic lifetimes recorded in reliability tests. A power equation is fitted in order to find parameters to a model that relates arbitrary plastic work divided by the crack length to the mean-cycles-to-failure. After that, a certain component, under some specific load conditions, can be analyzed, as a correlation between the plastic energy obtained by simulation and the test result has been established. Without the calibration curve, it is not possible to interpret the plastic energy values obtained by utilizing FEA in terms of lifetime.

According to [5], the crack growth rate can be written as

$$\frac{da}{dN} = K_3 \cdot \Delta W_{ave}{}^{K_4} \quad , \tag{35}$$

where a is the length of the crack, N is the number cycles, ΔW_{ave} is the average viscoplastic strain energy accumulated per cycle for the interface elements, and K_3 and K_4 are parameters. It may be suspected that the crack does not necessarily propagate at a constant rate. Actually, it has been noted in the literature that the crack growth rate is not always constant. This is the case especially if castellated solder joints are involved [91].

To check the validity of the constant crack growth rate assumption, the test results are depicted in Figure 22. It is noted that the assumption of constant crack growth rate is reasonable in case of –40…+125 °C test where results match a straight line acceptably. In case of 0…+100 °C test, the convergence of the data is not as good. The crack growth rate in the case of –40…+125 °C test is 3 μm/cycle, while in the 0…+100 °C test the crack growth rate is 0.8 μm/cycle, in other words, ca. one third of the growth rate in –40…+125 °C test, as expected. Here it is assumed that the crack initiates instantly after being exposed to thermal cycling. In [5], it was shown that the number of cycles to initiate the crack is usually less than 10% of the mean number of cycles to failure.

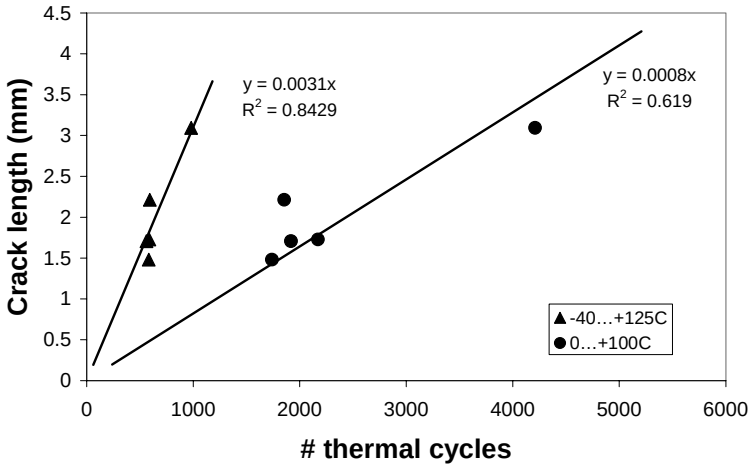

Figure 22. Crack length versus the number of thermal cycles in two thermal cycle tests.

In order to find out the values of parameters K_3 and K_4, the crack growth rate was plotted against the plastic strain energy density/cycle obtained by FEA. This can be seen in Figure 23.

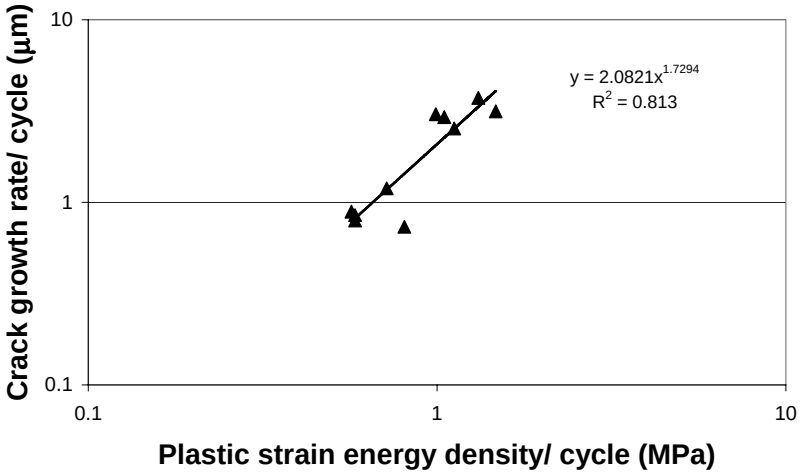

Figure 23. Crack growth rate in thermal cycling tests.

After curve fitting, the parameter values obtained are K_3=2.0821 $\mu m/cycle/MPa^{K_4}$ and K_4=1.7294.

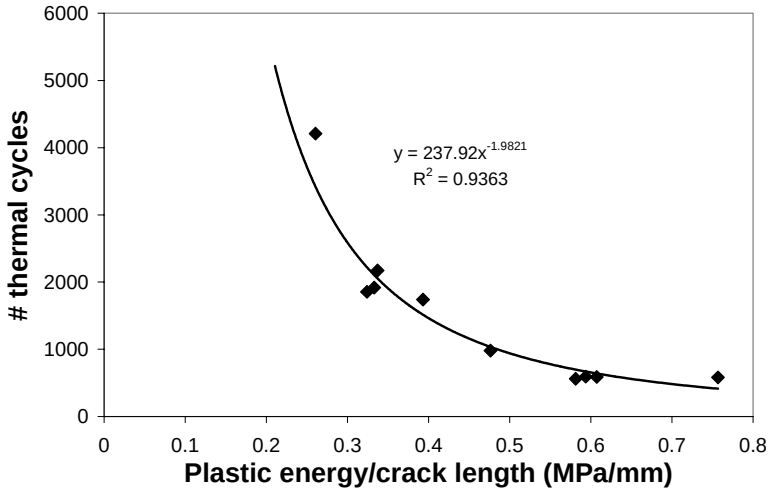

Figure 24. Calibration curve used in FEA.

In Figure 24, the calibration data used in conjunction with CLLCCs is depicted.

The data used to create the calibration curve originates from all the tests run. The curve fit seems to be acceptable. However, after having a closer look, it may be noted that, especially at higher cycle counts, individual data points deviate from the calibration curve. The absolute value of the deviation can be seen in Figure 25. As the magnitude of the error related to the calibration procedure has now been quantified, this information may be used later on when estimating the uncertainty of the lifetime predictions.

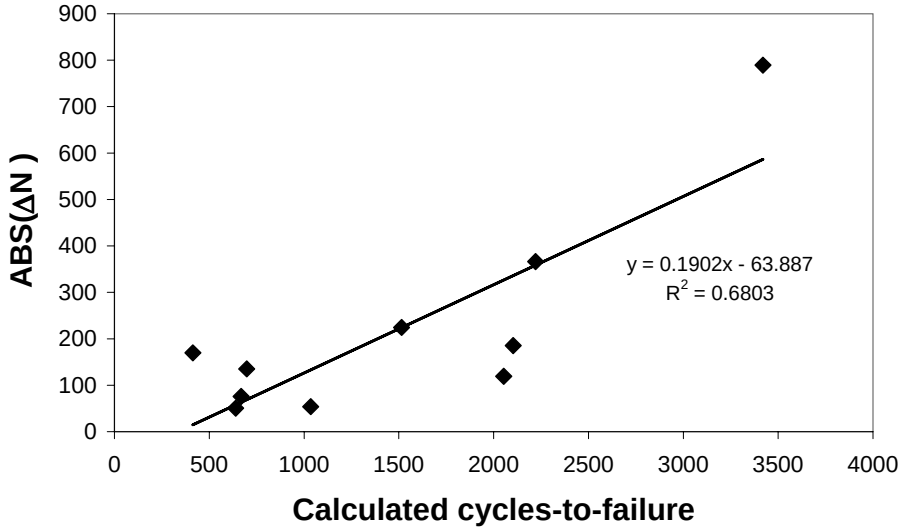

Figure 25. The absolute value of the deviation between the original data points and the fitted calibration curve.

Instead of using self-created calibration curves, it is possible to utilize generic parameter values available [5]. However, it is expected that when utilizing those, much larger errors may occur.

6.4.4 The Calibration of Engelmaier's Model

Engelmaier's semi-empirical model is based on a large amount of test data. The approximate nature of this model is presented by the non-ideality factor *F* with values

0.7...1.5. The non-ideality factor gives some flexibility to ‘calibrate’ Engelmaier’s model. For example, in [92], a component with gull-wing type extra-compliant leads was analyzed by using Engelmaier’s formulas, FEA, and accelerated life testing. A generic value of *F* for leaded components is 1. However, after correlating the Engelmaier’s model with the FEA results, an *F* value of 0.555 was obtained. When considering the actual test results, the *F* value gained was 0.356. This means, that both Engelmaier’s model with typical *F* values (at least by a factor of 4) and FEA (at least by a factor of 2) were more pessimistic than the actual thermal cycling test result.

In the following, the calibration is performed by equating the lifetime observed in the test and Engelmaier’s prediction. After that, the field lifetime prediction is obtained simply by multiplying the ‘calibrated’ test performance by the acceleration factor given by the Engelmaier model. This novel method may help to utilize Engelmaier’s model with better accuracy. After performing the calibration, the field performance predictions given by Engelmaier’s model and FEA were actually in closer agreement, as can be seen in Table 14.

Table 14. Field performance predictions given by ‘calibrated’ Engelmaier’s model. The difference to the values obtained by FEA is inside parenthesis.

	Characteristic lifetime, years			
Component	Fast soft	Fast hard	Day soft	Day hard
a	11.0 (+24.9%)	2.6(+13.1%)	92.7 (+61.5%)	6.6 (+38.1%)
b	20.9(-73.8%)	5.0(-85.2%)	164.7 (+20.3%)	11.5 (+51.9%)
c	10.7(-49.3%)	2.6(-84.4%)	84.4(+23.3%)	5.7 (+53.1%)
d	11.6(-111.7%)	2.8 (-133.8%)	90.6(+2.6%)	6.1(+52.9%)
e	10.6 (-32.5%)	2.5 (-48.2%)	87.6(+33.6%)	6.1 (+19.3%)

The sum of the differences (percentage) squared can be utilized in demonstrating the enhanced correlation between the two lifetime prediction techniques. Without the calibration this term obtains the value of 13.6 and after the calibration this term is almost halved to a value of 7.3. It seems that the calibration of Engelmaier's model results in a much closer agreement between the results obtained by two lifetime prediction methods. If assuming that FEA is more accurate, due to its better capabilities to take into account structural details, then by calibrating Engelmaier's model it is possible to obtain more realistic lifetime predictions than without calibration.

6.5 Parameter Sensitivity

6.5.1 General

In this section, the parameter sensitivity of both Engelmaier's model and thermo-mechanical FEA modeling are studied.

It is evident that Engelmaier's model is very sensitive to parameter changes, because the model consists of a power-law equation. Likewise, it is expected that thermo-mechanical modeling is prone to parameter fluctuations. This is due to the fact that generic solutions to 2^{nd} order differential equations are of exponential type. The strong parameter sensitivity gives rise to large error margins. Therefore, it is very important that an error estimation is given in conjunction with a reliability prediction.

6.5.2 Parameter Sensitivity

In this section, it is studied how large changes in terms of characteristic lifetime result from a small change of a certain parameter value. In the case of Engelmaier's model, the task is somewhat easy, because the sensitivity to a parameter change U_i may be studied by utilizing partial derivatives

$$U_i = \frac{\partial N}{\partial X_i} U_{\overline{Xi}}, \tag{36}$$

where N is the number of cycles, X_i is the i^{th} *parameter* and $U_{\overline{X}_i}$ is the uncertainty related to the parameter value.

Since Engelmaier's model is of analytical form, the calculation of the partial derivates is a straightforward task. The situation is not that simple when it comes to FEA, as no analytical solutions exist. However, if considering that the uncertainties/parameter changes are of infinitesimal magnitude, it is a valid operation to write

$$U_i = \frac{\partial N}{\partial X_i} U_{\overline{X}_i} \approx \Delta N_i, \tag{37}$$

where ΔN_i is the change in lifetime observed after changing i^{th} parameter from its nominal value.

Let's first study the component *e* in *test environment*. In Table 15, the nominal values, the deviations from the nominal values, and the related changes in the number of cycles to failure are shown. The changes (percentage) compared to nominal situation are inside parenthesis.

Parameter fluctuations resulted in almost equal magnitudes of uncertainty using both methods. Engelmaier's model is most sensitive to the fluctuations of PWB's CTE value, solder joint height, and DNP. The FEA method is most sensitive to changes in CTE value of PWB, CTE of the component, and DNP. The reason that FEA does not recognize solder joint height as a top-three factor affecting the solder joint reliability may be due to the some simplifications done on solder profile when setting up the simulation. The results obtained from the comparison between the two vendors (Table 10) also indicate this, as the FEA simulation could not duplicate very accurately the test performance of sample lots having different solder joint shapes.

In Table 16, the corresponding data in field environment is listed.

Table 15. Parameter sensitivity results in test environment 0…+100 °C for component *e*. The resulting deviation from the lifetime - obtained using nominal parameter values - compared to nominal lifetime value is inside parenthesis.

Parameter	*Nominal value*	*Deviation*	$\frac{\partial N}{\partial X_i} U_{\overline{X}_i}$, *Engelmaier*	ΔN_i, *FEA*
CTE, component (ppm/ºC)	7	0.2	91.2 (+4.4%)	98.7 (+7.5%)
CTE, PWB (ppm/ºC)	18	0.5	-227.9 (-11.0%)	-182.9 (-13.9%)
Solder joint height (cm)	0.026	+3.85%	192.9 (+9.3%)	30.3 (+2.3%)
Dwell time of half cycle (min)	5	0.3	-42.8 (-2.1%)	-0.9 (-0.1%)
DNP (cm)	0.475	0.01	-105.6 (-5.1%)	-69.3 (-5.3%)
Temperature low (ºC)	0	1	37.7 (+1.8%)	40.1 (+3.1%)
Temperature high (ºC)	100	1	-62.2 (–3.0%)	-43.1 (-3.3%)

In reality, larger deviations from the assumed nominal values may exist. For example, the CTE value of the PWB may vary in the range of 16…23 ppm/ºC.

In this case, it may seem that FEA is much more sensitive to parameter value changes than Engelmaier's model. This is due to the fact that the change in the number of cycles is much larger in FEA's case. It should, however, be remembered that the lifetime prediction given by FEA was larger (η=3624 cycles) compared to the lifetime prediction given by Engelmaier (η=1559 cycles). Therefore, it is natural that the small changes in parameter values in the case of FEA result in larger changes (in cycles) in lifetime prediction than in Engelmaier's case. A better way to compare the parameter sensitivity is to look at the change percentages. No large deviations between the two methods can be observed in those values.

Table 16. Parameter sensitivity results field environment (‘Day hard’) of component *e*. The resulting deviation from the lifetime - obtained using nominal parameter values - compared to nominal lifetime value is inside parenthesis.

Parameter	*Nominal value*	*Deviation*	$\frac{\partial N}{\partial X_i} U_{\overline{X_i}}$, *Engelmaier*	ΔN_i, *FEA*
CTE, component (ppm/ºC)	7	0.2	59.3 (+3.8%)	244.2 (+6.7%)
CTE, PWB (ppm/ºC)	18	0.5	-148.2 (-9.5%)	-492.4 (-13.6%)
Solder joint height (cm)	0.023	+4.35%	141.8 (+9.1%)	145.4 (+4.0%)
Dwell time of half cycle (min)	360	5	-3.2 (-0.2%)	1.5 (+0.04%)
DNP (cm)	0.475	0.01	-68.6 (-4.4%)	-163.1 (-4.5%)
Temperature low (ºC)	20	1	46.5 (+3.0%)	201.4 (+5.6%)
Temperature high (ºC)	80	1	-62.2 (-4.0%)	-176.7 (-4.9%)

In a ‘day hard’ field environment, Engelmaier’s model is most sensitive to parameter fluctuations of the CTE of PWB, solder joint height, and DNP, as was also the case in the test environment. FEA is most sensitive to changes in CTE of PWB, CTE of the component, and the low temperature end of thermal cycling profile.

It should be noted that the parameter deviation values used are somewhat arbitrary. However, if interested, the reader may easily select more suitable values and try those, instead.

6.6 Lifetime Predictions with Error Margin Estimates

In the following analysis, Eqs. (6) and (11) are utilized in order to calculate error margins. By using them, the maximum uncertainty and the uncertainty values, respectively, are obtained. Utilization of Eqs. (6) and (11) is straightforward when it concerns Engelmaier’s

analytical model, as the partial derivates are easy to calculate, because the equations used are of closed-form type. However, the situation is somewhat different when it comes to FEA, as no analytical solutions exist. In the following paragraphs, the parameter fluctuation related uncertainties are evaluated by assuming that the fluctuations are of virtually infinitesimal magnitude, cf. Eq. (37). Then, it is a valid operation to write

$$U_{\max} = \sum_{i=1}^{n} \left| \frac{\partial N}{\partial X_i} \right| U_{\bar{x}_{i,\max}} \approx \sum_{i=1}^{n} \left| \Delta N_i \right| \tag{38}$$

and

$$U = \sqrt{\sum_{i=1}^{n} \left(\frac{\partial N}{\partial X_i} U_{\bar{X}_i} \right)^2} \approx \sqrt{\sum_{i=1}^{n} (\Delta N_i)^2}\,, \tag{39}$$

where N is the number of cycles to failure and ΔN_i is the change in the number of cycles to failure compared to the 'nominal situation' related to the deviation of parameter *i* from its nominal value.

Now, it is possible to obtain the maximum uncertainty and the uncertainty values by summing up the uncertainty terms related to individual parameter fluctuations. The results, concerning component *e*, are summarized in Table 17.

When utilizing Engelmaier's model in a test environment of 0...100 °C, the uncertainties are 340 (761) cycles (in parenthesis the maximum uncertainty values and outside those the typical uncertainty values). These values may also be considered as error estimates for the lifetime of the component. Therefore, the test performance prediction may be written with the error margins as follows: 2072±340 cycles. As the actual test result was 2202 cycles, the prediction obtained by applying Engelmaier's model was within error margins.

Table 17. The lifetime predictions with error margins estimated for test and field environments of the component *e*.

Environment	η *, cycles (test)*	η *, cycles (prediction)*	U *, cycles*	U_{max} *, cycles*	*Within error margins*
Engelmaier					
0…100 ℃	2202	2072	340	761	Y
-40…+125 ℃	801	464	72	148	N
'Day hard'	N/A	1559	237	530	N/A
FEA					
0…100 ℃	2202	1313	227	446	N
'Day hard'	N/A	3624	635	1337	N/A

In –40…+125 ºC test profile, the corresponding uncertainties using Engelmaier's model are 72(148) cycles. In this case, the actual test result does not fit inside the error margins, as the result by using Engelmaier's model was 464±72 cycles and the actual test result was 801 cycles. Even if the maximum error had been used, the test result would still have been outside the error margins.

When using FEA, the test performance prediction does not fit inside the error margins. This implies that not all error sources may have been considered, or that the magnitudes of the selected uncertainties are not sufficiently large enough. However, if the uncertainty estimated due to the imperfect fit of the calibration curve is added, the error margins in the case of FEA may be reconsidered. If doing so, 186 cycles should be added to the uncertainty term in the test environment and 625 cycles in the field environment. However, even after taking into account this additional error term, the actual test result still does not fit inside the error margins.

It is possible that there is some interaction between different parameters. Then, the uncertainty analysis and error estimation should take this into account. However, this is

not likely the case in the above analysis, as the parameters, whose sensitivity was studied, are independent of each other.

It is now possible to obtain the lifetime prediction with some error margin values, which can give some insight into how trustworthy the predictions may be. The characteristic lifetime of component *e*, when utilizing Engelmaier's uncalibrated model is 4.3±0.7 years. After calibration according to Section 6.4.4, this prediction is 6.1±1.1 years. The lifetime prediction when using FEA is 9.9±1.7 years. If the error term related to the calibration curve is taken into account, the error margins double and the lifetime prediction becomes 9.9±3.5 years. It is impossible to decide which of these predictions is the most accurate one, since there is no field data with which to compare them available.

6.7 Discussion

Engelmaier's model could be applied in the case of castellated solder joints after interpreting the solder joint height in a novel way. The prediction was compared to the FEA modeling results. Relatively good correlation between the test performance and both the predictions was noted. Even better agreement could be obtained if Engelmaier's model was calibrated by test data. The performance deviation between the two vendors could be verified as being due to the different solder joint castellation shapes.

The analysis showed that both analytical and FEA modeling approaches have relatively large parameter sensitivity. This is, of course, unfortunate, but by estimating the parameter fluctuations, it is possible to give reliability predictions with proper error estimates. This is possible both in the case of analytical and numerical solutions, as was shown. Although not widely applied in solder joint lifetime predictions, the error estimates should always be given. Estimating errors also provides a possibility to study, which parameters are the most critical ones in the design analyzed. Their influence on adding uncertainty may be reduced after their effect has been recognized. This can be accomplished, e.g., by measuring the actual material parameters. When creating test acceptance criteria, safety margins may be set based on uncertainty estimations.

Based on the analysis above, the CTE values and the solder joint height were recognized as the ones that affect most the lifetime of the solder joint. This manifests the importance of using actual measured CTE values. Using handbook values may result in completely erroneous lifetime predictions. Virtually identical components may have a significantly different lifetime performance if the shape of the solder castellation is different. Therefore, detailed quality control of the components is of the utmost importance. It is also important to understand the field environment to which the components are going to be addressed, as this has a large effect on the forthcoming lifetime.

Table 18. Properties of Engelmaier's model and FEA modeling approach.

Property	***Engelmaier***	***FEA***
Accuracy	Moderate	Moderate
Sensitivity	Large	Large
Parameters having the largest effect on the lifetime prediction	CTE (PWB), solder joint height, DNP	CTE (PWB), CTE (component), DNP
Possibility to take into account structural details	Moderate	High
Level of expertise required	Moderate	High
Calibration data	Not needed	Required

FEA modeling requires some 'calibration data' in order to correlate a plastic energy value to a related characteristic lifetime. Due to an imperfect curve fitting it is expected that a certain additional error term is introduced. The effect of imperfect curve fitting may be severe, especially if the field environment and the test environment differ widely from each other. Creating a credible lifetime prediction, especially for mild environmental conditions, may be a demanding task, as the absolute errors due to FEA calibration are larger the milder the environment. Errors in lifetime prediction are expected to be large

also due to diverging lifetime predictions at low strain energy values when applying different FEA methods [5].

In Table 18, some key properties of both methods are listed.

Persons with little experience can utilize Engelmaier’s model, while FEA modeling typically requires in-depth understanding of numerical methods and tools.

7 Approximate Hazard Rate Selection for System Level Reliability Considerations

7.1 Introduction

It is well known that only exponential distribution has a constant hazard rate. The constant hazard rate is related to some random effects that take place during the lifetime of a component (bathtub curve with $\beta = 1$ in Figure 26).

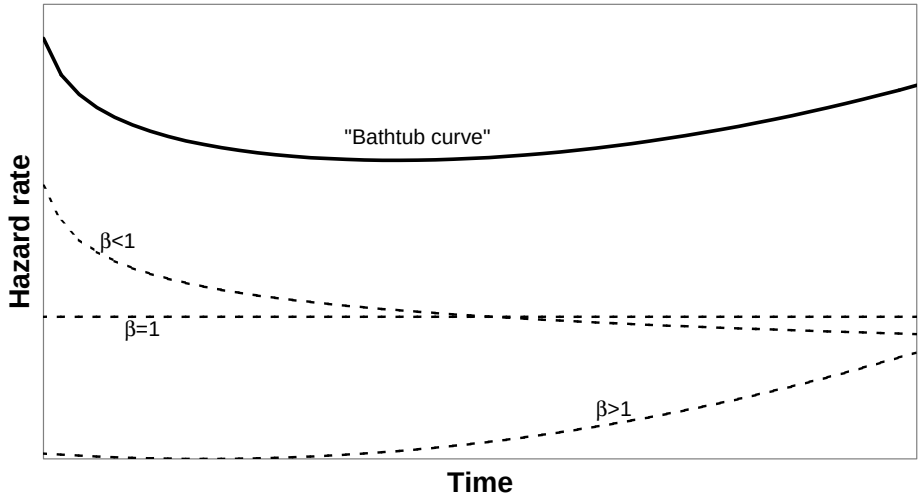

Figure 26. Bathtub curve and the different failure regions. When Weibull shape parameter $\beta < 1$, failures are predominantly of early failure type, when $\beta = 1$, random failures are dominant and when $\beta > 1$, wear-out is mostly responsible for failures.

Exponential distribution assumption with constant hazard rate is used quite a lot due to the resulting simplicity in system level reliability analyses. When utilizing constant hazard rate assumption in parts-count type reliability estimates, the hazard rates of individual

components $\lambda_{comp,i}$ can be summed up, and the end result is the system level hazard rate λ_{system} [9]

$$\lambda_{system} = \sum_{i=1}^{n} \lambda_{comp,i} \,. \tag{40}$$

The reciprocal of the system hazard rate is the MTTF (Mean Time To Failure) of the system

$$MTTF = \frac{1}{\lambda_{system}} \,. \tag{41}$$

Quite a lot of component lifetime data that has been gathered, is presented in terms of constant hazard rate. Many system level reliability prediction methods are also giving lifetime predictions in terms of constant hazard rate [93].

However, in reality, the constant hazard rate assumption is often not valid. Therefore, applying exponential distribution may not always be an appropriate choice [94]. Assuming a constant hazard rate makes the mathematical analyses easy, but assuming a constant hazard rate is in contradiction with the fact that most components fail either in the early failure or in the wear-out regime, where the hazard rate is either decreasing or increasing, respectively. The hazard rate in those regimes can be taken into account, for example, by utilizing Weibull statistics, but not by exponential distribution. Due to this fact there seems to be an unbridgeable situation, as component level reliability data can be interpreted by applying Weibull statistics, but these results cannot be utilized later on in simplistic system level MTTF calculations.

The relationship between the exponential and the Weibull distributions has already been studied in the past and the so-called Weibull-to-exponential transformation has been created [95], [96], [97]. The use of this transformation simplifies the estimation of the confidence bounds and some other parameters of Weibull distribution. When using the transformation, the Weibull data is first transformed into exponential form where the

mathematical analyses, for example, the determination of the confidence bounds, are done. After that, the results are converted back to Weibull form.

In our case, the Weibull data (hazard rate) is converted into exponential type data format (constant hazard rate) by time-averaging the hazard rate within certain time intervals. The approximate information created is readily applicable in parts-count type system level reliability analyses. Conversion back to the Weibull regime is not needed.

7.2 Some Constant Hazard Rate Approximations of the Weibull Distribution

Exponential distribution and Weibull distribution are of different form and they have a different time-dependency. The only exception is the case when shape parameter of Weibull distribution β=1, in which case the two distributions are identical, with $\eta = \theta = 1/\lambda$. In this case, Weibull distribution characteristic lifetime η is equal to the Mean Time To Failure (θ) value of the exponential distribution. At all other times, the distributions are not identical and therefore, some approximation is needed in order to present the Weibull distribution data in terms of exponential distribution.

There may be different strategies to create a suitable approximation of the Weibull distribution. Although it is impossible to match all the distribution functions (hazard function *h(t)*, probability density function *f(t)*, cumulative density function *F(t)*, and reliability function *R(t)*) between the two distributions simultaneously, there is a possibility to match perfectly some individual functions.

After the 2-parameter Weibull data is transformed into constant hazard rate form, it can be utilized in MTTF calculations for the whole system. Therefore, it would be beneficial if the reliability function of the approximate exponential distribution $R(t)_{WB \to EXP}$ *would imitate the reliability function of the original Weibull distribution* $R(t)_{WB}$ as closely as possible, in other words

$$R(t)_{WB \to EXP} \approx R(t)_{WB} . \tag{42}$$

Another criterion to be fulfilled is that the form of the hazard function $h(t)_{WB \to EXP}$ should be kept as simple as possible, but it should still present the main characteristics of the original distribution. This means that preferably $h(t)_{WB \to EXP}$ =*constant at least for some time intervals*. Still, oversimplification should be avoided when trying to satisfy this criterion. Otherwise, some false conclusions might be drawn from the MTTF calculations.

Typically, the reliability test results of components are of increasing hazard rate type. Weibull distribution with two parameters, shape parameter β and the characteristic lifetime η, can fit the data satisfactorily many times. This will be discussed in detail in Section 7.7.1. The Weibull hazard rate is of the form [98]

$$h(t) = \frac{\beta \cdot t^{\beta-1}}{\eta^{\beta}}. \tag{43}$$

In order to approximate this function, one of the below strategies can be chosen:

Option 1: Pick some representative value of the hazard function at some selected time t.

Option 2: Calculate a time-averaged hazard rate value for the whole lifetime.

Option 3: Calculate a time-averaged hazard rate value for some time intervals.

Option 4: Pick values from the time-averaged hazard rate curve (option 2) between selected time intervals.

Option 5: Calculate time-averaged reliability function values for selected time intervals and based on those, calculate equivalent hazard rate values λ_{eq} for each time interval. The actual procedure will be explained later on in more detail.

In the following section, the five strategies above are discussed in light of the criteria given earlier in this chapter.

Let’s first give the formal definitions for options 2-5:

Option 2

The hazard rate of the option 2 is defined as the time-averaged value over the whole lifetime of the component

$$\left\langle h(t)\right\rangle_t = \frac{\int_0^t h(t')dt'}{\int_0^t dt'} = \frac{t^{\beta-1}}{\eta^\beta}. \tag{44}$$

It is noted that this value is dependent on time t. The above approximation is useful, if the expected lifetime or lifetime requirement for the component $t = t_{lifetime}$ is known. By inserting this value into Eq. (44), it results in one constant hazard rate value for the whole lifetime of the component.

Option 3

The third option can be calculated in a similar way as above, but this time, the time-averaged hazard rate will be calculated for selected time-intervals $\Delta t = t_{i+1} - t_i$

$$\left\langle h(t)\right\rangle_{\Delta t} = \frac{\int_{t_i}^{t_{i+1}} h(t)dt}{\int_{t_i}^{t_{i+1}} dt} = \frac{1}{\eta^\beta}\cdot\frac{\left(t_{i+1}^\beta - t_i^\beta\right)}{t_{i+1}-t_i}. \tag{45}$$

In this case, the hazard rate has a constant value in a selected time interval from t_i to t_{i+1}, i=0,1,2,…n, where n is the number of time intervals.

Option 4

This option is making use of time-averaged hazard rate function defined by Eq. (44). The hazard rate values used are defined as $\left\langle h(t_{i+1})\right\rangle_t$ during selected time intervals $\Delta t = t_{i+1} - t_i$.

Option 5

Utilizing option 5 requires a little more rigorous analysis. The strategy is to first solve the time-averaged value of the reliability function $\langle R_{WB} \rangle$ for selected time intervals $t_i ... t_{i+1}$. This can be accomplished by writing

$$\langle R_{WB} \rangle = \frac{\int_{t_i}^{t_{i+1}} R(t)dt}{\int_{t_i}^{t_{i+1}} dt} = \frac{\int_{t_i}^{t_{i+1}} e^{-\left(\frac{t}{\eta}\right)^{\beta}} dt}{t_{i+1} - t_i} = -\frac{\eta}{\beta(t_{i+1} - t_i)} \left\{ \Gamma\left(\frac{1}{\beta}, \left(\frac{t_{i+1}}{\eta}\right)^{\beta}\right) - \Gamma\left(\frac{1}{\beta}, \left(\frac{t_i}{\eta}\right)^{\beta}\right) \right\}, \quad (46)$$

where $\Gamma(\cdot,\cdot)$ is the incomplete gamma function. In Figure 27, the time-averaged reliability function is depicted.

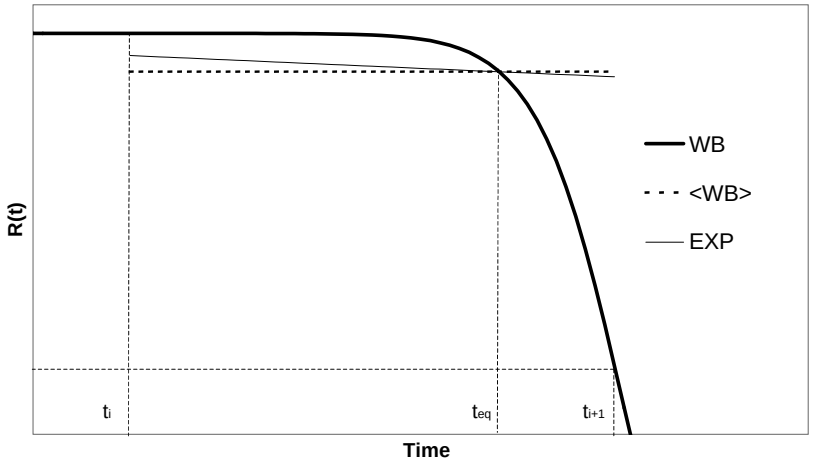

Figure 27. The Weibull reliability function $R(t)$ (WB), the time-averaged reliability function $\langle R_{WB} \rangle$ (<WB>), and the approximate exponential reliability function R_{EXP} (EXP) for time interval $t_i ... t_{i+1}$.

The instant in time t_{eq} ($t_i \le t_{eq} \le t_{i+1}$), at which the time-averaged reliability function is equal to the reliability function of the original Weibull distribution, may be written as

$$t_{eq} = \eta \cdot \left[\ln\left(\frac{1}{\langle R_{WB} \rangle} \right) \right]^{\frac{1}{\beta}}. \tag{47}$$

In order to obtain the corresponding equivalent constant hazard rate λ_{eq}, exponential reliability function R_{EXP} can be utilized

$$R_{EXP} = e^{-\lambda_{eq} \cdot t}. \tag{48}$$

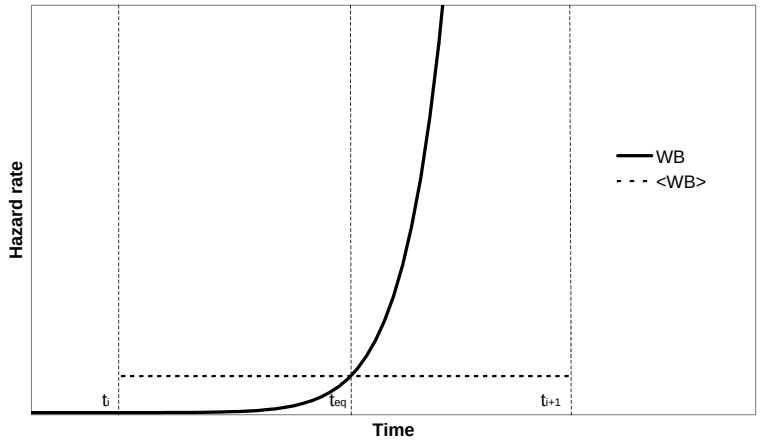

Figure 28. Hazard rate of Weibull distribution (WB) and the time-averaged value (<WB>).

To satisfy Eq. (42), it can be required that when $t = t_{eq}$, $R_{EXP} = \langle R_{WB} \rangle$. After solving for λ_{eq}, the following is obtained

$$\lambda_{eq} = \frac{\ln\left(\frac{1}{\langle R_{WB} \rangle}\right)}{t_{eq}}. \tag{49}$$

In Figure 28, the Weibull and time-averaged hazard rate λ_{eq} are depicted.

Later on, it will be shown that option 5 best fulfills the requirement given by Eq. (42). However, it may be demanding to calculate numerically the incomplete gamma function values accurately when time has large values, especially if β is large. In general, this is due to the lack of numerical solutions that are accurate enough for the incomplete gamma function, when variables have very large values.

7.3 Resulting Functions and Hazard Rates

In this section, the resulting functions and the approximate hazard rate values are studied in detail.

In Figure 29, all five approximate hazard rate options depicted for a component having η=3677 days and β=20 can be seen. The time interval selected in the time averaging was 5 years. The hazard rate for options 3, 4, and 5 is therefore constant in time-intervals 0…5 years, 5…10 years, 10…15 years, and 15…20 years.

The hazard rate for option 1 is selected to be 10,000 FITs corresponding to the hazard rate value of Weibull distribution in the middle of the lifetime (10 years=20 years/2). However, some other choice might have been justified as well. The hazard rate for option 2 is the time-averaged value for the whole 20-year lifetime obtained by utilizing Eq. (44).

The hazard rate for option 3 was obtained by utilizing Eq. (45) with time-interval $t_{i+1} - t_i$ = 5 years. Values for option 4 are picked from the curve plotted according to Eq. (44) at time instants of 5, 10, 15, and 20 years. The hazard rate for option 5 is calculated by utilizing the above-described method (Eqs. (46)-(49)), which is based on time-averaging of the reliability function.

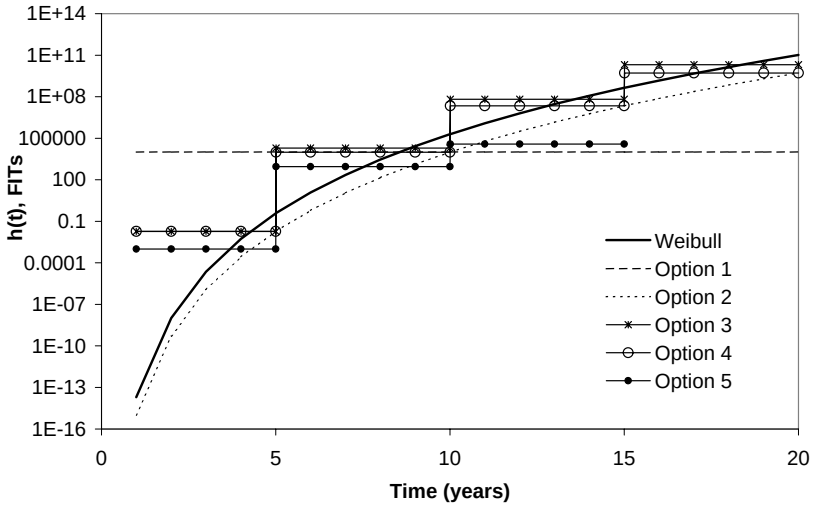

Figure 29. Weibull hazard rate and five approximate options. The selected time interval used in time-averaging is 5 years.

It is noted that the actual hazard rate obtains values from $2 \cdot 10^{-4}$ h to $1 \cdot 10^{11}$ h during the component's lifetime. Therefore, it might not be a good idea to use one single hazard rate value, as is the case in option 1. If doing so, there is a danger that the value picked is not representative of the risk level of the component at all instants of time. Also, utilizing option 2 with only one single hazard rate value results in a similar problem, although in this case the selection of the hazard rate is not arbitrary.

Keeping in mind the criterion stated in Eq. (42), the reliability function of the different options (Figure 30) should also be studied. Doing so, it can be noted that a perfect fit between the original Weibull reliability function and option 2 exists. The next best choices are options 5, 4, and 3. Option 1 has the worst performance. Therefore, it is not a suitable choice.

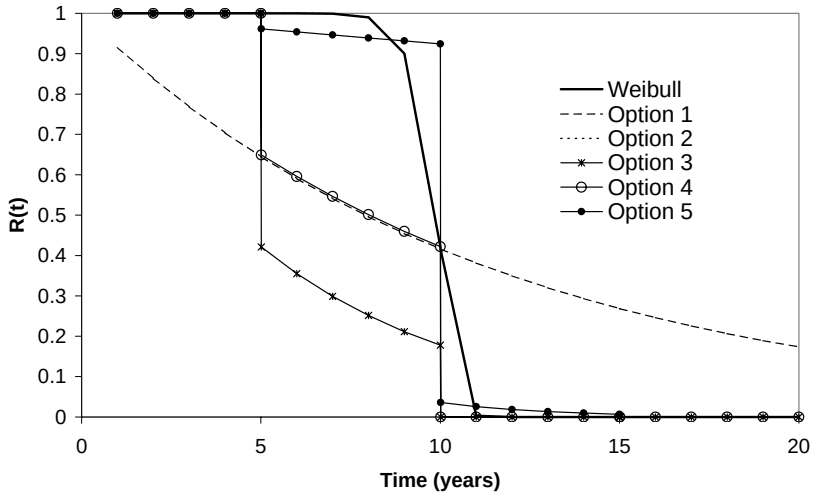

Figure 30. Reliability functions of the different approximation options. Option 2 data is overlapping with the Weibull data. The time interval used in the time-averaging is 5 years.

If the exact lifetime expectancy $t_{lifetime}$ of a component were known prior to the product launch, then option 2 would match exactly the original Weibull reliability function at $t = t_{lifetime}$. In this case, one would just pick $h(t_{lifetime})$ and use that in the MTTF calculations. This would represent the time-averaged value over the whole lifetime. However, in practice the true expected lifetime is not always known. Moreover, if wear-out is expected to take place during the operational lifetime, averaging over the whole lifetime may result in a very large hazard rate value. This would not give a proper picture of the reliability of the component during its early life period. Therefore, option 2 is attractive only if the hazard rate does not change much during the lifetime of a component.

Keeping in mind that

$$F(t) = 1 - R(t), \tag{50}$$

it is expected that the approximate options behave similarly when cumulative failure function $F(t)$ is concerned.

Looking at the density function $f(t)$, it may be noted that all the approximate solutions are a poor fit for the original Weibull distribution function (Figure 31).

One can also show, that

$$\int_0^\infty f(t)dt < 1 \tag{51}$$

in the case of options 2-4. Therefore, those options cannot be considered as true statistical distribution functions. The integration of a true distribution density function over time should always be equal to 1 [99].

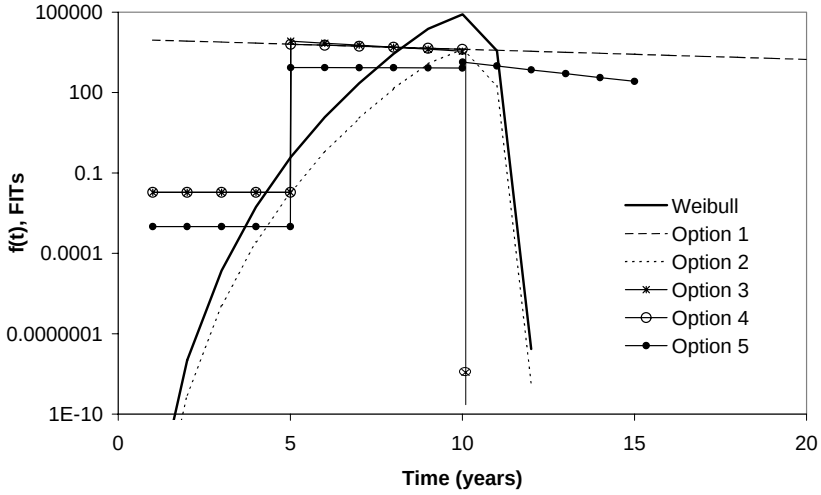

Figure 31. Reliability density function of the Weibull and those related to the approximate solutions.

When using options 3, 4, and 5, simple constant hazard rate values can be found for some selected time intervals, for example, in a tabulated form. This is demonstrated in Table 19 where the data of the above example is listed. Using option 4 does not gain a hazard rate value during time interval 15…20 years due to the lack of accurate numerical solutions to incomplete gamma function, as discussed earlier.

Table 19. Time-averaged hazard rate values for different approximate options.

	Approximate hazard rate (FITs)					
Time (years)	*Weibull*	*Option 1*	*Option 2*	*Option 3*	*Option 4*	*Option 5*
0…5	$2 \cdot 10^{-14}$...0.4	10,000	10^{-15}...0.02	0.02	0.02	0.001
5…10	0.4...200,000	10,000	0.02...10,000	20,000	10,000	899
10…15	200,000...$4 \cdot 10^{8}$	10,000	10,000...$22 \cdot 10^{6}$	$65 \cdot 10^{6}$	$22 \cdot 10^{6}$	37857
15…20	$4 \cdot 10^{8}$...10^{11}	10,000	$22 \cdot 10^{6}$...$5 \cdot 10^{9}$	$20 \cdot 10^{9}$	$5 \cdot 10^{9}$	N/A

This kind of data can be utilized directly in parts-count type system level MTTF calculations.

7.4 Properties of Different Options

Let's first look at option 2 in detail. The definitions of the statistical functions of option 2 are based on the exponential distribution function using the hazard rate obtained from Eq. (44). This is accomplished just by replacing the constant hazard rate value λ by the hazard rate value given by the above definition (Eq. (44)). The functions of the exponential distribution and option 2 are listed below in Table 20. The distribution functions derived for other options were also derived by replacing the exponential hazard rate function with the time-averaged hazard rate values.

Table 20. Exponential distribution functions and Option 2 related functions.

Statistical distribution function / Statistical function value		
	Exponential	*Option 2*
Hazard rate	$h(t) = \lambda$	$h(t) = \langle h(t) \rangle_t$
Distribution function	$f(t) = \lambda e^{-\lambda t}$	$f(t) = \langle h(t) \rangle_t e^{-\langle h(t) \rangle_t t}$
Cumulative distribution function	$F(t) = 1 - e^{-\lambda t}$	$F(t) = 1 - e^{-\langle h(t) \rangle_t t}$
Reliability function	$R(t) = e^{-\lambda t}$	$R(t) = e^{-\langle h(t) \rangle_t t}$

As already shown, the reliability function of option 2 is equal to the original Weibull reliability function at any selected instant in time t. Simple relations can be written between all statistical functions of 2-parameter Weibull distribution and those of option 2. Table 21 lists these relations. Inserting the hazard rate defined by Eq. (44) into option 2 distribution functions in Table 20 can verify that the relations are correct.

An important note is that although closed form results can be derived for option 2, option 2 is not a true distribution function, as it does not satisfy all the criteria required from a true reliability statistical function (Eq. (51)). Actually, it can be shown that the integration of this function, over time, is equal to $1/\beta$. This may sound a bit odd, as both the cumulative distribution function and the reliability function for option 2 get reasonable values and reach values in the whole scale (0…1). The explanation for this apparent contradiction is simply the fact that the cumulative distribution function, in this case, is defined by making use of exponential function - not by actually integrating the distribution density function of the option 2 over time.

Table 21. Statistical functions of the Weibull distribution, and their relationship to those of option 2.

Statistical distribution function / Statistical function value		
	Weibull	*Option 2, in terms of Weibull distr.*
Hazard rate	$h(t) = \frac{\beta t^{\beta-1}}{\eta^{\beta}}$	$\beta \cdot h(t)$
Distribution function	$f(t) = \frac{\beta}{\eta^{\beta}} t^{\beta-1} e^{-\left(\frac{t}{\eta}\right)^{\beta}}$	$\beta \cdot f(t)$
Cumulative distribution function	$F(t) = 1 - e^{-\left(\frac{t}{\eta}\right)^{\beta}}$	$F(t)$
Reliability function	$R(t) = e^{-\left(\frac{t}{\eta}\right)^{\beta}}$	$R(t)$

Option 3 fitted both to hazard rate and reliability functions of the true Weibull distribution (Figure 29 and Figure 30) relatively accurately. Looking more carefully at the hazard rate function of this option, it is noted that at the end of the first time interval, the value of the hazard rate function is equal to the time-averaged value of the hazard rate (option 2). During the next time intervals, the hazard rate of option 3 starts to approach the original (instantaneous) Weibull distribution hazard rate. In actual fact, it can be shown that when the number of time intervals n approaches infinity, the hazard rate functions of option 3 and instantaneous Weibull distribution approach each other. This is shown in Appendix C. The reliability function of option 3 has always got smaller values than the true Weibull distribution (Figure 30).

Option 4 is making use of the time-averaged hazard rate function defined by Eq. (44) at the end points of the time intervals. The reliability function is smaller than, or equal to, the

original Weibull distribution function at all instants in time. At the end points of the time intervals, the reliability function is equal to the values given by the Weibull distribution and is smaller elsewhere. Option 4 is a better match to the original Weibull reliability function than option 3.

Option 5 most resembles the original Weibull reliability function among those approximations that utilize time intervals. However, for very large time values, the calculation of the hazard rate may become cumbersome due to numerical solution accuracy limitations discussed earlier.

7.5 Comparison of the Selected Options

As discussed already in Section 7.2, there are at least two things that must be taken into account, when making practical choices about the hazard rate approximation function. The first one is that the reliability function of the approximation should closely imitate the original Weibull reliability function. Option 2 is superior to the others in this respect as it matches perfectly the original Weibull reliability function. The next best choices are options 5, 4, and 3. The use of a single, constant hazard rate value (option 1) has the worst accuracy over the lifetime.

The other important criterion is to keep the expression of the hazard rate as simple as possible. By doing so, it is possible to apply the calculated hazard rate values directly into the system level parts-count type MTTF calculations. In this respect, option 2 might not be a suitable choice, as it cannot be used in a tabulated form. All other options can be presented in a simple table form having constant hazard rate values either for the whole lifetime or for part of it.

To satisfy both criteria, option 5 seems to be the best choice, having the possibility to be used in a simplistic form (for example, table) and still match reasonably well the true reliability behavior of the component.

7.6 Selection of Time Intervals

When using the simplistic time-averaged hazard rates, the time intervals should be selected in a way that the reliability behavior can be imitated with acceptable accuracy. In order to be able to satisfy this criterion, the reliability function should be plotted in conjunction with the hazard rate of the component and then the lifetime should be divided into suitable time intervals. There should be at least one, but preferably several, time intervals in which wear-out has not yet fully occurred (let's say, $F(t) < 1\%$). The following time intervals may already include the wear-out phenomena related to high hazard rate values, and therefore the resulting time-averaged hazard rate value may be large in those intervals. When wear-out has occurred almost completely, the hazard rate gets values of infinite magnitude and using those in the MTTF calculations will result in a clear message; this component will fail at latest in the selected time interval. One interval indicating the end of the life of the component is enough for practical purposes.

7.7 Discussion

7.7.1 The motivation for selecting 2-parameter Weibull distribution

In this chapter, the 2-parameter Weibull distribution was selected to present the statistical behavior of components that face wear-out phenomena. Some other choice might have been possible, too. The selection of suitable statistical distribution has raised some discussion in the science community. In [49] 2-parameter Weibull distribution is recommended, whereas in [71] and [100] 3-parameter Weibull is considered superior over 2-parameter Weibull. Also, lognormal distribution is considered to fit the test results better than 2-parameter Weibull distribution. The conclusion that 2-parameter Weibull distribution is not very accurately presenting the test data is based on least-squares curve fitting results and the related small correlation coefficients obtained when fitting the test data to 2-parameter Weibull distribution.

Another argumentation used against 2-parameter Weibull distribution is that it is expected that there is a failure-free period of time (presented by the failure-free time γ in 3-parameter Weibull distribution) when testing solder attachments. One fact supporting this

is that according to Darveaux [5], it takes some finite time to initiate a crack in the solder material. One further observation made is that when fitting the test data to 2-parameter Weibull distribution the test data has a tendency to have downward sloping in the beginning of the wear-out period [71]. This is believed to indicate that there is a failure-free time that 2-parameter Weibull distribution cannot satisfactorily take into account. Furthermore, it is noted that if using 2-parameter Weibull distribution the reliability requirement based on it will be very demanding [71], [100].

Now, we try if we can verify that the 2-parameter Weibull distribution is accurate enough for practical purposes. The author is aware that using 2-parameter Weibull distribution will result in more demanding reliability requirement if very small percentages of failed items are considered. This is evident if comparing the behaviour of cumulative distribution functions. It is also ‘natural’ to consider that there is a failure-free period of time until first items start failing in the test. However, we think that in reality it is not impossible that items may fail very early. This may happen if the test vehicles are inherently very weak or if the test itself is very harsh. One should remember that as lifetime is often monitored in terms of number of cycles, this measure used is discretized, as the length of thermal cycle is finite. The first cycle may include the incubation period of some weak components. Still, from number-of -cycles viewpoint, it would seem that the failure occurs instantly. Therefore, the assumption of incubation period is not necessarily in conflict with the selection of 2-parameter Weibull distribution. Furthermore, author is not aware that there would be well-documented tests that would prove either 2-parameter or 3-parameter Weibull statistics to best describe the behaviour of test population, especially when very small cumulative failure percentages, such as 0.01%, are considered. This would require testing of hundreds or thousands of items, which is very difficult to arrange in practice. Therefore the discussion on the distribution function selection is at least partly speculative, as no actual proof exists.

Table 22. The top three distribution functions (in ranking order) that best fit the test data and their correlation coefficients [63].

	Top-3 distributions (ρ)	
Test env.	*Prototype*	*Production*
-40…+125 ºC	Lognormal (0.97)	3-P Weibull (0.95)
Batch 1	3-P Weibull (0.97)	2-P Weibull (0.92)
	2-P Weibull (0.97)	Normal (0.93)
	3-P Weibull (0.97)	2-P Weibull (0.96)
Batch 2	Normal (0.97)	Lognormal (0.99)
	2-P Weibull (0.96)	3-P Weibull (0.99)
0…+100 ºC	Lognormal (0.95)	3-P Weibull (0.97)
Batch 1	3-P Weibull (0.98)	Normal (0.98)
	2-P Weibull (0.97)	2-P Weibull (0.97)
	3-P Weibull (0.98)	3-P Weibull (0.99)
Batch 2	2-P Weibull (0.97)	2-P Exp. (-0.94)
	Normal (0.97)	2-P Weibull (0.94)
+30…+80 ºC	3-P Weibull (0.99)	2-P Weibull (0.99)
Batch 1	Lognormal (0.99)	Normal (0.97)
	2-P Weibull (0.96)	3-P Weibull (0.99)
	3-P Weibull (0.99)	-
Batch 2	Lognormal (0.96)	
	2-P Weibull (0.96)	

On conceptual level it is impossible to decide which argumentation is more correct. In [63] more than 200 CBGA components assembled using lead-free solder were tested using thermal cycling. Weibull++© software was used to fit the test results. Three most obvious statistical distributions were observed and their parameters were recorded. Also the correlation coefficient ρ values were recorded in order to check how accurately the distribution fits the test data (Table 22). The values for 2-parameter Weibull distribution were in all cases very high (ρ =0.92...0.99). This implicates that the 2-parameter Weibull

distribution is a proper selection if applied to solder fatigue lifetime data. However, it must be admitted that in most cases 3-parameter Weibull distribution has slightly larger correlation coefficient values than 2-parameter Weibull distribution has (Table 22). However, the differences measured in terms of correlation coefficient are very small.

In the references [71] and [100], only least-squares method and the related correlation coefficients were used to compare the curve-fitting accuracy. However, there are also some other methods to check the accuracy of the curve-fitting results [99]. The ranking procedure built-in Weibull++© software was tried. The weighting based - on which the ranking was performed - was: Kolmogorov-Smirnov test 50%, least-squares method 20% and maximum likelihood method 30%. In all cases, the 2-parameter Weibull distribution proved to be in the top-3 list of distributions among 6 possible distributions.

Our test data cannot support the ‘downward sloping’ described in [71]. A term defined in Section 5.6, Comparison Ratio (C.R.) was used to test if the first failure recorded in the test fits well the distribution function selected.

In Table 23, the C.R. values are shown. In four cases the C.R. value is within 10% of the nominal value of 1 representing a very good fit. In four cases the ‘downward sloping’ (C.R.>>1) is recognized and in two cases ‘upward’ sloping (C.R.<<1) is noted. The reason, that our data does not support the ‘downward sloping’ to be a common phenomenon, may be partly explained by the fact that we did not remove ‘drops’ from the test data. In [71], some data points were removed as they were considered as ‘early drops’ due to ‘data transcription error, test set-up problems, bad test parts, or faulty solder joints’. Removing ‘drops’ may have resulted in both the ‘downward sloping’ phenomenon and the 3-parameter Weibull distribution to appear superior over 2-parameter Weibull distribution.

One problem related to 3-parameter Weibull distribution lies in the fact that the failure-free time parameter γ sometimes obtains meaningless, negative values. This occurred in 3 out of 11 cases in our test population. Therefore, the use of 3-parameter Weibull is limited if meaningful parameters are expected.

Table 23. Comparison ratio (C.R.) values for different test set-ups.

	C.R.	
Test env.	*Prototype*	*Production*
-40…+125 ºC	1.03 (Batch 1) 1.10 (Batch 2)	1.82 (Batch 1) 1.60 (Batch 2)
0…+100 ºC	1.03 (Batch 1) 1.53 (Batch 2)	1.06 (Batch 1) 0.98 (Batch 2)
+30…+80 ºC	0.86 (Batch 1) 0.85 (Batch 2)	1.22 (Batch 1) - (Batch 2)

Based on our experience 2-parameter Weibull distribution is an acceptable choice due to its good correlation to the test data and the parameters that always obtain reasonable values.

7.7.2 Constant failure rate and its origin in the field failure data

In the field environment, constant hazard rate at the product level is often recorded although components may fail due to wear-out phenomena. The reason that we observe the exponential portion of the bathtub curve for a population of products is in part because of repairs, and in part because of random overstress events through the lifetime of the population. If the data is grouped by failure mechanisms, then it is highly doubtful that we would see an exponential distribution for each group. It is more likely that we will see a collection of Weibull distributions, each with $\beta \neq 1$, indicating that either early failures or wear-out mechanism are taking place. However, at the system level, this can be represented with an averaged quasi-constant hazard rate.

7.8 Conclusions

In this chapter, some options to approximate the Weibull hazard rate are proposed and studied. The time-averaged options are studied both from a theoretical and a practical point of view. It seems that a reasonable compromise between accuracy and usability, and easy

applicability in the MTTF calculations can be found. Attention should be paid to the selection of time intervals, so that the true reliability behavior can be imitated with reasonable accuracy.

Option 1 cannot be recommended due to its limited accuracy. Time-averaging over the whole lifetime (option 2) is a good choice if the hazard rate does not change very much during the expected lifetime of the component. However, if the hazard rate changes considerably during the life span of a component, it is recommended that the options with time intervals be applied.

Among options utilizing time intervals, option 5 seems to be the most accurate one. This is due to the fact that its reliability function best matches the reliability function of the original Weibull function. Option 4 is also a good selection, although its accuracy is not as good as that of option 5. In the case of option 3, the time-averaged hazard rates in a series of time intervals, approach the instantaneous Weibull hazard rate as the number of time intervals approach infinity. Therefore, option 3 is not a very good choice.

If wear-out is expected during the lifetime of a component, option 5 seems to be the best choice due to its acceptable accuracy and easy applicability. The incomplete gamma function, utilized when calculating hazard rate values for option 5, may be difficult to calculate accurately due to a lack of suitable numerical solutions. This problem is, however, expected to take place only in cases when wear-out has already severely damaged the performance of the component population.

The methodology to create time-averaged constant hazard rates described above has been successfully utilized in conjunction with the 2^{nd} level interconnection reliability issues. This work has been documented in several conference papers [61], [82], [101].

8 The Effect of the Introduction of High-Risk Electronic Components into 3rd Generation Telecommunications Systems

8.1 Terminology

The terminology when considering non-repairable and repairable systems is unfortunately far from being well established [57], [98], [102]. In this chapter, at component level considerations, the term ‘hazard rate’ is used. In conjunction with repairable systems, ROCOF (rate of occurrence of failures) is applied. The hazard rate is a function of the life distribution of a single unit and an indication of the ‘proneness to failure’ in a time unit after time *t* has elapsed, while ROCOF is the occurrence rate of failures for a stochastic point process.

In the latter part of this chapter, a repairable system is considered. Some terms need to be explained in order to be able to understand the following text.

IID is an acronym for Independent, Identically Distributed. This term is used in conjunction with times to failure in a stochastic process. IID property means that the times to failure are independent samples from the same distribution function.

IIED is an acronym for Independent, Identically Exponentially Distributed. This term means that the times to failure are independent samples from the same *exponential* distribution.

HPP stands for Homogeneous Poisson Process. HPP is a counting process with IIED inter-arrival times. HPP has a constant ROCOF.

8.2 Introduction

In this chapter, the dependability of the 3rd generation telecommunications network systems is studied. Special attention is paid to a case when increased-reliability-risk electronic components are introduced to the system. Earlier in this thesis, only component

level reliability assessments have been performed. However, as discussed in Section 4.5, component reliability should be considered in conjunction with reliability targets and requirements of larger entities. By doing so, it is easier to set realistic reliability requirements for the components based either on the PWB or the product level reliability requirements. Thus, the component selection can be optimized, and at the same time, the satisfaction of the lifetime expectations can be guaranteed. In the following, the reliability assessment is further extended to cover a whole telecommunications system. The acceptable operation of the telecommunications system is needed, as it may even be a matter of safety, since dropped calls in case of emergency situation are highly undesirable. Furthermore, the telecom operators expect that the manufacturers can provide them with systems that are trustworthy and perform predictably.

The chapter consists of three parts: First, the reliability data of four electronic components is considered. This includes statistical analysis of the reliability test data, thermo-mechanical Finite Element Analysis of the printed wiring board assemblies, and based on those, a field reliability estimate of the components is given. Second, the component level reliability data is introduced into the network element reliability analysis. This is accomplished by using a reliability block diagram technique and Monte Carlo simulation of the network element. The end result of the second part is a reliability estimate of the network element with and without the high-risk components. Third, the whole 3rd generation network, having multiple network elements is analyzed. In this part, the criticality of introducing high-risk electronic components into 3rd generation telecommunications network is considered.

8.3 Background

The telecommunications infrastructure industry has a tradition of having demanding quality and reliability requirements close to those of military and space applications and having similar reliability prediction methods [93], [103]. This is due to the need to guarantee high availability of telecommunications systems at all times. This requirement is based on telecom operators' needs and requirements.

In the past, the military industry was driving the electronic components industry. At that time, high reliability was of the utmost importance and cost was not a major issue. After the cold war period, the volume of military industry has diminished. Nowadays, the electronic component technologies are driven primarily by consumer industry demands. Those include low cost and small size electronic components. Reliability is not always the major driver. Therefore, it is not anymore self-evident that all the components in the marketplace conform to high reliability requirements.

In order to satisfy the long-term reliability goals the manufacturers of the infrastructure equipment must take an active role in selecting and validating components that are used in their products. The component level reliability work should be linked to system level dependability goals. In this chapter, reliability qualification, starting from component level reliability tests and concluding with network level availability considerations are described.

Similar approaches to link physical lifetime predictions with the higher hierarchy level reliability assessment to be presented in this chapter can be found in the literature [26]. The methods utilized are partly the same. For example, Monte-Carlo simulation and Reliability Block Diagrams (RBD) have been utilized, as will be done also in this chapter. However, some fundamental differences exist. In the reference, ‘the system’ studied is a semiconductor device and ‘the elementary object’ studied is, e.g., a metal run if electromigration of conductors is considered. Here, ‘the system’ is a full telecommunications network and ‘the elementary object’ is a component. Furthermore, in this chapter, both systems that are repaired and those are not repairable are studied. In the reference, the reliability assessment is limited to non-repairable devices.

The effect of physical failure mechanisms on the functionality of electrical devices has been studied in [46] and [104]. These references provide some alternative ways to account for physical lifetime models in reliability assessment of larger entities. In these references, the link between the physical reliability prediction for an elementary object and the functionality of the device is established through circuit simulation techniques.

8.4 Component Level Reliability Assessment

The empirical part of this chapter consists of some thermal cycling tests, the statistical analysis of the results of these tests, and the field failure prediction based on Finite Element Analysis.

Three components were tested [105]: The first one (component A) was a Multi-Chip-Module (MCM) made of Low Temperature Cofired Ceramics (LTCC) (CTE=5.8 ppm/°C) material and having a Ball Grid Array (BGA) type of 2nd level interconnection. The size of the module was ca. 20 mm*30 mm. All the critical solder balls (ϕ=1.27 mm) were confined in a 7.6mm*7.6mm matrix in the middle of the substrate. Besides the central ball matrix, larger 3.4 mm *3.4 mm size pads were also used, where four balls per pad were soldered. Special pad metallurgy and other proprietary, structural arrangements were used to strengthen the interconnection structure.

The second component (component B) was an alumina (CTE=7.0 ppm/°C) based Dual In Line (DIL) component having solder castellations as an interconnection media. The size of the component was 19.0 mm* 6.5 mm. The solder castellations (altogether 12 pcs.) were placed in the middle of the longer edges having a pitch of 1.9 mm.

The third component (component C) was an MCM made of HTCC material (CTE=7.0 ppm/°C). The size of this BGA (ϕ=0.80 mm) 21*21 ball matrix was ca. 36 mm* 36 mm.

The fourth component (component D) was a very large organic BGA component having 1788 solder balls (ϕ=0.6 mm) as interconnection media. The thickness of the organic board was 1.15 mm and the area was ca. 45 mm * 45 mm. A silicon chip of size ca. 18 mm * 18 mm was attached to an organic substrate. The chip was covered with a copper lid. This component was not actually tested. The reliability prediction is therefore based on Finite Element Analysis only.

The components were assembled on a 1.6 mm thick FR-4 printed wiring board. The thermal cycle was a 1-hour cycle from –40 to +125 °C with 15 minutes dwell times at both temperature extremes. The failure analysis consisted of cross-sectioning and visual inspection. In some cases, X-ray was also used to discover the failure mechanism. Before

the tests were run, there were some doubts whether the harsh test environment could induce failure mechanisms that were different from those that take place in the field. To check this, some test vehicles were exposed to a more benign 20-minute thermal cycle from 0 to +100 °C (Figure 8). However, no signs of change of failure mechanism were observed. Therefore, the assumption that the discovered failure mechanism was representative of the true failure mechanism to be found also in the field was made. The failure mechanism in all cases was solder fatigue.

8.5 Test Results and Their Interpretation

After fitting the test results using least-squares method, the Weibull parameters listed in Table 24 is obtained.

It is noted that almost all components had difficulty in passing the often-used no-failures-in-1000-cycles criterion. The relatively large shape parameter β values reflect the fact that the quality deviation of the components tested was small.

Finite Element (FE) analysis was used to calculate the acceleration factors. The number of cycles in the field environment was obtained by multiplying the number of cycles in the test environment by the acceleration factor. It was assumed that the components were addressed to a ‘Day hard’ thermal cycling in the field. This field environment is described in Section 5.7 in detail. The shape parameter was considered to be the same in both test and field environments.

Table 25 lists the predicted field performance of the tested components.

Table 24. Reliability test results of the increased-reliability-risk components.

Component	*Characteristic lifetime, η / # cycles*	*Shape parameter, β*
A	1886	5.82
B	981	7.53
C	821	5.42
D	2414*	20

* This value is based on Finite Element Analysis, not on test results.

The characteristic lifetimes η are relatively large in all cases. This, however, does not necessarily guarantee that the reliability of these components would be at an acceptable level, as η represents an instant in time at which 63.2% of the component population has already failed.

Table 25. Field lifetime prediction of the increased-reliability-risk components.

Component	*Predicted characteristic lifetime in the field, η / years*	*Shape parameter, β*
A	25.8	5.82
B	12.9	7.53
C	11.2	5.42
D	10.1	20

Therefore, the statistical behavior of the component population needs to be considered.

8.6 Network Element Dependability

8.6.1 General

Since the four components tested have an increased reliability risk related to their 2nd level interconnections, it is important to study what the effect is, if such components would be used in a network element (NE). This gives a concrete indication if the components studied are at an acceptable reliability level or if they should not be used. In the following sections, the network element dependability is studied. NE with and without the high-risk components is considered.

A WCDMA base station (Node B) is used as an example of a network element. It should, however, be noted that the reliability figures used here are arbitrary, although the magnitude may be close to representative. The same also holds when considering the other NEs to be introduced later on in the following section. Actually, it is assumed that the lifetime of all network elements are distributed exponentially with Mean Time To Failures (MTTF) of 793.95 years (6,955,000 hours). The repair distribution of all NEs is considered to be exponentially distributed with a Mean Time To Recovery (MTTR) of 1 hour. The reliability function of the exponential distribution is given as [106]

$$R_{EXP} = e^{-\left(\frac{t}{\theta}\right)}, \tag{52}$$

where $\theta = MTTF$ and t is time.

The reliability function of the 2-parameter Weibull distribution is given as [106]

$$R_{WB} = e^{-\left(\frac{t}{\eta}\right)^{\beta}}, \tag{53}$$

where η is the characteristic lifetime and β is the shape parameter.

Because the lifetime of the network is exponentially distributed and the high-risk components follow 2-parameter Weibull distribution, the arrangement can be presented as a reliability block diagram (RBD), as depicted in Figure 32.

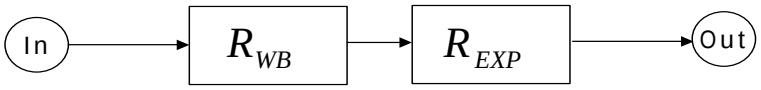

Figure 32. Reliability block diagram of a series connection of a network element whose lifetime is exponentially distributed (EXP) and a high-risk component with lifetime distribution of 2-parameter Weibull type (WB).

This series configuration represents the most pessimistic scenario, as it is assumed that no redundancy is used and that the failure in the high-risk component always causes the whole NE to fail. This may not always be the case in reality.

8.6.2 Non-Repairable NE

As the complexity of the RBD of the series connection is relatively low, it is possible to obtain most of the distribution functions in closed form. For example, the reliability of the NE is given simply as

$$R = R_{EXP} \cdot R_{WB} = e^{-\left(\frac{t}{\theta}\right)} \cdot e^{-\left(\frac{t}{\eta}\right)^{\beta}}, \tag{54}$$

where R is the reliability function of the NE after the introduction of a high-risk component with interconnection related reliability risk, R_{EXP} is the reliability function of the NE without the high-risk component, and R_{WB} is the reliability function of the component having the interconnection related reliability risk.

The probability density function $f(t)$ and the hazard rate function $h(t)$ of the series-connection can be attained by applying the definitions of the $f(t)$ and $h(t)$ [106] resulting in

$$f(t) = \frac{dF(t)}{dt} = -\frac{dR(t)}{dt} = \frac{1}{\theta} e^{-\left(\frac{t}{\theta}\right)} e^{-\left(\frac{t}{\eta}\right)^{\beta}} + \frac{\beta}{\eta}\left(\frac{t}{\eta}\right)^{\beta-1} e^{-\left(\frac{t}{\eta}\right)^{\beta}} e^{-\left(\frac{t}{\theta}\right)} \tag{55}$$

$$h(t) = \frac{f(t)}{R(t)} = \frac{1}{\theta} + \frac{\beta}{\eta}\left(\frac{t}{\eta}\right)^{\beta-1}. \tag{56}$$

Now, the reliability behavior can be anticipated, as all the relevant reliability functions of the series-connected system are defined.

In Figure 33, the reliability functions of the series connection of the NE with and without the high-risk components are depicted.

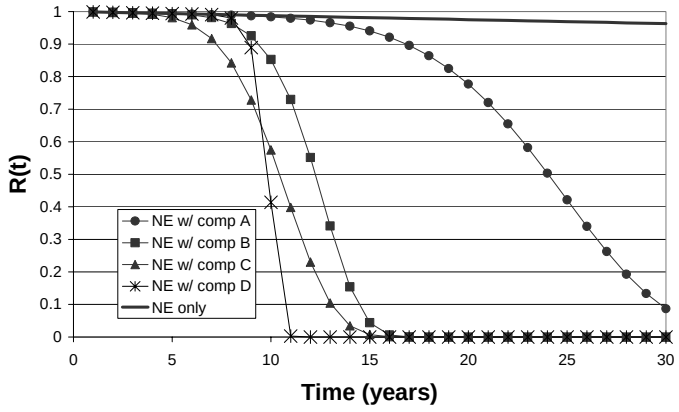

Figure 33. Reliability function of the network element with and without the high-risk components.

It can be seen, that without the high-reliability-risk components the NE performs very well. The performance degradation related to the high-risk components is clearly visible. Without the high-risk components it would be anticipated that the share of the failed components would be less than 5% for the whole 30-year lifetime of the system. However, after introducing the new components, the 5% failure limit is already reached after 14, 8, 6, and 9 years for the NE with components A, B, C, and D, respectively.

The probability density function of the system, with the high-risk components introduced is depicted in Figure 34. It is noted that the reliability behavior of the whole system follows, quite closely, the reliability behavior of the critical components, as the peaks in the density function are coincidental with the attainable lifetime values of the high-risk components.

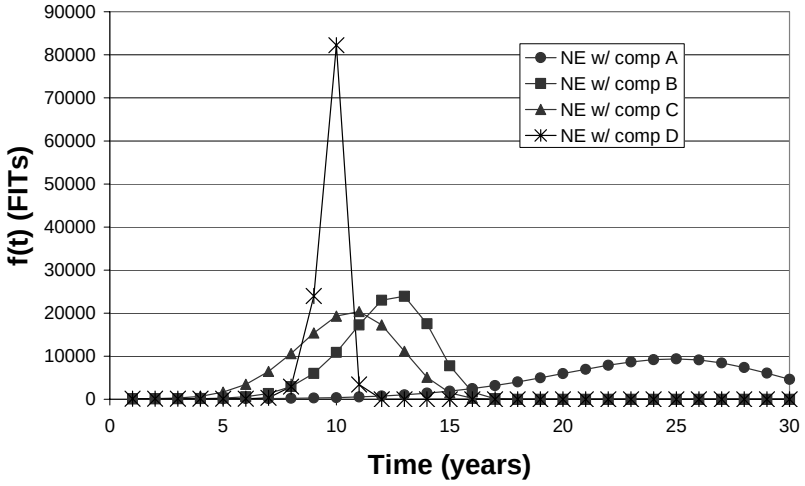

Figure 34. Probability density function of the network element with high-risk components included.

Two common measures, the mean lifetime and the variance, for the NE including the high-risk component can be calculated, but this time the integration must be accomplished numerically, as no closed-form solution exists.

The mean $E = \int_0^\infty t f(t) dt$ has the form

$$E = \int_0^\infty \left[\frac{1}{\theta} e^{-\left(\frac{t}{\theta}\right)} e^{-\left(\frac{t}{\eta}\right)^\beta} + e^{-\left(\frac{t}{\theta}\right)} \left(\frac{t}{\eta}\right)^\beta \left(\frac{\beta}{t}\right) e^{-\left(\frac{t}{\eta}\right)^\beta} \right] t dt . \quad (57)$$

And the variance is $Var = \int_0^\infty \left(t - E^2\right) \cdot f(t) dt$.

The mean and the variance values of the lifetime of the NE are tabulated in Table 26.

Table 26. Mean lifetime and variance values of the series connection of the network element with the high-risk components.

NE w/ component	*Mean, E / years*	*Var / years*
A	23.5	27.6
B	12.0	4.3
C	10.3	5.2
D	9.77	0.8

8.6.3 Repairable NE

When considering a repairable system, the RBD depicted in Figure 32 is interpreted as a Superimposed Renewal Process (SRP). This means that the two blocks are renewed (=replaced by ‘as good as new’) after they have failed and that the overall SRP observed is a superposition of the two independent renewal processes.

In Figure 35, a general SRP is depicted. It consists of several renewal processes (RP), whose superposition is the SRP. The interarrival times $X_1, X_2, X_3, ... X_n$ describe the time between subsequent failures.

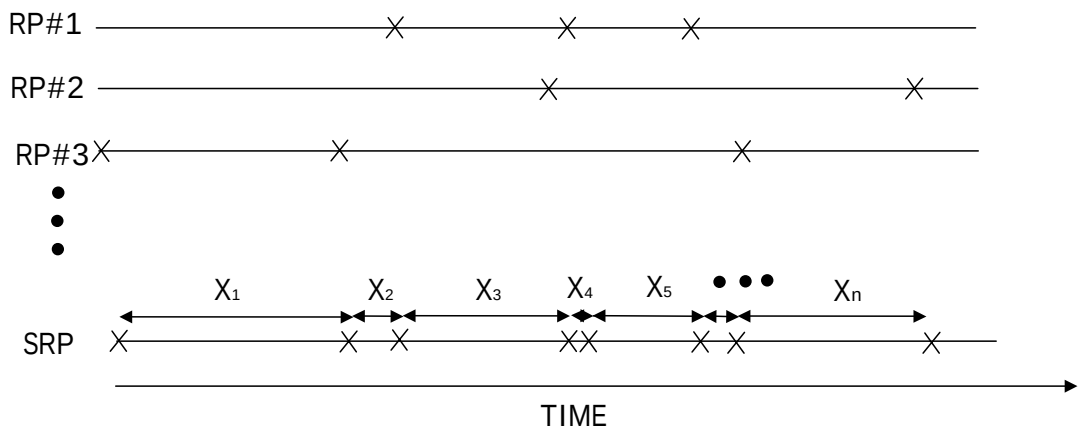

Figure 35. Superimposed renewal process. Crosses denote failures and $X_1, X_2, X_3, ...X_n$ are the interarrival times. Times needed to recover the system are not depicted, as they are typically much smaller than the interarrival times.

Drenick has shown that the superposition of an infinite number of independent renewal processes approaches a Homogeneous Poisson Process (HPP) after an infinite number of system failures has occurred [107]. This means, that although underlying lifetime distributions of the individual renewal processes may not be exponentially distributed, the lifetime distribution of the superposition of those will approach independent, identically exponentially distributed (IIED) behavior when time approaches infinity. In practice, a limited number of renewal processes, with only some tens of system failures already approach the HPP [102], [111]. The asymptotic behavior is very often assumed, although that may not always be the case in reality [102].

A repairable system can be analyzed by applying the concept of availability. The *steady-state* availability A is defined as [98]

$$A = \frac{MTBF}{MTBF + MTTR}, \tag{58}$$

where $MTBF$ is Mean Time Between Failures and $MTTR$ is Mean Time To Recovery. Assuming that $MTBF >> MTTR$ and that the interarrival times $X_1, X_2, ...X_n$ are independent and identically, exponentially distributed (IIED), then $MTBF \approx MTTF$ can be written. When the interarrival times are independent, and identically distributed (IID),

but not exponentially distributed, the $MTBF$ can be approximated by the mean lifetime E. The mean lifetime of the Weibull distribution E, can be discovered by utilizing Gamma function $\Gamma(\cdot)$ [108] as

$$E = \eta \cdot \Gamma(1 + \frac{1}{\beta}). \tag{59}$$

The steady-state availability A of the series connection of two components having availabilities A_1 and A_2, can be stated as [98]

$$A = A_1 \cdot A_2. \tag{60}$$

By applying the above formulas it is possible to calculate the availability of the NE with and without the introduction of the high-risk components.

In the following sections, it is assumed that a representative value of $MTTR = 1$ hour for both the NE and the high-risk component can be utilized. In Table 27, the results for the repairable system are listed.

Table 27. Steady-state availability, Mean-Time-Between-Failures, and Mean-Down-Time values for the network element with and without the increased-reliability-risk components [109].

Configuration	*Availability*	*MTBF, years*	*MDT/ year, minutes*
NE only	0.999 999 856	793.95	0.08
NE w/ comp A	0.999 995 085	23.20	2.58
NE w/ comp B	0.999 990 445	11.93	5.02
NE w/ comp C	0.999 988 822	10.20	5.88
NE w/ comp D	0.999 988 233	9.69	6.19

It can be seen that even a single high-risk component may introduce a very serious effect on the NE performance, as both *MTBF* and *MDT* are degraded by almost two orders of magnitude if utilizing a high-risk component in the NE. Although the example used here represents the ultimately unfavorable situation (a series connection), it can be assumed that the introduction of high-risk components may also have a serious effect on the NE performance in real life. Preventive maintenance would probably be beneficial in this case, especially if long lifetime requirements for the NE are used. Preventive maintenance can, at least partly, restore the original favorable NE reliability situation. Other options to rectify the situation are the replacement of the high-risk component with another one that has better reliability performance or by making a design modification. Such a modification may mean, for example, the use of a leadframe package, which adds flexibility to the interconnection structure and thus enhances the 2nd level interconnection reliability. The realignment of solder joints in order to decrease the distance to the neutral point, or the change of solder material or the amount used can be tried as well. The change of solder metallurgy may in some cases play an important role.

The above availability analysis was made under steady-state assumption. In reality, the availability values are time-dependent and differ from the above mentioned.

This can be seen when looking at Figure 36-Figure 39, where the estimated interarrival times $E[X_i]$ are plotted against the number of NE failures. Monte Carlo simulations were run in order to calculate the time-dependent interarrival times. The software used was Raptor [110]. To guarantee an acceptable convergence of the results, the following number of iterations was used: 2000 iterations for 1st and 2nd failures, 1500 iterations for 5 failures, 1000 iterations for 10 failures, and 500 iterations for 20 and 35 failures. The non-repairable and the steady-state data are also depicted in the same figures.

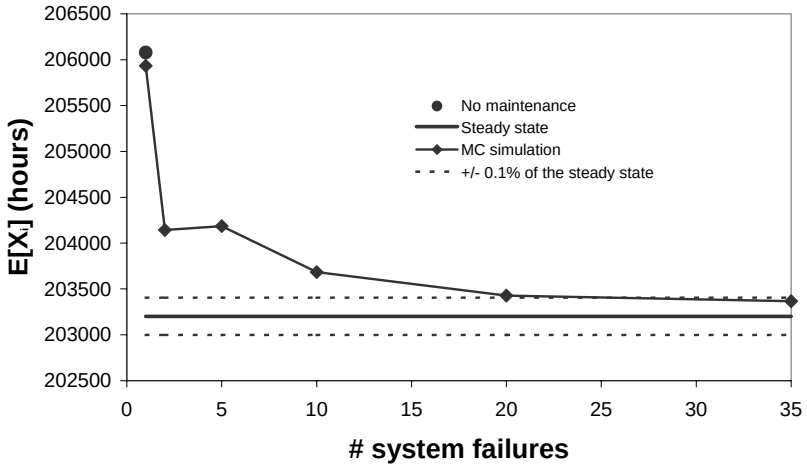

Figure 36. Estimated interarrival times of the network element with high-risk component A.

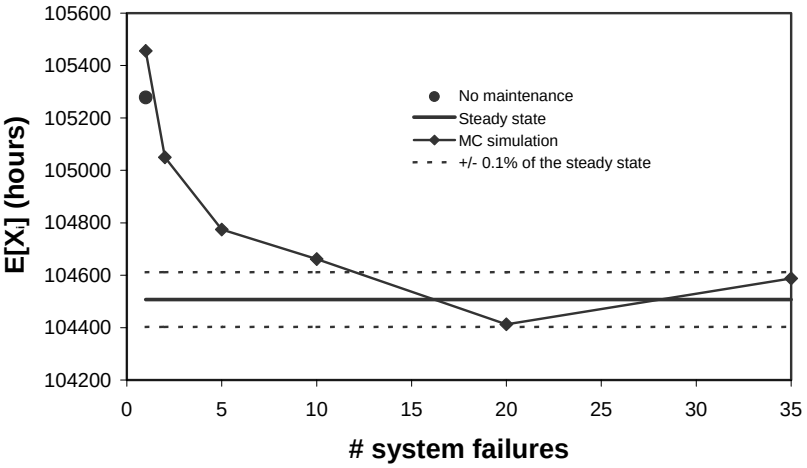

Figure 37. Estimated interarrival times of the network element with high-risk component B.

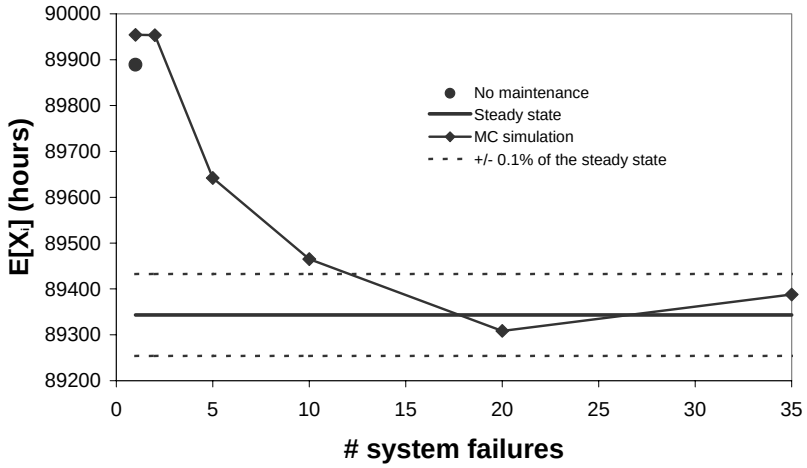

Figure 38. Estimated interarrival times of the network element with high-risk component C.

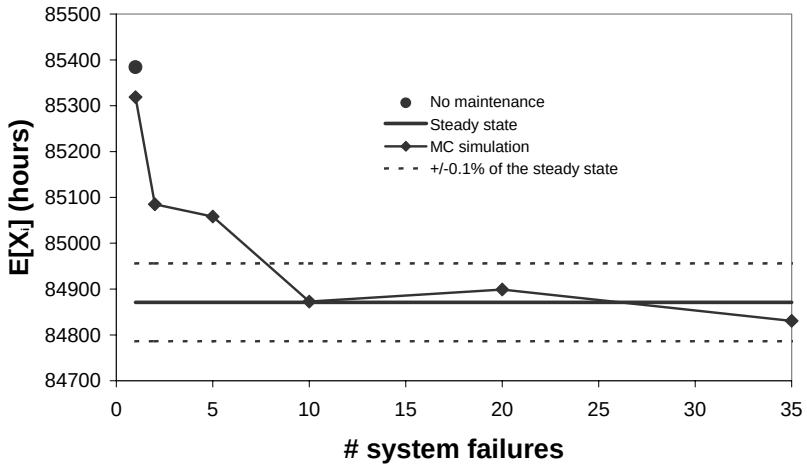

Figure 39. Estimated interarrival times of the network element with high-risk component D.

Looking at the figures, it is noted that a relatively good correlation between the manual calculations (steady-state and non-repairable system data) and the Raptor simulation results. It looks like the steady-state is reached already after ca. 10 system failures. The fact that interarrival times are approaching a steady-state, constant interarrival time condition does not necessarily indicate that the SRP is approaching HPP. This is due to the fact that the actual lifetime distribution is not known. It should be of exponential type if the process is HPP. When utilizing a shareware version of the Raptor software it was not possible to monitor the individual interarrival times. Therefore, it is not possible to verify if the lifetime is of exponential type and if the steady-state is truly reached after 10 system failures. However, 10 system failures seem to be a smaller number than proposed by Keats and Chambal [111]. It should, however, be remembered that the value of 30 system failures until the steady-state given by Keats and Chambal is reached is a generic limiting value for convergence given for an arbitrary complexity level and underlying component statistical distribution.

However, as the interarrival times (10…24 years) are quite large compared to the expected lifetime of the NEs in the field it is clear that it is enough to study the time-interval having the first 1…3 failures. Therefore, in the following paragraphs, time-averaged availability figures are utilized.

The time-dependent average availability is defined as [112]

$$A_{avg} = \frac{1}{T}\int_0^T A(t)dt\,, \tag{61}$$

where T is the time-interval along which the availability is monitored and $A(t)$ is the point availability. In the following, $T = 20$ years was used. After a Monte Carlo simulation (2000 iterations) the following availabilities were obtained (Table 28).

Table 28. Time-averaged availability values of the network element with increased-reliability-risk components.

NE w/ component	*Mean A(20 years)*
A	0.999 998 810
B	0.999 993 664
C	0.999991 849
D	0.999 990 589

It is noted that when comparing Table 27 and Table 28, the time-averaged availability values are slightly larger than the steady-state values, as expected.

8.7 Dependability of the 3GPP Network System

8.7.1 Network Architecture

In the following section, the dependability of the third generation telecommunications networks is studied. The topology analyzed is based on 3GPP (3rd Generation Partnership Project) Release 99 recommendations. The somewhat simplified model utilized here is based on the work of Kumar et al [113]. The simplifications used are mostly related to the integration of some NEs, which makes the analysis somewhat easier. The simplified version of the network is depicted in Figure 40. A more detailed description can be found in the technical specification document (3GPP TS-TS 23.002, 2002 V3.5.0) on the Internet [114].

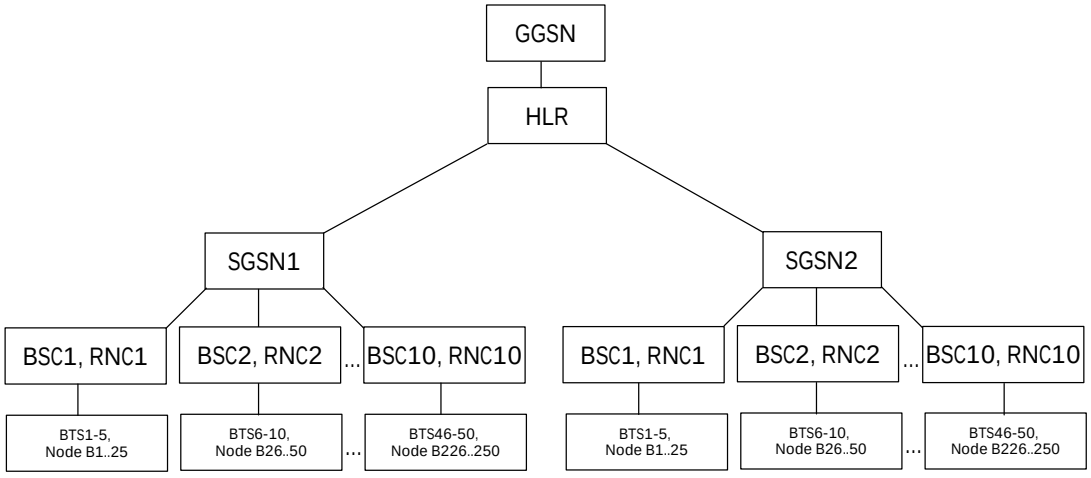

Figure 40. Simplified 3rd generation telecommunications network.

A network system can be divided into two parts: Access Network (AN) and Core Network (CN). Furthermore, Access Network is sub-divided into GERAN (GSM/EDGE Radio Access Network) network and UTRAN (UMTS Terrestrial Radio Access Network) network. GERAN consists of base station transceivers (BTS) and base station controllers (BSC), while UTRAN is composed of base stations (Node B) and Radio Network Controllers (RNC). GERAN offers Time Division Multiple Access (TDMA) based radio technology, such as GSM and/or GPRS, whereas UTRAN offers Wideband Code Division Multiple Access (WCDMA) based radio technology.

Core Network (CN) has two domains: Circuit Switched (CS) and Packet Switched (PS). The CS domain handles real-time type of traffic/services and PS domain handles non-real-time type traffic/services.

The Core Network in the following is somewhat simplified. It is assumed that it consists of a Mobile Switching Center (MSC), Home Location Register (HLR), Serving GPRS Support Node (SGSN), and Gateway GPRS Support Node (GGSN) only. In reality, some other functions do exist, but for simplicity's sake some functions are considered to be integrated into the above-listed NEs. MSC is managing CS connections. HLR stores

mobile subscriber parameters. SGSN is in charge of mobility management, packet transfer, charging, and admission control. GGSN is the interface to external data networks.

In the availability analysis, it is assumed that there are no functional dependencies between the NEs.

8.7.2 Availability Analysis of the 3rd Generation Network

In the following section: *first*, it is assumed that in order for the network to be in 'up' state *all NEs need to be functional*. This may add some pessimism to the analysis, as some other choice of definition for a functional network could have been chosen. In this analysis, the systems with and without the high-risk components are analyzed. In case high-risk components are introduced to the system, only Node Bs are considered to contain the high-risk components. All other NEs have the generic availability value of $A = 0.999\ 998\ 856$ at all times. The availability values of Node Bs are chosen to be average availabilities calculated for the first 20 years of operation. This is probably the best approximation, because the steady-state values seem to be slightly over-pessimistic, as discussed in Section 8.6.3.

In the *second case, some Node Bs are allowed to be in 'down' state*. Also, in this case, all other NEs are required to be in 'up' state. All the NEs in 'up' state can be easily handled with a simple multiplication of availabilities, while in case some Node Bs are allowed to be in 'down' state, *k-out-of-n* calculus will be deployed.

In the following paragraphs, the formulas are introduced. The availability of the GERAN network consisting of *n* BTSs per one BSC and *m* BSCs can be presented as [113]

$$A_{GERAN} = \prod_{i=1}^{m} \left(A_{BSCi} \cdot \sum_{j=k}^{n} \left(\frac{n!}{j!(n-j)!} A_{BTSj}^{j} (1 - A_{BTSj})^{n-j} \right) \right). \qquad (62)$$

In the above, it is assumed that all BSCs are required to be in 'up' state, while some BTS elements may be in 'down' state. Since in the following analysis all BTS elements are

required to be functional, the formula of the GERAN availability can be simplified into form

$$A_{GERAN} = \prod_{i=1}^{m}(A_{BSCi} \cdot \prod_{j=1}^{n}(A_{BTSj})) = A_{BSC}^{m} \cdot A_{BTS}^{n} \ . \tag{63}$$

The latter form of the formula comes from the fact that in the following it is assumed that all BSCs and BTSs have similar availabilities. The availability of the UTRAN can be similarly presented as [113]

$$A_{UTRAN} = \prod_{i=1}^{m}(A_{RNCi} \cdot \sum_{j=k}^{n}(\frac{n!}{j!(n-j)!} A_{Node\,Bj}^{j}(1 - A_{Node\,Bj})^{n-j})) . \tag{64}$$

The 2G- and 3G-service availabilities $A_{2GservicePS}$ and $A_{3GservicePS}$ for the PS domain can be presented as [9]

$$A_{2GservicePS} = A_{HLR} \cdot \prod_{i=1}^{n}\left(A_{MSCi} \cdot A_{GERANi}\right) \tag{65}$$

$$A_{3GservicePS} = A_{GGSN} \cdot A_{HLR} \cdot \prod_{i=1}^{n}\left(A_{SGSNi} \cdot A_{UTRANi}\right). \tag{66}$$

Maintenance availability $A_{maintenancePS}$ for the PS domain as a whole can be given as [113]

$$A_{maintenancePS} = A_{GGSN} \cdot A_{HLR} \cdot \prod_{i=1}^{n}\left(A_{SGSNi} \cdot A_{UTRANi}\right) \cdot \prod_{j=1}^{m}\left(A_{MSCj} \cdot A_{GERANj}\right). \tag{67}$$

For the CS domain the availability formulas strongly resemble the PS formulas given above and they are as follows

$$A_{2GserviceCS} = A_{HLR} \cdot \prod_{i=1}^{n}\left(A_{MSCi} \cdot A_{GERANi}\right) \tag{68}$$

$$A_{3GserviceCS} = A_{HLR} \cdot \prod_{i=1}^{n} \left(A_{MSCi} \cdot A_{UTRANi} \right) \tag{69}$$

$$A_{maintenanceCS} = A_{HLR} \cdot \prod_{i=1}^{n} A_{UTRANi} \cdot \prod_{j=1}^{m} \left(A_{MSCj} \cdot A_{GERANj} \right). \tag{70}$$

In all cases, the subscripts of the availability terms refer to the NEs whose availability is in question, for example, A_{BTS} is the availability of the BTS network element etc.

8.7.3 Analysis Results

In Table 29, the availability, Mean Time Between Failures (MTBF), and Mean Down Time /year (MDT) values are tabulated in case *all NEs (including all Node Bs) are required to be in 'up' state*. In the calculations, the number of BTSs was assumed to be 5 per BSC and the number of BSCs per SGSN element is 10. The number of Node Bs was assumed to be 25 per RNC and the number of RNCs per SGSN element was 10. The number of SGSNs and MSCs was 2. The network was assumed to include only one single HLR and GGSN.

It is noted that the introduction of high-risk components has a large effect on the availability of the network in this case. As expected, the introduction of a high-risk component does not have an effect on the 2G functionality. This can be seen when looking at Table 29 where the availabilities of the GERAN network and the 2G services for PS and CS domains are unaltered by the introduction of the high-risk components. However, the 3G part of the network suffers quite heavily from the introduction of the high-risk components, as the availabilities of the UTRAN network and 3G services are severely reduced. This results in the fact that the MDT values of the PS domain increase by a factor of 6.6…50.7, and in the CS domain the increment of MDT values is in the order of 6.6…50.9 times. Looking at the MTBF values, the corresponding degradation of network dependability can be noted.

A much better performance can be expected, if it is assumed that *some Node Bs are allowed to be in 'down' state*. In Table 30, this fact is demonstrated. The figures are

related to a case, in which one Node B per RNC is allowed to be in ‘down’ state. The improvement is significant, as in this case the yearly downtimes are less than 4 minutes. Another interesting fact is that the introduction of the high-risk components has virtually no effect on the system availability. It can even be demonstrated that the high availability is not affected by the number of Node Bs allowed to be in ‘down’ state (except for the case, where all Node Bs are required to be in ‘up’ state).

The above, somewhat surprising, result can be understood, if a closer look at taken at Eq. (64) that defines the UTRAN availability. If $n > k$, then a very good approximation is

$$A_{UTRAN} = \prod_{i=1}^{m} A_{RNCi} , \tag{71}$$

as

$$\sum_{j=k}^{n} \left(\frac{n!}{j!(n-j)!} A_{Node\,Bj}^{j} (1 - A_{Node\,Bj})^{n-j} \right) \approx 1 , \text{ if } n > k \text{ and } A_{Node\,B} \approx 1. \tag{72}$$

The latter condition given by Eq. (72) is easily kept in our case, as the average availability values of the Node B, even after the introduction of high-risk components, is >0.999 990 in all cases studied. The conclusion of the above is slightly surprising, in other words, the availability of the Node Bs nor the number of Node Bs in the ‘down’ state do not have an effect on the availability of the telecommunications network. It should, however, be remembered that if the network availability is defined so that all NEs (including *all Node Bs*) must be in ‘up’ state then the effect of introducing high-risk components is profound.

How to define the network availability, then? Or what is the correct availability value that should be used? Is the system ‘up’ even if some Node Bs are in ‘down’ state? Using simplistic RBD techniques or other non-state space analysis techniques cannot give an answer to these questions. What would be necessary is an in-depth state space analysis that can take into account the dependencies of the NEs and the resilience behavior of the network and other complex phenomena. The state space analysis techniques include, for example, Markov modeling and Petri Nets. However, as the 3rd generation network is a

very complex system, it is not very easy to apply these more sophisticated techniques to the whole system. Therefore, it would be useful to limit the state space analysis into a smaller entity. By doing so, answers may be expected to the question: what is the proper way to define the 3rd generation network system.

It may be assumed that it is probable that one Node B failure does not cause the whole network to fail. But what if the number of NEs is something other than 25 pcs? Is the approximation stated in Eq. (72) still valid?

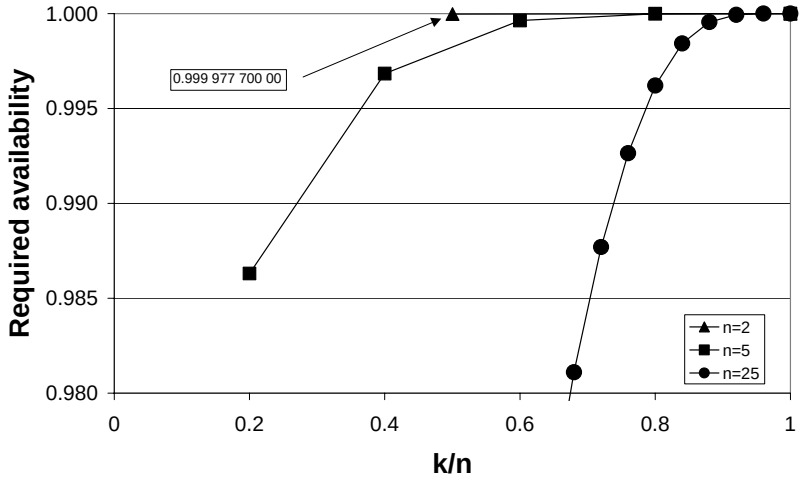

Figure 41. The required availability of a single network element in order to fulfill A>0.999 999 9995 requirement for a k-out-of-n configuration.

If it is assumed that the approximation in Eq. (72) is valid, if the summation $= 0.999\,999\,999|5 \approx 1$, the required minimum availability can be plotted for a single NE in terms of k-out-n ratio as depicted in Figure 41. It is noted that the larger the n, the smaller the minimum availability of NEs for a given *k/n* ratio. Therefore, the Node B case with n=25 was a favorable one. The introduction of weaker components had virtually no effect at all on the entity. However, if n is smaller, for example, n=2, then a very high availability for individual NEs is needed. For example, in the case where n=2 and k=1 the required minimum availability is 0.999 977 700. This required value already approaches the capability of the NEs with high-risk components (cf. Table 27). Therefore, the introduction of high-risk components, in general, is not a straightforward issue.

Furthermore, sometimes all NEs are needed to be in ‘up’ state, especially if the NE is critical from the network functionality point of view. For example, all SGSN, MSC, HLR, and GGSN NEs are required for proper operation of the network. Therefore, it is not acceptable that any of those could be in ‘down’ state and that the network would still be in ‘up’ state. More in-depth state space analysis can also help in this case to reveal the real dependencies of the NEs.

8.8 Discussion

In this chapter, the dependability of the 3rd generation telecommunications network has been covered. Special attention is paid to a case when components with 2nd level interconnection related reliability risk have been introduced to Node B NEs. From NE availability point of view the introduction of high-risk components has a very profound effect, as expected. In order to take this into account, some proper maintenance actions, at least, should be planned. Also, it can be considered if the components create such risks that those cannot be utilized at all. If a component with a better reliability performance could be used instead of the high-risk component, then it is recommended to abandon the high-risk components studied. Some component design modifications that could amend the reliability may also be considered.

From a network availability point of view, the effect of introducing high-risk components to some individual Node Bs may not always be critical. Whether this is the case, however, depends a lot on the definition that is used for network availability. The RBD technique used here should be complemented with state space analysis in order to get a deeper insight into this aspect. That is, however, beyond the scope of this thesis.

One interesting finding is that if the NE is not critical from a network availability point of view and therefore some of the elements are allowed to be in the ‘down’ state then (under some special circumstances) the number of NEs in ‘down’ state, or the fact that whether the NEs have high-risk components included or not, has virtually no effect on the network availability. It should, however, be remembered that this is the case only if availability of the NEs is already at a very high level.

As a conclusion, it seems that using high-risk components in the higher-hierarchy level NEs should be avoided. This is due to the low number of parallel elements and the criticality of the whole network performance. Even at lower-hierarchy level NEs the use of high-risk components cannot be recommended. This is due to the fact, although not studied in this thesis, it is expected that from economical point of view this is not feasible. The increased preventive maintenance and retrofit costs may easily overcome the potential savings on component costs.

Table 29. 3rd generation telecommunications network dependability figures of merit in case no network elements in 'down' state are allowed.

	NE only	*NE w/ comp A*	*NE w/ comp B*	*NE w/ comp C*	*NE w/ comp D*
A_{GERAN}	0.999991360	0.999991360	0.999991360	0.999991360	0.999991360
A_{UTRAN}	0.999962561	0.999701105	0.998415811	0.997962879	0.997648568
$A_{2GservicePS}$	0.999982288	0.999982288	0.999982288	0.999982288	0.999982288
$A_{3GservicePS}$	0.999924547	0.999401723	0.996833558	0.995929335	0.995302092
$A_{maintenancePS}$	0.999906980	0.999384165	0.996816046	0.995911839	0.995284606
$A_{2GserviceCS}$	0.999982288	0.999982288	0.999982288	0.999982288	0.999982288
$A_{3GserviceCS}$	0.999924691	0.999401867	0.996833701	0.995929479	0.995302235
$A_{maintenanceCS}$	0.999907412	0.999384597	0.996816476	0.995912269	0.995285036
MTBF, years					
GERAN	13.19	13.19	13.19	13.19	13.19
UTRAN	3.04	0.38	0.07	0.06	0.05
2GservicePS	6.44	6.44	6.44	6.44	6.44
3GservicePS	1.51	0.19	0.04	0.03	0.02
MaintenancePS	1.23	0.19	0.04	0.03	0.02
2GserviceCS	6.44	6.44	6.44	6.44	6.44
3GserviceCS	1.51	0.19	0.04	0.03	0.02
MaintenanceCS	1.23	0.19	0.04	0.03	0.02

MDT/year, minutes					
GERAN	4.54	4.54	4.54	4.54	4.54
UTRAN	19.68	157.10	832.65	1070.71	1235.91
2GservicePS	9.31	9.31	9.31	9.31	9.31
3GservicePS	39.66	314.45	1664.28	2139.54	2469.22
MaintenancePS	48.89	323.68	1673.49	2148.74	2478.41
2GserviceCS	9.31	9.31	9.31	9.31	9.31
3GserviceCS	39.58	314.38	1664.21	2139.47	2469.15
MaintenanceCS	48.66	323.46	1673.26	2148.51	2478.19

Table 30. 3rd generation telecommunications network dependability figures of merit in case one Node B per RNC in 'down' state is allowed.

	NE only	*NE w/ comp A*	*NE w/ comp B*	*NE w/ comp C*	*NE w/ comp D*
A_{GERAN}	0.999998560	0.999998560	0.999998560	0.999998560	0.999998560
A_{UTRAN}	0.999998560	0.999998560	0.999998560	0.999998560	0.999998560
$A_{2GservicePS}$	0.999996688	0.999996688	0.999996688	0.999996688	0.999996688
$A_{3GservicePS}$	0.999996544	0.999996544	0.999996544	0.999996544	0.999996544
$A_{maintenancePS}$	0.999993376	0.999993376	0.999993376	0.999993376	0.999993376
$A_{2GserviceCS}$	0.999996688	0.999996688	0.999996688	0.999996688	0.999996688
$A_{3GserviceCS}$	0.999996688	0.999996688	0.999996688	0.999996688	0.999996688
$A_{maintenanceCS}$	0.999993808	0.999993808	0.999993808	0.999993808	0.999993808
MTBF, years					
GERAN	79.17	79.17	79.17	79.17	79.17
UTRAN	79.17	79.17	79.17	79.17	79.17
2GservicePS	34.42	34.42	34.42	34.42	34.42
3GservicePS	32.99	32.99	32.99	32.99	32.99
MaintenancePS	17.21	17.21	17.21	17.21	17.21
2GserviceCS	34.42	34.42	34.42	34.42	34.42
3GserviceCS	34.42	34.42	34.42	34.42	34.42
MaintenanceCS	18.41	18.41	18.41	18.41	18.41

MDT/year, minutes					
GERAN	0.76	0.76	0.76	0.76	0.76
UTRAN	0.76	0.76	0.76	0.76	0.76
2GservicePS	1.74	1.74	1.74	1.74	1.74
3GservicePS	1.82	1.82	1.82	1.82	1.82
MaintenancePS	3.48	3.48	3.48	3.48	3.48
2GserviceCS	1.74	1.74	1.74	1.74	1.74
3GserviceCS	1.74	1.74	1.74	1.74	1.74
MaintenanceCS	3.25	3.25	3.25	3.25	3.25

9 Summary of the Thesis

In this thesis, first, the effect of constant temperature on the lifetime of electronic devices is considered. A novel temperature derating method is proposed. By using this method it is possible to take into account the true temperature dependency of the lifetime of a device. The end result enables the utilization of electronic devices at a higher operating temperature without compromising the reliability level required for successful completion of the required function.

Then, cyclic temperature effects on solder attachments are studied. First, IPC (The Institute for Interconnecting and Packaging Electronic Circuits) surface mount guidelines are surveyed. The underlying principles are revealed and the validity of the assumptions related is commented. In order to rectify some shortcomings of the guideline-based reliability requirements, a component specific reliability requirement approach and tool are introduced. Using this tool the applicability of certain ceramic components under certain typical telecommunications field environments is evaluated. A new method of how to predict the reliability of a component population that is addressed to several, different field environments is introduced.

Analytical and simulation based solder fatigue prediction models are benchmarked. The absolute accuracy of both approaches is found to be moderate. Different error sources are discussed and the effect of those on lifetime estimates is quantified. Two methods to improve the accuracy of Engelmaier's model are suggested: re-interpretation of solder joint height-term in conjunction with solder fillets, and the calibration of the lifetime prediction with actual test results.

Ways to time-average the hazard rate of 2-parameter Weibull distribution were researched in order to link the component level lifetime predictions with the PWB and higher hierarchy level lifetime predictions. The most accurate approximation was observed when equating a time-averaged reliability function of the 2-parameter Weibull distribution with the value of an exponential distribution.

Finally, the availability of a full 3rd generation telecommunications network was considered. The application of high-risk electronic components in network elements was considered. The effect of introducing high-risk components was not, in all cases, very large. However, if the number of parallel elements is small, then the required availability of individual network elements increases to a level that does not allow the use of high-risk components. From an economical point of view it may not be sensible to save on marginal component costs and by doing so compromise the reliability performance at the cost of potentially increased field returns.

One of the goals of this thesis was to create stronger links between component and system level reliability considerations. It has been attempted to reach this goal by using system level information when specifying component lifetime requirements and by studying the effects of introducing high-risk components to a telecommunications system. In Chapter 3, a new temperature derating approach is introduced. By using it, it is possible to take into account an arbitrary lifetime requirement. In Chapter 4, guideline-based thermal cycling requirements are reviewed, and in Chapter 5, a new approach on how to define thermal cycling requirements is described. By applying the new approach, it is possible to base the requirements on product-specific lifetime requirements. This is increasingly important, as many components have difficulties to pass generic rule-of-thumb type lifetime requirements. This means that safety margins must be based on realistic assumptions. Optimal requirements make sure that lifetime expectations are fulfilled under all circumstances but no excess safety margins are added.

Another goal of this thesis was to increase the accuracy of lifetime prediction methods. This is needed in order to create solid product-specific lifetime requirements. In Chapter 6, analytical and simulation based reliability prediction methods are compared. Their error sources are discussed and the error magnitudes are quantified. A new method to define solder joint height term for solder fillet attachments is introduced. By applying this a better agreement between the prediction and the actual test result is gained. A new method to calibrate Engelmaier's model is introduced. When error sources and their magnitudes are estimated, it is possible to reduce the errors, e.g., by utilizing more accurate material property data. If this is not a possibility, knowing the error magnitudes gives at least a

possibility to give lifetime estimates with proper error margins. Nowadays, error estimates have many times lacked, especially when applying numerical simulation methods. It is important that methods to improve the reliability prediction accuracy are going to be taken into use more widely.

In Chapter 7, some time-averaging methods are studied in order to be able to utilize component level reliability data on simplistic system level reliability considerations. In Chapter 8, a full 3rd generation telecommunications network is analyzed. General methodology for how to link component level data to the system level availability considerations is disclosed. The effect of introducing high-risk components, in particular, is studied. System level studies need to be developed further on so that more complex phenomena, such as network resilience behavior, can be taken better into account.

Suggestions for other future work contain the development of lifetime models for lead-free solder materials. This work has already started with the re-calibration of Engelmaier's model - originally developed for eutectic tin-lead solder - to be applicable in conjunction with SnAgCu solder [63], [64], [65].

Understanding the actual field environment needs to be studied in more detail in order to be able to effectively utilize the introduced mixed field environment concept. This is important also due to the fact that the extrapolation of test behavior from highly accelerated test environment to the actual field environment may otherwise cause huge errors. This is evident, as numerical simulation methods have a tendency to diverge at low strain energy values [5]. The lifetime behavior close to actual field environment - in general - is an issue that needs some further studies.

Although the development of reliability prediction methods and tools is important, it is at least equally important to know how to improve reliability. In this task a thorough understanding of metallurgical and other fundamental aspects of physical reliability is needed.

Appendices

Appendix A . Some corrections to the IPC-SM-785 guideline.

Appendix B. Component test data (Chapter 5).

Appendix C. Proof that option 3 approaches the instantaneous hazard rate of 2-parameter Weibull distribution as time approaches infinity.

Appendix A . Some corrections to the IPC-SM-785 guideline.

The IPC-SM-785 Guidelines for Accelerated Reliability Testing for Surface Mount Solder Attachments document contains some errors in the formulas and misuse of the units. As IPC-9701 Performance Test Methods and Qualification Requirements for Surface Mount Solder Attachments applies the Engelmaier formulas, it is expected that correcting the errors found in the IPC-SM-785 guideline also helps those utilizing the new IPC document. In the following paragraphs, the errors found are listed and corrected.

There are several errors in the IPC-SM-785 document. Most of them are probably just misprints or slight simplifications. Some of the errors seem to be systematic and therefore more serious.

Page 18, equation (no number) in the low part of the page after Equation (10).

This formula presents the acceleration factor in terms of MTTF values and cyclic frequencies. The IPC version is

$$A.F.(t) = \frac{MTTF(use)}{MTTF(test)} = A.F.(N)\frac{f_c(use)}{f_c(test)} \quad . \qquad \textit{(wrong)} \qquad (73)$$

The correct version should read

$$A.F.(t) = \frac{MTTF(use)}{MTTF(test)} = A.F.(N)\frac{f_c(test)}{f_c(use)} \quad . \qquad \textit{(corrected)} \qquad (74)$$

It is very probable that this is just a misprint, as this equation is presented correctly elsewhere [115].

Page 19, Equations (13) and (14)

Eqs. (13) and (14) are inconsistent with the literature [116].

The IPC-SM-785 version of Equation (13) is in the form

$$\Delta D = \frac{FL_D \Delta\alpha \Delta T_e}{2\varepsilon_f^{'} h_{s.j.}}, \qquad \textit{(inconsistent)} \qquad (75)$$

while the correct version is shown as Eq. (15) of this thesis. The excess $2\varepsilon_f^{'}$ term is the fatigue ductility coefficient, which has a value of $\cong 0.65$ for near-eutectic tin-lead solder material. Similarly, Eq. (14) in the IPC-SM-785 guideline has an excess term of $2\varepsilon_f^{'}$ in the denominator

$$\Delta D = \frac{FK_D \left(L_D \Delta\alpha \Delta T_e\right)^2}{2\varepsilon_f^{'} \left(200\, psi\right) A_{2/3} h_{s.j.}}. \qquad \textit{(inconsistent)} \qquad (76)$$

The consistent version of this equation can be found in this thesis (Eq. (14)). The unit of the constant term in the denominator is reversed into SI units in Eq. (14).

Page 19, Equation (15)

Equation (15) in IPC-SM-785 is an approximate solution of the acceleration factor, like Eq. (12) in this thesis. However, the approximate nature of this equation is not indicated in IPC-SM-785

$$A.F.(t) = \frac{N_f(use, 50\%)}{N_f(test, 50\%)} = \frac{\left(\Delta D(use)\right)^{\frac{1}{c(use)}} \cdot f_c(test)}{\left(\Delta D(test)\right)^{\frac{1}{c(test)}} \cdot f_c(use)}. \qquad (77)$$

In this equation, $N_f(use, 50\%)$ is the number of cycles in the use environment until 50% of the population has failed, and $N_f(test, 50\%)$ is the same figure of merit in the test environment. To be precise, the latter equals sign should be '$\cong$' instead of '='. Another option is to give a more precise value of the acceleration factor as

$$A.F.(t) = \frac{N_f(use,50\%)}{N_f(test,50\%)} = \frac{\Delta D(use)^{\frac{1}{c(use)}} \cdot f_c(test)}{\Delta D(test)^{\frac{1}{c(test)}} \cdot f_c(use)} \left(\frac{1}{2\varepsilon_f'} \right)^{\frac{1}{c(use)} - \frac{1}{c(test)}} \tag{78}$$

In general, the approximate nature of Engelmaier's formulas should be kept in mind. This is presented in the formulas by the empirical non-ideality factor *F*.

Page 21, Equations (17) & (18)

Equations (17) and (18) show how to determine the minimum acceptable failure-free cycle count in thermal cycling tests. The formula below (Eq. (17) in IPC-SM-785) relates the minimum number of failure-free cycles $N(test, n_t, x\%)$ to the number of cycles to failure in the test $N(test, x\%)$

$$N(test, n, x\%) = N(test, x\%) \left[\left(\frac{\ln 0.5}{\ln(1-0.01x)} \right)^{\frac{c(use)}{c(test)}} \left(\frac{\ln\left(1-\frac{1}{n_t}\right)}{\ln 0.5} \right) \right]^{\frac{1}{\beta}} \tag{79}$$

where n_t is the number of devices being tested and β is the Weibull distribution shape parameter. It is noted that the requirement can be somewhat eased if the number of samples tested n_t is increased. Equation (18) in IPC-SM-785 further gives $N(test, x\%)$ in terms of a so-called acceleration transform, introduced in [116].

The above form of Eq. (79) is overly complex, as what is actually needed is to move along the Weibull distribution with fixed parameters, shape parameter β and characteristic lifetime η. All that is required is to move from x% failed to the $(1/n_t)\cdot 100\%$ failed position. Therefore, a more compact and more accurate equation could simply be

$$N(test, n_t, x\%) = N(test, x\%)\left(\frac{\ln\left(1-\frac{1}{n_t}\right)}{\ln(1-0.01x)}\right)^{\frac{1}{\beta}} . \quad (80)$$

It is noted that the two equations are exactly equal, if and only if $c(use) = c(test)$. In all other cases, there is a slight discrepancy between the two equations.

The unit of the K_D term

It seems that in the literature [49], [116], [117], [118], the unit for the diagonal flexural stiffness of the lead K_D is wrong. The unit used is lb/in (kg/m in SI units), when it should actually be lbf/in (N/m in SI units). Although the wrong unit has been systematically applied in the literature, it looks like the calculations using this term have been performed correctly (as if the unit had been correct in the first place). One further point that supports this assumption is that unless the correct unit for K_D was selected, ΔD would not be unitless.

Appendix B. Component test data (Chapter 5).

Table 31. Statistical parameters of the tested components.

Component	Manufacturer	Parameter *)	-40…+125°C	0…100°C	$C.F.(N)$
a	I	n_t	11	10	
		p	11	10	
		β	7.8	8.3	
		η	609	1988	3.27
		$N_{1st\ failure}$	466	1533	
		$N_{1/n}$	427	1442	
		$C.R.$	0.92	0.94	
a	II	n_t	20	15	
		p	20	15	
		β	12.3	14.5	
		η	579	1724	2.98
		$N_{1st\ failure}$	469	1416	
		$N_{1/n}$	441	1396	
		$C.R.$	0.94	0.99	
b	III	n_t	10	5	
		p	10	0	
		β	6.1		

		η	813		
		$N_{1st\ failure}$	512		
		$N_{1/n}$	525		
		C.R.	1.03		
b	I	n_t	10	5	
		p	7	0	
		β	7.6		
		η	1058		
		$N_{1st\ failure}$	806		
		$N_{1/n}$	745		
		C.R.	0.92		
b	II	n_t	8	15	
		p	5	4	
		β	8.9	3.5	
		η	1072	4210	3.93
		$N_{1st\ failure}$	813	1769	
		$N_{1/n}$	816	1739	
		C.R.	1.00	0.98	
c	III	n_t	4	0	
		p	4	0	

		β	16.2		
		η	512		
		$N_{1st\ failure}$	457		
		$N_{1/n}$	460		
		C.R.	1.01		
c	II	n_t	20	15	
		p	20	15	
		β	9.1	6.9	
		η	612	1919	3.13
		$N_{1st\ failure}$	485	1393	
		$N_{1/n}$	423	1230	
		C.R.	0.87	0.88	
d	IV	n_t	20	15	
		p	20	14	
		β	9.1	5.9	
		η	663	2228	3.38
		$N_{1st\ failure}$	451	1360	
		$N_{1/n}$	456	1323	
		C.R.	1.01	0.97	
d	V	n_t	11	10	

		p	11	9	
		β	5.0	4.4	
		η	516	2117	4.10
		$N_{1st\ failure}$	288	1244	
		$N_{1/n}$	296	1149	
		C.R.	1.03	0.92	
e	III	n_t	7	10	
		p	7	10	
		β	10.1	11.1	
		η	365	1277	3.50
		$N_{1st\ failure}$	317	1058	
		$N_{1/n}$	290	1005	
		C.R.	0.91	0.95	
e	II	n_t	20	15	
		p	16	15	
		β	7.9	9.4	
		η	801	2202	2.75
		$N_{1st\ failure}$	534	1735	
		$N_{1/n}$	525	1591	
		C.R.	0.98	0.92	

*)

n_t	the number of tested items
p	the number of failed items
β	Weibull shape parameter
η	Weibull characteristic lifetime
$N_{1st\ failure}$	the number of cycles until the first failure observed in the test
$N_{1/n}$	the number of cycles until the first failure is anticipated in the test according to Weibull distribution
C.R.	Comparison Ratio

Appendix C. Proof that option 3 approaches the instantaneous hazard rate of 2-parameter Weibull distribution as time approaches infinity.

It is proven below that as $n \to \infty$, then $\langle h(t) \rangle_{\Delta t} \to h(t)$, where $\langle h(t) \rangle_{\Delta t}$ is the time-averaged hazard rate function of option 3 and $h(t)$ is the Weibull hazard rate function.

Let's first consider the instant in time at the end of the *first time interval* $t=t_1$. Keeping in mind the definitions of the hazard rate of the Weibull distribution Eq. (43) and of the hazard rate of option 3, Eq. (45) and writing $t_0=0$, the ratio of the two hazard rate functions can be written as

$$\frac{h(t)}{\langle h(t) \rangle_{\Delta t}} = \frac{\beta t_1^{\beta-1}}{\eta^\beta} \cdot \frac{\eta^\beta t_1}{t_1^\beta} = \beta \,. \tag{81}$$

For the *following time intervals*, the ratio of hazard rates can be written, keeping in mind that $t_{i+1} = (i+1)t_1 = mt_1$ and $t_i = it_1$, where $i = 1,2,3,...n$, as

$$\frac{h(t)}{\langle h(t) \rangle_{\Delta t}} = \frac{\beta (mt_1)^{\beta-1}}{\eta^\beta} \cdot \frac{\eta^\beta [mt_1 - it_1]}{(mt_1)^\beta - (it_1)^\beta}, \tag{82}$$

which simplifies after some manipulation into the form

$$\frac{h(t)}{\langle h(t) \rangle_{\Delta t}} = \frac{\beta}{m\left[1 - \left(1 - \frac{1}{m}\right)^\beta\right]}. \tag{83}$$

Part of the denominator of this can be presented as a binomial series, in other words,

$$\left(1 - \frac{1}{m}\right)^\beta = \sum_{i=0}^{\infty} \binom{\beta}{j} \left(-\frac{1}{m}\right)^j = 1 + \binom{\beta}{1} \cdot -\frac{1}{m} + \binom{\beta}{2} \cdot \left(-\frac{1}{m}\right)^2 + \ldots, \tag{84}$$

as the convergence criterion $\left|-\frac{1}{m}\right| < 1$ is fulfilled.

Looking at the full denominator, it can be written

$$m\left[1-\left(1-\frac{1}{m}\right)^{\beta}\right]=m\left[1-\left(1+\binom{\beta}{1}\cdot-\frac{1}{m}+\binom{\beta}{2}\cdot\left(-\frac{1}{m}\right)^{2}+\ldots\right)\right], \tag{85}$$

which simplifies into the form

$$\beta-\binom{\beta}{2}\cdot\frac{1}{m}+\binom{\beta}{3}\left(\frac{1}{m}\right)^{2}+\ldots. \tag{86}$$

Looking at the ratio again, it is easy to see that

$$\lim_{n\to\infty}\left(\frac{h(t)}{\langle h(t)\rangle_{\Delta t}}\right)=\frac{\beta}{\beta}=1, \tag{87}$$

which was the above claim that had to be proved.

References

[1] C.E. Pelaez and J.B. Bowles, “Applying Fuzzy Cognitive Maps Knowledge Representation to Failure Modes Effects Analysis”, *Proc. of the IEEE Annual Symposium on Reliability and Maintainability*, 1995, 450-456.

[2] M. Silva and S. Velilla, “ Error Detection and Correction on Petri net models of Discrete Events Control Systems”, Proc. *IEEE Int. Symposium Circuits and Systems*, 1985, 921-924.

[3] *IEEE Standard Methodology for Reliability Prediction and Assessment for Electronic Systems and Equipment*, #1413-1998, IEEE, 1998.

[4] *IEEE Guide for Selecting and Using Reliability Predictions Based on IEEE 1413*, #1413.1-2002, IEEE, 2002.

[5] R. Darveaux, “ Effect of Simulation Methodology on Solder Joint Crack Growth Correlation”, *Proc. of the 50th Electronics Components & Technology Conference*, Las Vegas, 2000, 1048-1058.

[6] J. Galloway, L. Li, R. Dunne, and H. Tsubaki, “Analysis of Acceleration Factors Used to Predict BGA Solder Joint Field Life”, *Proc. SMTA International*, Chicago, 2001, 357-363.

[7] *Military Standard MIL-STD-721C*, Definitions for Terms for Reliability and Maintainability, June, 12 1981.

[8] *International Standard, Information technology – Software product quality, Part 1: Quality model*, ISO/IEC FDIS 9126-1, ISO/IEC 2000.

[9] *MIL-HDBK-217*, Reliability Prediction of Electronic Equipment, version E, 1986, October 27.

[10] S. Arrhenius, "On the Reaction Velocity of the Inversion of Cane Sugar by Acids," *Zeitschrift für physikalische Chemie* **4**, 226ff (1889).

[11] D.L. Crook, “Evolution of VLSI Reliability Engineering”, *Proc. Int. Reliability Physics Symposium*, 1990, 2-11.

[12] W. Perry, “Specifications & Standard – A New Way of Doing Business”, *US Department of Defense Policy Memorandum*, June 1994.

[13] TS-TSY-000332, *Reliability Prediction Procedure for Electronic Equipment*, Issue 2, 1988 July, Bellcore.

[14] *Standard Reliability Table for Semiconductor Devices*, 1985, March, Nippon Telegraph and Telephone Corporation.

[15] *Handbook of Reliability Data for Components Used in Telecommunications Systems*, Issue 4, 1987 January, British Telecom.

[16] *Recuiel De Donnes De Fiabilite Du CNET* (Collection of Reliability Data from CNET), 1983, Centre National D’Etudes des Telecommunications (National Center for Telecommunication Studies).

[17] SN29500, *Reliability and Quality Specification Failure Rates of Components*, Siemens Standard, 1986.

[18] J.B. Bowles, “A Survey of Reliability-Prediction Procedures For Microelectronic Devices”, *IEEE Trans. On Reliability*, **41**(1992), 2-12.

[19] CALCE WWW URL: http://www.calce.umd.edu/

[20] N. Kelkar, A. Fowler, M. Pecht, and M. Cooper “Phenomenological Reliability Modeling of Plastic Encapsulated Microcircuits”, *Int. J. of Microcircuits and Electronic Packaging*, vol. 19 no. 1, 1996.

[21] T. Stadterman, B. Hum, D. Barker, and A. Dasgupta. “A Physics-of-Failure Approach to Accelerated Life Testing of Electronic Equipment”, *Proc. for the Test Technology Symposium '96*, U.S. Army Test & Evaluation Command, John Hopkins University/Applied Physics Laboratory, 4-6 Jun 1996.

[22] J. R. Black, “Physics of Electromigration”, *Proc. International Reliability Physics Symposium*, 1974, 142-164.

[23] P. Lall, M. Pecht, E. Hakim, *Influence of Temperature on Microelectronics and System Reliability*. CRC Press, 1997.

[24] J.-P. Clech, “Solder Reliability Solutions, A PC-Based Design-For –Reliability Tool”, Proc. of Surface Mount International, SMTA, 1996.

[25] A. Syed, “Predicting Solder Joint Reliability for Thermal, Power & Bend Cycle within 26% Accuracy”, *Proc. of the 51st Electronics Components & Technology Conference*, Orlando, 2001, 255-263.

[26] M.S. Moosa, K.F. Poole, “Simulating IC Reliability with Emphasis on Process-Flaw Related Early Failures”, *IEEE Trans. on Reliability* **44**(1995): 556-561.

[27] E. Demko, “Commercial-Off-The-Shelf (COTS): A Challenge To Military Equipment Reliability”, Proc. Annual Reliability and Maintainability Symposium, 1996, 7-12.

[28] T. Ejim, “High Reliability Telecommunications Equipment: A Tall Order for Chip-Scale Packages”, *Chip Scale Review* **5** (1998): 44-48.

[29] P. Frisk, M. Lindgren, B. Isaksson, P. Sneitz, and K. Hagelin, “Novel Packages and Packaging Technologies for Use in Harsh Environments”, *Proc. of IMAPS Nordic*, 2002.

[30] O. Salmela, *Interconnection Reliability Scales*, Nokia internal presentation, Nokia Networks, 2001.

[31] M. Pecht, “Why the Traditional Reliability Prediction Models Do Not Work – Is There an Alternative?”, *ElectronicsCooling*, vol. 2, No. 1, Jan 1996.

[32] Military Standard, MIL-STD-454, Standard General Requirements for Electronic Equipment, Requirement 18, *Derating of Electronic Parts and Materials*.

[33] Military Standard, MIL-STD-975 (NASA), NASA Standard (EEE) Part List, Appendix A, *Standard Parts Derating Guidelines*.

[34] *Electronic Derating for Optimum Performance*, Reliability Analysis Center, 2000.

[35] M.A. Jackson P. Lall, D. Das, “Thermal Derating – A Factor of Safety or Ignorance”, *IEEE Trans. Components, Packaging, and Manufacturing Technology* – Part A **20**(1997): 83-85.

[36] M. Pecht, “Issues Affecting Early Affordable Access to Leading Electronics Technologies by the US Military and Government”, *Circuit World* **22**(1996): 7-15.

[37] JEDEC newsletter: *Solid State Times*, vol. 4, no. 2, 2001, 8-10.

[38] M. White, M. Cooper, Y. Chen and J. Bernstein, “Impact of Junction Temperature on Microelectronics Device Reliability and Considerations for Space Applications”, *Proc. Integrated Reliability Workshop*, Final Report, 2003, IEEE International, Oct. 20-23, 2003.

[39] F. Jensen, *Electronic Component Reliability: Fundamentals, Modelling, Evaluation, and Assurance*, John Wiley & Sons, 1995, 202-207.

[40] R. Goyal, *Monolithic Microwave Integrated Circuits: Technology & Design*, Artech House, Norwood, 1989.

[41] A. Kleyner, J. Boyle, “Reliability Prediction of Substitute Parts Based on Component Temperature Rating and Limited Accelerated Test Data”, *Proc. Annual Reliability and Maintainability Symposium*, 2003, 518-522.

[42] C.R. Cooper and C.D. McGillen, *Probabilistic Methods of Signal and System Analysis*, Holt, Rinehart and Winston, New York, 1971.

[43] P. Yang and J-H Chern, "Design for Reliability: The Major Challenge for VLSI", *Proc. of the IEEE* **81**(1993): 730-744.

[44] C. Hu, "IC Reliability Simulation", *IEEE J. of Solid-State Circuits* **27**(1992): 241-246.

[45] D.F. Frost and K.F. Poole, "RELIANT: A Reliability Analysis Tool for VLSI Interconnects", *IEEE J. of Solid-State Circuits* **25**(1989): 458-462.

[46] X. Xuan, A. Chatterjee and A. Singh, "ARET for System Level IC Reliability Simulation" *Proc. 41st Annual Int. Rel. Phys. Symp*., Dallas Texas, 2003, 572-574.

[47] H.C. Mogul, J.W. McPherson, and T.M. Parrill, "Building-In Reliability into VLSI Junctions", *IEEE Trans. Semiconductor Manufacturing* **10** (1997): 495-497.

[48] L.J.T. Hinton, "Uncertainty and Confidence in Measurements", Chapter 21 in *Microwave Measurement Including Supplementary Volume*, ed. A.E. Bailey, Peter Peregrinus Ltd., London 1988, 418-443.

[49] *Guidelines for Accelerated Reliability Testing of Surface Mount Solder Attachments*, IPC-SM-785, November 1992.

[50] *Performance Test Methods and Qualification Requirements for Surface Mount Solder Attachments*, IPC-9701, January 2002.

[51] J.D. Morrow, "Cyclic Plastic Strain Energy and Fatigue of Metals", *ASTM STP* **378**, ASTM, Philadelphia, 1964

[52] S.S. Manson, *Thermal Stress and Low Cycle Fatigue*, McGraw-Hill, New York, 1966.

[53] O. Salmela, “Commentary on the IPC Surface Mount Attachment Reliability Guidelines”, accepted for publication in *Quality and Reliability Engineering International*.

[54] R.D. Gerke, and G.B. Kromann, “Solder Joint Reliability of High I/O Ceramic Ball Grid Arrays and Ceramic Quad-Flat-Packs in Computer Environments: The PowerPC 603™ and PowerPC 604™ Microprocessors”, *IEEE Transactions on Components and Packaging Technology* **22**(1999): 488-496.

[55] R.D. Banks, T.E. Burnette, R.D. Gerke, E. Mammo, and S. Mattay, “Reliability Comparison of Two Metallurgies for Ceramic Ball Grid Array”, *IEEE Trans. Components and Packaging Technology, Part B* **18**(1995): 53-57.

[56] A. Syed, and R. Darveaux, “LGA vs. BGA: What is More Reliable? A 2nd Level Reliability Comparison”, *Proc. SMTA International* 2000, 347-352.

[57] A. Høyland, and M. Rausand, *System Reliability Theory, Models and Statistical Methods*, John Wiley & Sons, New York, 1994.

[58] M. Osterman, T. Stadterman, “Failure Assessment Software for Circuit Card Assemblies”, *Proc. Annual Reliability and Maintainability Symposium*, 1999, 269-276.

[59] J. Lau, G. Harkins, D. Rice, and J. Kral, “Thermal Fatigue Reliability of SMT Packages and Interconnections“, *Proc. International Reliability Physics Symposium 1987.*

[60] G.V. Clatterbaugh and H.K. Charles, “Thermomechanical Behavior of Soldered Interconnects for Surface Mounting: A Comparison of Theory and Experiment“, *Proc. Electronic Components 35th Annual Conference*, Washington 1985.

[61] J. Särkkä, K. Andersson, O. Salmela, and M. Tammenmaa, “Interconnection Reliability of Some Lead-free RF-Components in Leadless Packages”, *Proc. IMAPS Nordic, Espoo 2003.*

[62] J. Särkkä, K. Andersson, O. Salmela, and M. Tammenmaa, “Interconnection Reliability of SnAgCu Soldered Ceramic Leadless Packages”, *Proc. PIC Jedec 5th Lead-free Conference*, San Jose, April 2004.

[63] O. Salmela, K. Andersson, A. Perttula, J. Särkkä, and M. Tammenmaa, “Recalibration of Engelmaier’s Model for Lead-Free Solder Attachments”, submitted to *Quality and Reliability Engineering International*.

[64] O. Salmela, K. Andersson, A. Perttula, J. Särkkä, and M. Tammenmaa, “Modified Engelmaier’s Model Taking Account of Different Stress Levels”, submitted to *Quality and Reliability Engineering International*.

[65] O. Salmela, K. Andersson, J. Särkkä, and M. Tammenmaa, “Reliability Analysis of Some Ceramic Lead-Free Solder Attachments”, *Proc. Pan Pacific Microelectronics Symposium Conference*, Kauai, SMTA, January 2005.

[66] O. Salmela, J. Särkkä, K. Andersson, and M. Tammenmaa, “Reliability Testing of Some Ceramic Components and Evaluation of the Results Using Test Interpretation Tool”, *Proc. European Microelectronics and Packaging Symposium*, Prague, June 2004.

[67] D.R. Banks, et al, “Reliability Comparison of Two Metallurgies for Ceramic Ball Grid Array, *IEEE Trans. Components, Packaging, and Manufacturing Technology- Part B* **18** (1995).

[68] L.G. Johnson, *The Statistical Treatment of Fatigue Experiments*, Elsevier, Amsterdam, 1964.

[69] G.S. Wasserman, I.S. Reddy, “Practical Alternatives for Estimating the Failure Probabilities of Censored Life Data”, *Quality and Reliability Engineering International*, **8**(1992), 61-67.

[70] F. Jensen, *Electronic Component Reliability, Fundamentals, Modelling, Evaluation, and Assurance*, John Wiley & Sons, 1995.

[71] E. Nicewarner,"Historical Failure Distribution and Significant Factors Affecting Surface Mount Solder Joint Fatigue Life", *Proc. International Electronic Packaging Conference*, Wheaton, USA, 1993.

[72] K.C. Norris and A.H. Landzberg, "Reliability of Controlled Collapse Interconnections", *IBM J. Res. Develop.* **13** (1969), 266-271.

[73] J.-P. Clech, "Solder Reliability Solutions: A PC-Based Design-For-Reliability Tool", *Proc. of Surface Mount International*, SMTA, 1996.

[74] A. Syed and M. Doty, "Are We Over-Designing for Solder Joint Reliability? – Field vs. Accelerated Conditions, Realistic vs. Specified Requirements", in *Proc. of the 49th Electronics Components & Technology Conference*, San Diego, 1999, 111-117.

[75] A. Kleyner and J. Boyle, "Reliability Prediction of Substitute Parts Based on Component Temperature Rating and Limited Accelerated Test Data" *Proc. Annual Reliability and Maintainability Symposium*, Tampa, 2003, 518-522.

[76] C.K. Hansen and P. Thyregod, "Component Lifetime Models Based on Weibull Mixtures and Competing Risks", *Quality and Reliability Engineering International*, **8**(1992), 325-333.

[77] L. Anand, "Constitutive Equations for Hot-Working of Metals", Int. Journal of Plasticity, **1**(1985), 213-231.

[78] J-P Clech, "Solder Reliability Solutions, A PC-Based Design-For –Reliability Tool", Proc. of Surface Mount International, SMTA, 1996.

[79] A. Syed, “Predicting Solder Joint Reliability for Thermal, Power & Bend Cycle within 26% Accuracy”, *Proc. of the 51st Electronics Components & Technology Conference*, Orlando, 2001, 255-263.

[80] S. Stoyanov and C. Bailey, “Optimisation and Finite Element Analysis for Reliability Electronic Packaging”, *Proc. 4th Int. Conf. On Thermal & Mechanical Simulation and Experiments in Micro-Electronics and Micro-Systems*, EuroSIME 2003, Aix-en-Provence, 391-398.

[81] C. Bailey, “Exploiting Virtual Prototyping for Reliability Assessment”, *Proc. Int. IEEE Conf. On the Business of Electronic Product Reliability and Liability*, 2003.

[82] K. Andersson, O. Salmela, J. Särkkä, and M. Tammenmaa, “The Effect of Material and Dimension Related Parameters on the FIT-Figures of Interconnections in Reliability Calculations”, *Proc. IMAPS, Boston*, 2003.

[83] R. Darveaux, K. Banerji, A. Mawer, and G. Dody, “Reliability of Plastic Ball Grid Array Assembly” in *Ball Grid Array Technology*, Ed. J. Lau, McGraw-Hill, New York, 1995.

[84] *The Restriction of Hazardous Substances in Electrical and Electronic Equipment* (ROHS) Directive (2002/95/EC).

[85] P. Roubaud, G. Ng, G. Henshall, “Impact of Intermetallic Growth on the Mechanical Strength of Pb-Free BGA Assemblies”, *Proc. APEX* 2001.

[86] P.M. Hall, T.D. Durrerar, and J.J. Argyle, “Thermal Deformations Observed in Leadless Ceramic Chip Carriers Surface Mounted to Printed Wiring Boards”, *IEEE Trans. Components, Hybrids, and Manufacturing Technology*, vol. CHMT-6, No. 4, Dec. 1983, 544-552.

[87] D.E. Riemer, “Prediction of Temperature Cycling Life for SMT Solder Joints on TCE-Mismatched Substrates”, Proc. Electronic Components and Technology Conference, 1990, 418-425.

[88] P. M. Hall, “Solder Attachment of Leadless Ceramic Chip Carriers”, *Solid State Technology*, March 1983, 103-107.

[89] R.T. Howard, S.W. Sobeck, C. Sanetra, “A New Package-Related Failure Mechanism for Leadless Ceramic Chip Carriers (LC-3s) Solder-Attached to Alumina Substrates”, *Solid State Technology*, February 1983, 115-122.

[90] H.D. Solomon, V. Brzozowski, D.G. Thompson, “Predictions of Solder Joint Fatigue Life”, *Proc. Electronic Components and Technology Conference*, May 1990, 351-359.

[91] H.D. Solomon, “Life Prediction and Accelerated Testing” in *Mechanics of Solder Alloy Interconnects*, Eds. D.R. Frear, S.N. Burchett, H.S. Morgan, and J.H. Lau, Kluwer academic Publishers, Dordrecht, 1994.

[92] P.E. Baker and D.K. Kaspari, “ Low Cycle Fatigue Analysis and Test Methodology for Fine Pitch Leaded Surface Mount Components”, *Proc. IEEE InterSociety Conference on Thermal Phenomena*, 1996, 74-80.

[93] J.B. Bowles, “A Survey of Reliability-Prediction Procedures For Microelectronic Devices”, *IEEE Transactions on Reliability*, **41**(1992), 2-12.

[94] J.B. Bowles, “Commentary-Caution: Constant Failure-Rate Models May Be Hazardous to Your Design”, *IEEE Transactions on Reliability*, **51**(2002), 375-377

[95] W. Nelson, “Weibull Analysis of Reliability Data with Few or No Failures”, *J. Quality Technology*, **17**(1985) 140-146.

[96] J.B. Keats, P.C. Nahar, and K.M. Korbel , “A Study of the Effects of Mis-Specification of the Weibull Shape Parameter on Confidence Bounds Based on the

Weibull-to-exponential Transformation", *Quality and Reliability Engineering International*, **16**(2000), 27-31.

[97] M. Xie, Z. Yang, O. Gaugoin, "More on the Mis-Specification of the Shape Parameter with Weibull-to-exponential Transformation", *Quality and Reliability Engineering International*, **16**(2000), 281-290.

[98] P.D.T. O'Connor, *Practical Reliability Engineering*, John Wiley & Sons, 1991.

[99] W. Nelson, *Accelerated Testing, Statistical Models, Test Plans, and Data Analyses*; John Wiley & Sons, New York, 1990.

[100] J-M Clech, D.M. Noctor, J.C. Manock, G.W. Lynott, F.E. Bader, "Surface Mount Assembly Failure Statistics and Failure Free Time", *Proc. 44th Electronic Components and Technology Conference*, May 1994.

[101] O. Salmela, K. Andersson, J. Särkkä, and M. Tammenmaa, "Interconnection Reliability Studies of Some Ceramic Components and the Introduction of the Results Into MTBF Calculations", *Proc. Ceramic Interconnection Initiative: Next Generation Conference*, IMAPS, Denver, April 2003.

[102] H. Ascher, H. Feingold, *Repairable Systems Reliability – Modelling, Inference, Misconceptions, and Their Causes*, Marcel Dekker, New York and Basel, 1984.

[103] J. Jones, J. Hayes, "A Comparison of Electronic-Reliability Prediction Models", *IEEE Transactions on Reliability*, **48**(1999), 127-134.

[104] X. Xuan, and A. Chatterjee, "Sensitivity and Reliability Evaluation for Mixed-Signal ICs Under Electromigration and Hot-Carrier Effects", *Proc. IEEE Symp. On Defect and Fault Tolerance in VLSI Systems*, IEEE, 2001.

[105] O. Salmela, K. Andersson, J. Särkkä, and M. Tammenmaa, “Reliability of Some Ceramic Components and the Related Effect on System Performance”, *Proc. IMAPS Nordic*, Espoo 2003.

[106] W. Nelson, *Accelerated Testing, Statistical Models, Test Plans, and Data Analyses*. John Wiley & Sons, New Work, 1990.

[107] R.F. Drenick, “The Failure Law of Complex Equipment”, *The Journal of the Society for Industrial Applications in Mathematics*, **8**(1960), 680-689.

[108] F. Jensen, *Electronic Component Reliability, Fundamentals, Modelling, Evaluation, and Assurance*. John Wiley & Sons, 1995.

[109] O. Salmela, “The Effect of Introducing Increased-Reliability-Risk Electronic Components into 3rd Generation Telecommunications System”, accepted for publication in *Reliability Engineering & System Safety*.

[110] Free download: www.raptorplus.com

[111] J.B. Keats, S.P. Chambal. “Transient Behavior of Time-Between-Failures of Complex Repairable Systems”, *Quality and Reliability Engineering International*, **18**(2002), 293-297.

[112] C.R. Cassady, E.A. Pohl, “Introduction to Repairable-System Modelling”, *Annual Reliability and Maintainability Symposium* 2003, Tutorial Notes.

[113] D. Kumar, A. Miyabayashi, and K. Ojala, “Availability Modelling of the 3GPP R99 Telecommunication Networks”, *Proc European Safety and Reliability Conference,* 2003.

[114] www.3GPP.org

[115] W. Engelmaier, “The Use Environments of Electronic Assemblies and Their Impact on Surface Mount Solder Attachment Reliability”, *IEEE Transactions on Components, Hybrids, and Manufacturing Technology* **13**(1990): 903-908.

[116] W. Engelmaier, “Functional Cycles and Surface Mounting Attachment Reliability”, *Circuit World* **11**(1985):61-68.

[117] J.-P. Clech, W. Engelmaier, R.W. Kotlowitz, and J.A. Augis, “Reliability Figures of Merit for Surface-Soldered Leadless Chip Carriers Compared to Leaded Packages”, *IEEE Transactions on Components, Hybrids, and Manufacturing Technology* **12**(1989): 449-458.

[118] W. Engelmaier, “Generic Reliability Figures of Merit Design Tools for Surface Mount Solder Attachments”, *IEEE Transactions on Components, Hybrids, and Manufacturing Technology* **16**(1993): 103-112.